universität wien

MASTERARBEIT

Titel der Masterarbeit

„Chiral Methylmetals – Configurational Stability and Applications“

Verfasserin

B.S. Petra Malova

angestrebter akademischer Grad

Master of Science (MSc)

Wien, 2010

Studienkennzahl lt. Studienblatt:	A 066 862
Studienrichtung lt. Studienblatt:	Chemie
Betreuerin / Betreuer:	Ao. Univ.-Prof. Dr. Friedrich Hammerschmidt

To Fritz, my advisor, who has helped me incredibly in my work,
to my parents and my whole family who have always stood by me,
to Milan and all of my friends who were there for me,
to Ania and Renzhe for all of their help and fun in the lab,
and last but not least to everyone in our group who has offered me a helping hand,

Thank you!

Table of contents

1 Organolithiums

1.1 Carbanions

"Carbanion" as a term was introduced by Wallis and Adams in the year 1933[1] and it is used for compounds that have a negative charge on a carbon atom. Carbanions can be found in several hybridization states (Figure 1.1).[2]

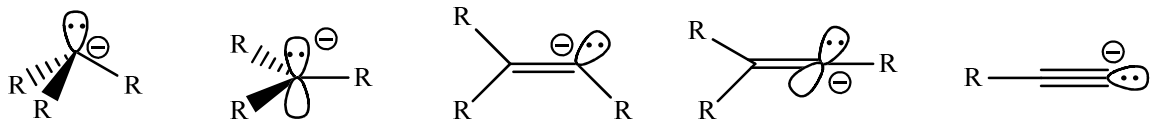

sp^3/sp^3 p/sp^2 sp^2/sp^2 p/sp sp/sp

Figure 1.1 - Hybridization states of carbanions

1.1.1 Stability

The stability of a carbanion increases with *s* character and is influenced by the substituents on the carbon atom – the order of stability is *tert* > *sec* > *prim* due to stabilization through polarisability.[2] Heteroatom-substituted functional groups in α position greatly increase the stability of carbanions[3] through resonance (groups like CN, NO_2, COR) and polar (F, OH) effects (Figure 1.2).[2]

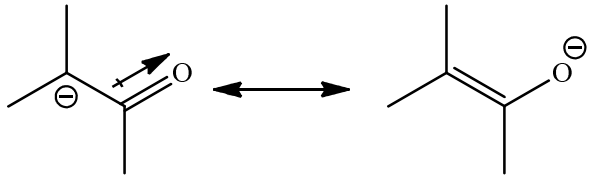

Figure 1.2 - Stabilization through resonance

Carbanions that are sp^3 hybridized are tetrahedral and therefore can be configurationally stable.[1]

1.2 Organolithiums

Organometallic derivatives of very electropositive metals like lithium have the same properties as salts of carbanions.[2]

Organolithiums exist as aggregates – dimers (bulky organolithiums), tetramers (β-branched primary, secondary and tertiary organolithiums), hexamers (primary organolithiums)[4] and higher[5,6] in solution (Figure 1.3). The degree of aggregation depends on the solvent and the organic group.[2]

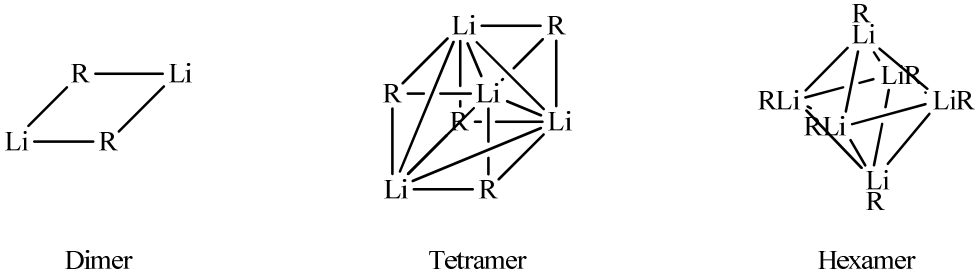

Figure 1.3 - Aggregates of organolithiums

Various ligands have the ability to dissolve these aggregates – *N*,*N*,*N*′,*N*′-tetramethylethylenediamine (TMEDA) is a very common one, but others may be used as well. The order of activation is: hexamethylphosphoramide (HMPA) > *N*,*N*,*N*′,*N*″,*N*″-pentamethyldiethylenetriamine (PMDTA) > (-)-sparteine > *N*,*N*′-dimethyl-*N*,*N*′-propylene urea (DMPU) > 1,2-Dimethoxyethane (DME) > TMEDA > THF > Et_2O.[4]

1.2.1 Preparation

1. Preparation of organolithiums using metallic lithium

It is the simplest way to prepare organolithiums. Alkyl, aryl, and alkenyl halides can be used but the stereochemical integrity is mostly lost.[7]

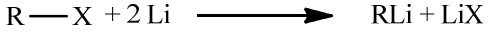

2. Preparation of organolithiums by lithiation (hydrogen-metal exchange, metalation)

It is the method of choice in many cases. The position of lithiation depends on the directing effect of the substituents and the acidity of the hydrogens in the substrate.[7]

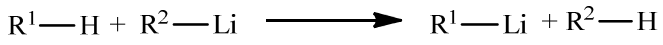

3. Preparation by halogen-metal exchange

It proceeds in the direction of the more stable organolithium that is formed from the more acidic compound. It is very useful for converting aryl and alkenyl halides to aryl and alkenyl lithiums.[7]

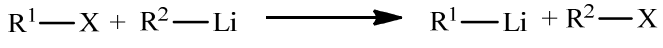

4. Preparation by metal-metal exchange (transmetalation)

It proceeds in the direction of the more electropositive metal on the more acidic carbon atom.[7]

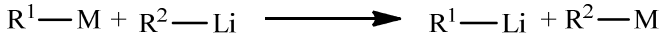

1.2.1.1 Tin-Lithium Exchange

Tin-lithium exchange is the most important way of making salt free organolithiums. Most of the evidence shows that it proceeds stereospecifically with retention of configuration towards the formation of the most stable organolithium, especially in case of a stabilized organolithium. It is a great way of synthesizing organolithiums that contain aryl or vinyl groups or heteroatoms in α position because they are more stable than alkyllithiums like MeLi or BuLi.[8]

Still[9] and Seebach[10] proposed a mechanism for tin-lithium exchange with an ate complex **1.2** as an intermediate (Scheme 1.1). If there is a heteroatom in α position it can work as an anchor for the lithium and thus lead to the overall retentive mechanism.

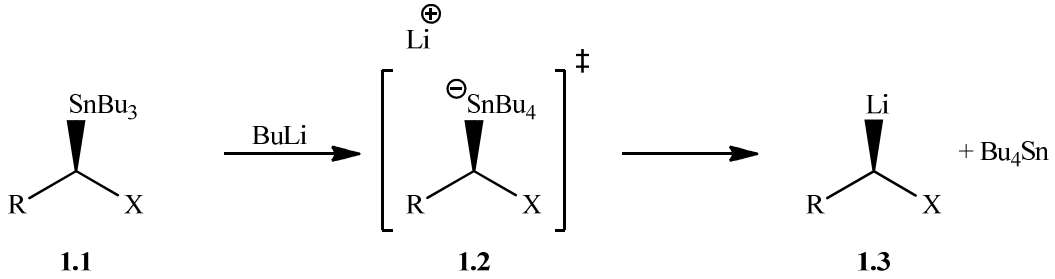

Scheme 1.1 - Proposed mechanism for the tin-lithium exchange

If this intermediate ate complex is stable enough, it can be characterized by NMR spectroscopy as is the case in a mixture of tetramethylstannane and MeLi in THF after the addition of HMPA. At first, only one peak representing the tetramethylstannane at 0 ppm was present in the ^{119}Sn NMR spectrum but when HMPA was added, another peak corresponding to a stannate complex at -277 ppm showed up[11] (Scheme 1.2).

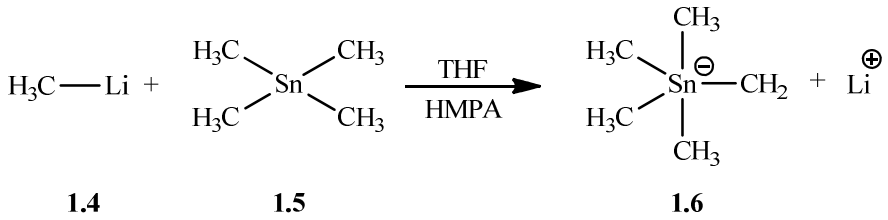

Scheme 1.2 - Formation of the ate complex after the addition of HMPA

1.2.2 Classes of Organolithiums

1. Unfunctionalized organolithiums

They do not contain any heteroatom in α position and are not synthetically interesting. The first chiral, nonracemic organolithium, that was formed from (-)-2-iodooctane 60 years ago, belongs to this class. It was quenched with carbon dioxide at -70˚C to give the optically active (-)-2-methyloctanoic acid in enantiomeric excess of 20%[12] (Scheme 1.3).

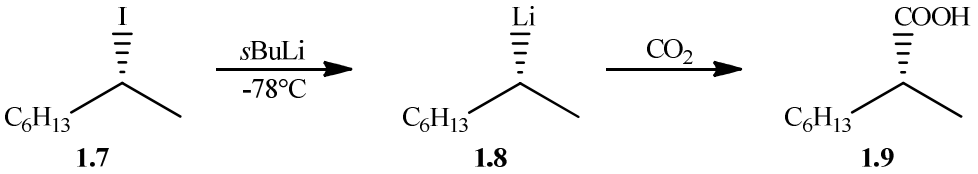

Scheme 1.3 - Formation of the (-)-2-methyloctanoic acid

The configurationally most stable ones are cyclopropyllithiums (due to the ring strain) followed by vinylic, tertiary, secondary, primary and benzylic organolithiums.[8]

2. α-Heteroatom-substituted organolithiums

They contain heteroatoms like oxygen, nitrogen, sulfur and halogens. They can be divided into two groups based on their stabilization.

- Non-stabilized organolithiums

They contain a tetrahedral centre that also contains lithium. Their reactions usually proceed through retention of configuration which makes them useful for the syntheses of chiral, nonracemic compounds.[4]

- Dipole-stabilized organolithiums

If the group Y is capable of inducing a formal positive charge on the heteroatom X, then the heteroatom can produce a local inductive effect that can promote the removal of the hydrogen from the carbon α to it (Scheme 1.4).[13]

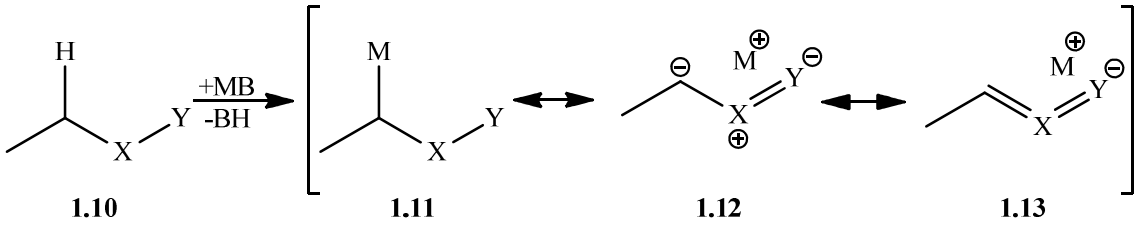

Scheme 1.4 - Stabilization of carbanions by a dipole

A good stabilizing effect is observed if there is another heteroatom (oxygen, nitrogen) in the γ-position to the carbanion – lithium can coordinate to this heteroatom and form a five membered chelate ring[13] (Scheme 1.5).

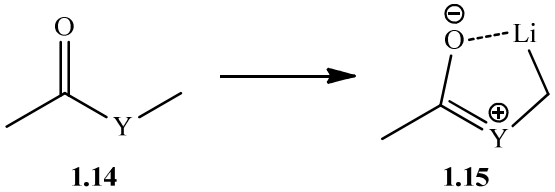

1.14 **1.15**

Scheme 1.5 - Stabilization through heteroatom

1.2.3 Configurational Stability

Configurational stability is a relative concept that depends very much on external conditions like temperature, solvent, timescale of interest and the reaction itself.[14, 15]

1. Macroscopic configurational stability

It is characteristic for compounds that racemize slowly, over the period of minutes and hours. It is examined by quenching a single pure enantiomer of organolithium with an electrophile after various periods of time and determining the enantiomeric excess of the product.

2. Microscopic configurational stability

It is characteristic for compounds that racemize within seconds or less. It refers to the rate at which the organolithium adds to an electrophile which is usually present in the reaction mixture or to the rate at which it undergoes an intramolecular rearrangement.
For compounds that racemize in a matter of 1/10 or 1/100 of a second there is a test that employs variable temperature NMR spectroscopy. It is based on the line shape analysis of peaks of the interconverting diastereotopic signals at different temperatures.

1.2.4 Inversion of Configuration (Enantiomerization)

With the development of NMR spectroscopy it has been possible to determine barriers for the inversion of configuration and thus draw conclusions about the possible mechanism. So far three mechanisms for enantiomerization have been proposed.[16]

1. Dissociative mechanism

At first a solvent-separated ion pair (SSIP) forms followed by planarization of the carbanion, flipping of the substituents and ion-pair recombination (Scheme 1.6). The rate-determining step is the dissociation of the lithium cation from the carbanionic carbon atom.

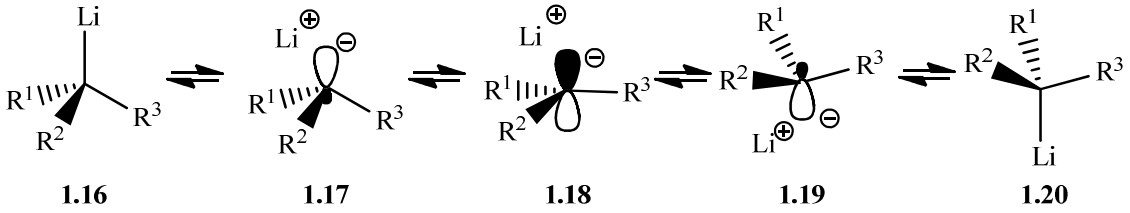

Scheme 1.6 - Enantiomerization through dissociative mechanism

2. Conducted tour mechanism

The lithium ion coordinates to a Lewis base like a nitrogen atom and is so delivered to the other side of the carbanion. This mechanism has been suggested on the basis of the crystal structure of α-lithio-*N*,*N*-dimethylbenzylamine (Scheme 1.7).

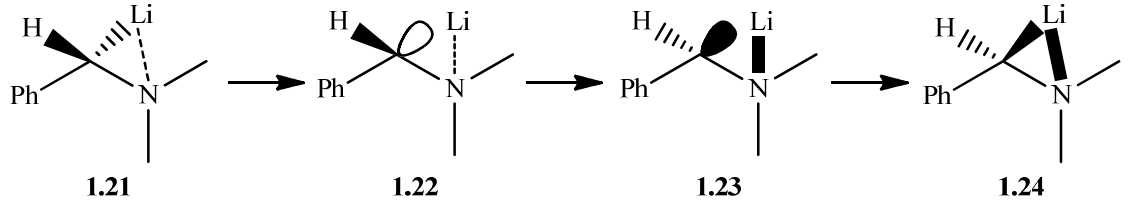

Scheme 1.7 - Enantiomerization through conducted tour mechanism

3. Bond rotation

The rate-determining step of this mechanism is the rotation about the C-X bond which is influenced by the bulkiness of the substituents. It is characteristic for the organolithiums containing sulfur or selenium in α position (Scheme 1.8).

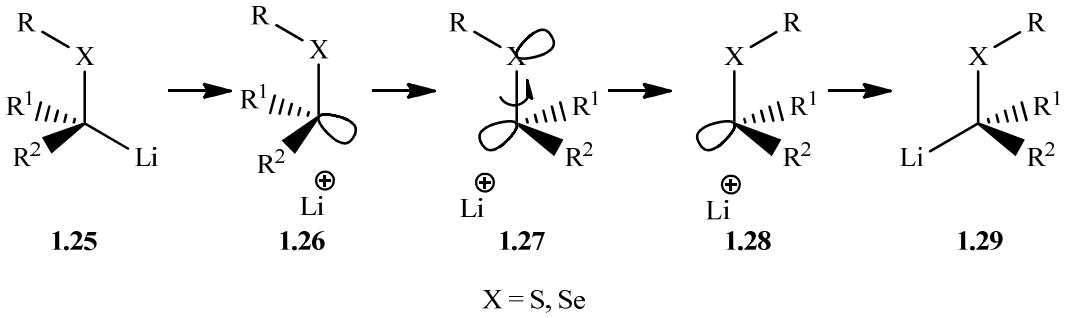

Scheme 1.8 - Enantiomerization through bond rotation

1.2.5 Hoffman test

This test was developed by Hoffman et al. for the determination of the configurational stability of chiral organolithiums and is based on kinetic resolution during the electrophilic substitution step.[16, 17]

It consists of two reactions – in the first one, the control reaction, the racemic organolithium compound reacts with a chiral racemic electrophile and the ratio of diastereomeric products should lie between 1.5 and 3.0. In the second reaction the racemic organolithium reacts with a single enantiomer. If the resulting ratio of diastereomers is the same as in the control reaction, the organolithium is configurationally labile, but if it is different, it is at least partially configurationally stable. If the resulting ratio is equal to 1, the organolithium is completely configurationally stable.[16]

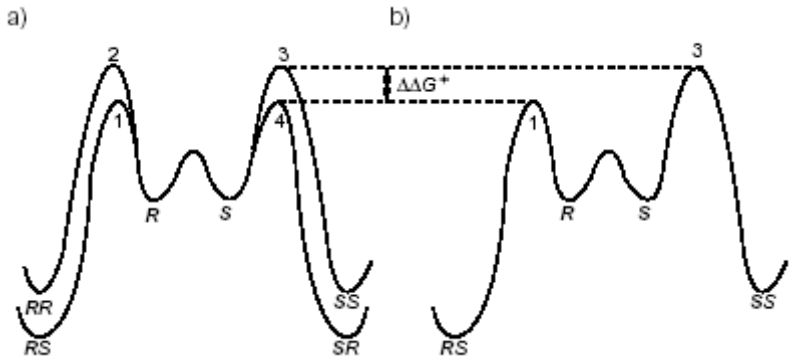

Figure 1.4 - Energy diagram for a reaction of a configurationally labile organolithium

Figure 1.4 shows the energy diagram for a reaction between a) a configurationally labile racemic organolithium and a racemic electrophile and b) the pure (*S*)-enantiomer of the electrophile. The outcome in this situation is only dependent on the transition state energy difference $\Delta\Delta G^{\ddagger}$

because the inversion barrier between (*R*) and (*S*), which is represented by the smallest peak, is much smaller than the transition state energies for the formation of both products.[16]

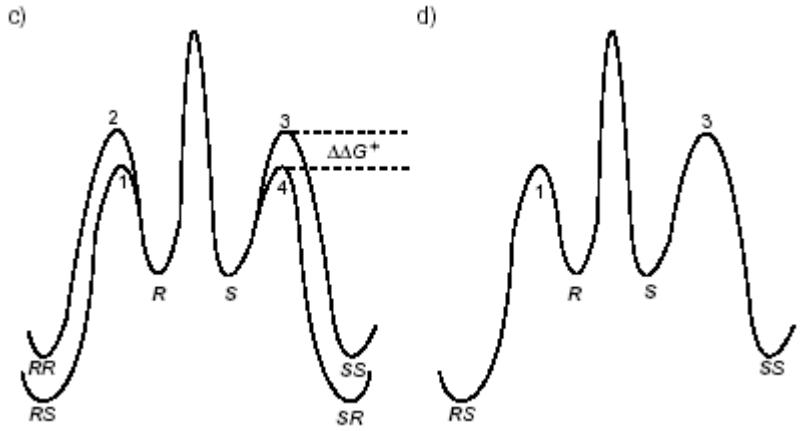

Figure 1.5 - Energy diagram for a reaction of a configurationally stable organolithium

In Figure 1.5, a configurationally stable organolithium reacts with c) a chiral racemic electrophile and d) the (*S*)-enantiomer. Since the inversion barrier between (*R*) and (*S*) is bigger that the transition state energy difference $\Delta\Delta G^{\ddagger}$, it is the $\Delta\Delta G^{\ddagger}$ that determines the ratio of diastereomers when the organolithium reacts with the racemic electrophile. If however only one enantiomer is present, only one pathway is possible because the inversion barrier which is represented by the biggest peak is much bigger that the transition state energies for the formation of both products.[16]

1.2.6 Reactions of Organolithiums with Electrophiles

Organolithiums readily undergo substitution reactions with electrophiles with both retention (S_E2ret) and inversion (S_E2inv) of configuration (Scheme 1.9). The non-stabilized ones react preferentially with retention of configuration. The stabilized organolithiums can react either way since both pathways are energetically and symmetry allowed.[8]

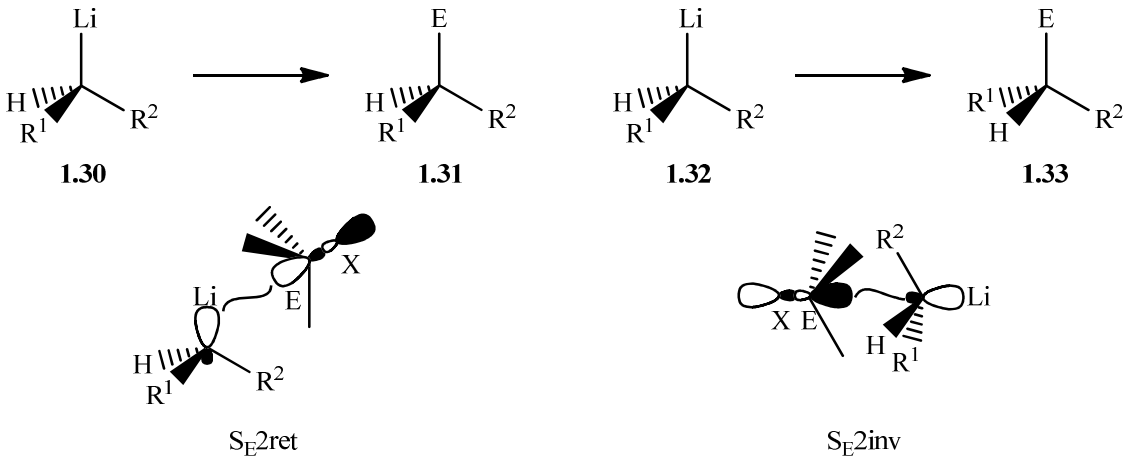

Scheme 1.9 - Possible reaction mechanisms of organolithiums with electrophiles

Sometimes the reaction follows a radical mechanism which results in a mixture of products that are formed by inversion and retention of configuration (stepwise single-electron transfer pathway) (Scheme 1.10).[8]

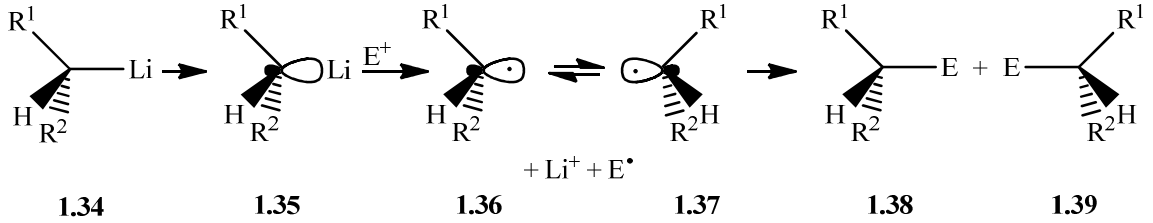

Scheme 1.10 - Stepwise single-electron transfer pathway

1.2.7 α-Oxyalkylllithiums

α-Oxyalkyllithiums are the most important group of functionalized organolithiums[4], but their formation is not easy. An oxygen atom deactivates the metalation of the adjacent carbon atom because the electron pair repulsion between oxygen's lone pair and the C-Li bond overcome the inductive effect of the oxygen atom.[13]

α-Silyloxyalkyllitiums are non-dipole stabilized organolithiums that undergo a retro-Brook rearrangement with retention of configuration and are thus synthetically useful[18] (Scheme 1.11).

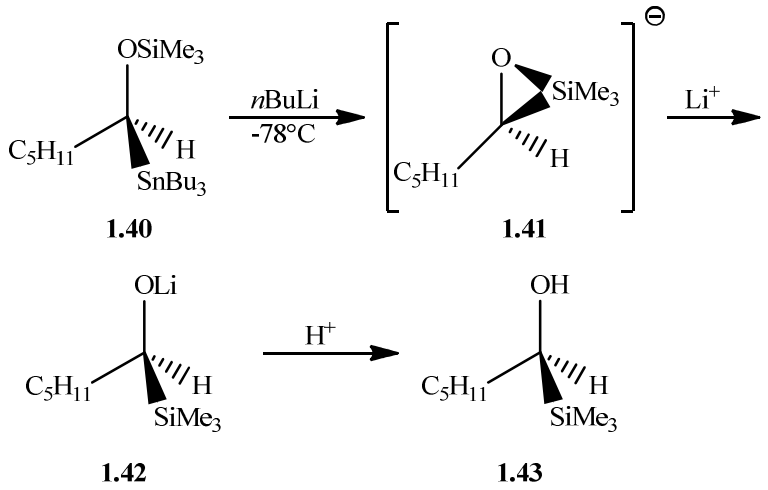

Scheme 1.11 - Retro-Brook rearrangement of an α-silyloxyalkyllitium

Dipole-stabilized organolithiums are considered to be one of the most configurationally stable organolithiums and their research has attracted a lot of attention. The majority of it has been spent on alcohols protected by carbamoyl groups like Cb, Cbx and Cby which activate the α-hydrogen atoms for removal by a strong base (Fugure 1.6).[16]

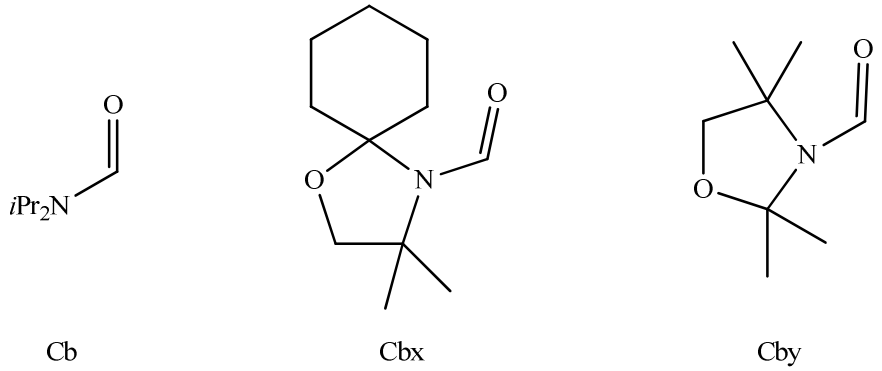

Figure 1.6 - Carbamoyl protecting groups for alcohols

There are a lot of examples of tertiary α-oxyorganolithiums with alkyl, heteroalkyl, vinyl and phenyl substituents that are stable over long periods in Et_2O in the absence of THF.[19]

1.2.8 α-Aminoalkyllithiums

α-Aminoalkyllithiums are less configurationally stable than the α-oxyalkyllithiums because the destabilizing effect of the lone pairs is bigger. In order to obtain the same results they require

lower temperature and absence of chelating agents.[20] The only exceptions to this rule are the lithiated *N*-methyl pyrrolidines and piperidines which can be stable up to -40˚C.[21]

Dipole-stabilized α-aminoalkyllithiums are synthetically useful and they have been used in asymmetric alkylations as chiral auxiliaries.[22] Most of the non-dipole-stabilized and the acyclic organolithiums racemize very quickly. Therefore they are not very interesting for asymmetric syntheses.[4]

1.2.9 α-Thioalkyllithiums

Non-dipole stabilized organolithiums derived from sulfides are usually only microscopically configurationally stable. This observation is useful for intramolecular rearrangements or reactions where the electrophile is already present when the α-thioalkyllithium is generated.[4]

Tertiary α-thioalkyllithium **1.44**, a dipole-stabilized one is the most stable α-thioalkyllithium so far known (Figure 1.7).[19]

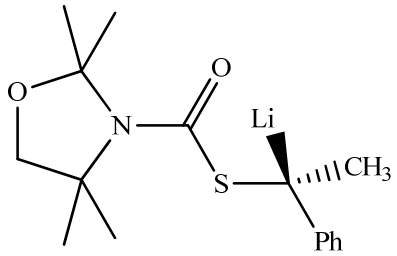

1.44

Figure 1.7 - Tertiary dipole-stabilized α-thioalkyllithium

Sulfoxides and sulfones can be macroscopically configurationally stable at low temperatures.[4]

1.2.10 α-Haloalkyllithiums

Most of these species are chemically very unstable. Therefore the determination of their configurational stability is a challenging task. Their stability is dependent on the number of halogen atoms that they contain and also on which halogen they contain. In case of bromoorganolithiums, the more bromine atoms the organolithium contains the more stable it is. In case of chloroorganolithium, the disubstituted species is more stable than the trisubstituted organolithium and the monosubstituted organolithium is the least stable of all three.[15]

1.3 Chiral heteroatom-substituted methyllithiums

The term chiral methyllithium corresponds to a methyllithium being chiral by virtue of two isotopes of hydrogen and a heteroatom[24] (Figure 1.8).

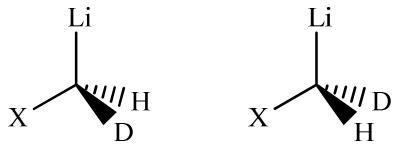

(*R*)-**1.45** (*S*)-**1.45**

X = heteroatom

Figure 1.8 - Chiral methyllithiums containing a heteroatom

1.3.1 Chiral Oxymethyllithium

Research of the Hammerschmidt group has showed that (diisopropyloxy)phosphinyl methyllithium derived from tributylstannylmethyl phosphate **1.46** is microscopically configurationally stable up to 0˚C and isomerizes through a phosphate-phosphonate rearrangement to α-hydroxymethylphosphonate **1.47** with retention of configuration[24] (Scheme 1.12).

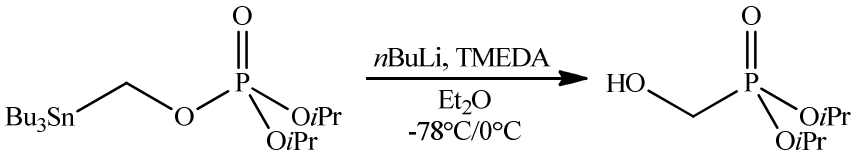

1.46 **1.47**

Scheme 1.12 - Phosphate-phosphonate rearrangement

All of the compounds in Figure 1.9 were found to be microscopically configurationally stable. Compounds **1.48**, **1.49** and **1.50** undergo a retro-Brook rearrangement and compound **1.51** isomerizes through a [2,3]-sigmatropic rearrangement to give a homoallylic alcohol.[24]

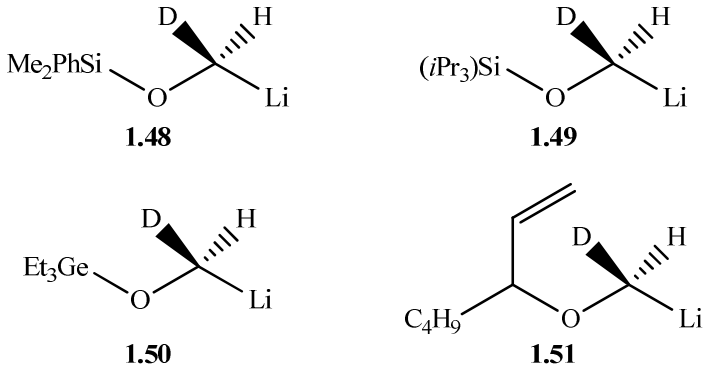

Figure 1.9 - Microscopically configurationally stable α-oxymethyllithiums

N,*N*-diisopropylcarbamoyloxymethyllithium, the intermediate in the reaction given in Scheme 1.13, is macroscopically configurationally stable at -78˚C in Et_2O/TMEDA for at least 10 min and in Et_2O and THF for 3 h but its chemical instability increases with increasing temperature.[24]

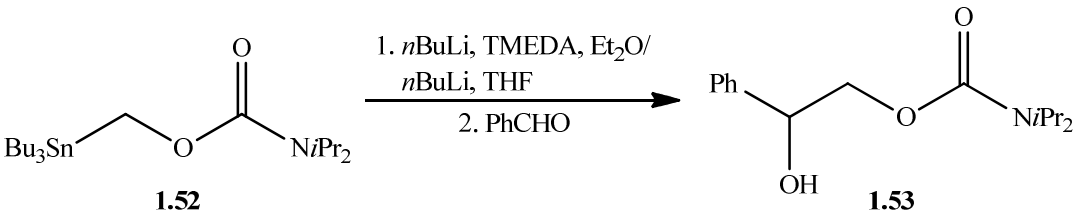

Scheme 1.13 - Test for the macroscopic configurational stability of *N*,*N*-diisopropylcarbamoyloxymethyllithium

The (2,4,6-triisopropropylbenzoyloxy)-[D_1]methyllithiums shown in Figure 1.10 are macroscopically configurationally stable, but less than the carbamoyloxy-[D_1]methyllithiums. The configurationally most stable α-oxymethyllithiums are the ethers **1.55** and **1.56**.

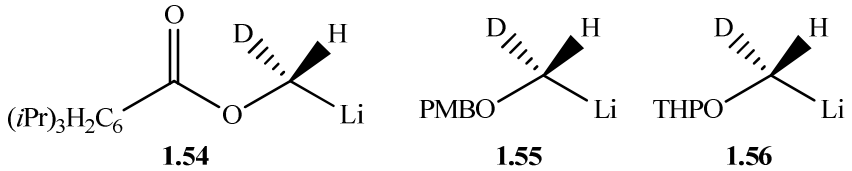

Figure 1.10 - Macroscopically configurationally stable α-oxymethyllithiums

1.3.2 Chiral Aminomethyllithium

Research of the Hammerschmidt group showed phosphoramidate **1.57** to be microscopically configurationally stable up to 0˚C for a rearrangement to the aminomethylphosphonate. The compounds **1.58** and **1.59** were found to be at least partially macroscopically configurationally

stable but less than their oxygen analogues. **1.58** was the least stable of the two, giving enantiomeric excess of 65% at -95˚C after aging for 30 s while the enantiomeric excess of **1.59** was 90% at the same temperature after aging for 15 min (Figure 1.11).[15]

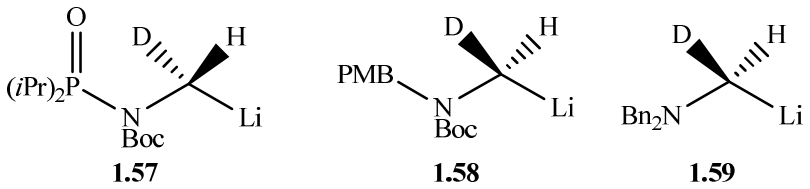

1.57 **1.58** **1.59**

Figure 1.11 - Microscopically and macroscopically configurationally stable α-aminomethyllithiums

1.3.3 Chiral Chloromethyllithium

Kapeller found that chloromethyllithium **1.60** is macroscopically configurationally stable up to 30 s at -78˚C in THF but chemically very labile (Figure 1.12).[23]

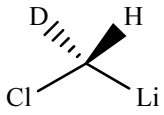

1.60

Figure 1.12 - Chiral chloromethyllithium

1.3.4 Fluoromethyllithium

Some research on the configurational stability of fluoromethyllithium was already carried out by Kapeller. Many calculations for the (configurational) stability have been performed for it, but it has never been prepared. In a recent review[25] it has been stated, that fluoromethyllithium cannot be analyzed spectroscopically because of its chemical instability. Chiral fluoromethyllithium is the smallest chiral organometallic compound possible, allowing only stable isotopes as substituents (Figure 1.13).

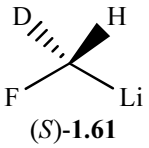

(*S*)-**1.61**

Figure 1.13 - (*R*)-fluoro[D_1]methyllithium

Kapeller accessed chiral tributyl(fluoro-[D_1]methyl)stannane from the respective stannylmethanol and DAST.[15] The enantiomeric excess could not be determined, because it was assumed that fluoride cannot be substituted by a sulfur-containing homochiral derivatizing reagent to generate diastereomers for the evaluation of the enantiomeric excess by ^{1}H NMR spectroscopy. She found that chiral fluoromethyllthium can be formed from fluoromethylstannane by tin-lithium exchange with MeLi at -78 °C and intercepted by benzaldehyde already present in the reaction mixture (Scheme 1.14).

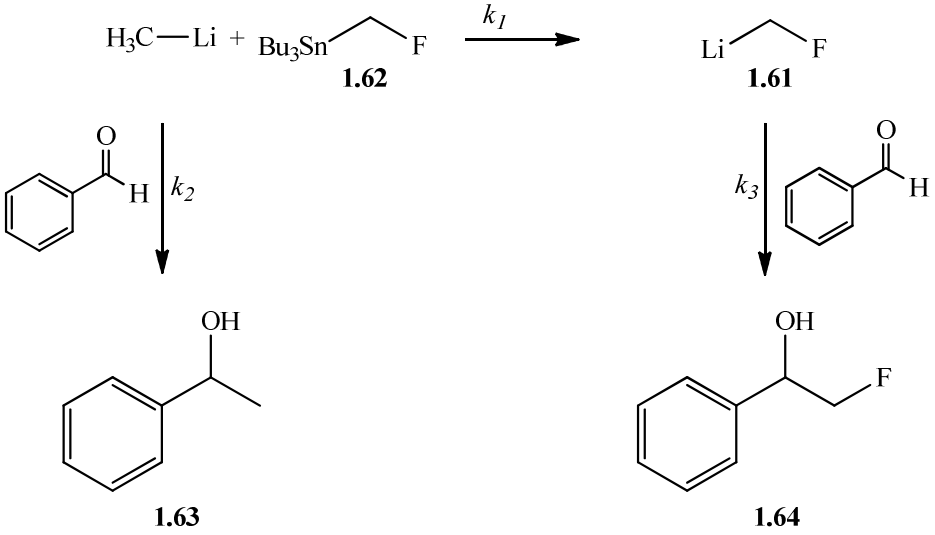

Scheme 1.14 - Test of the microscopic configurational stability of fluoromethyllithium done by Kapeller

It was found that chiral fluoromethyllithium is microscopically configurationally stable, but chemically less stable than chloromethyllithium. Furthermore, transmetalation was also significantly slower than with chloromethylstannane and a large amount of 1-phenylethanol was formed as side product. Therefore, in all experiments performed with various ligands the yield of 2-fluoro-1-phenylethanol (**1.64**) was 43% at best. However, 50% or more of the fluoromethyllithium which was generated decomposed very likely by elimination of LiF. When Kapeller tried to determine the macroscopic configurational stability of chiral fluoromethyllithium, the yield dropped to only 25% at best. The amount of starting material in

the crude product increased and losses due to decomposition increased as well, even if benzaldehyde was added shortly (10 or 30 sec) after the addition of MeLi for transmetalation, and decreasing the temperature to -100 °C.

The reaction rate k_2 of the addition of MeLi to benzaldehyde was greater than the rate k_1 of transmetalation. Therefore not much of the fluoromethyllithium was formed. To get around this problem, I replaced benzaldehyde by acetophenone as an electrophile, because it is less reactive than benzaldehyde. The reaction rate k_2 should get smaller while k_1 remains the same. Before doing any experiment in the labeled series, preliminary experiments were performed in the unlabeled series (Scheme 1.15).

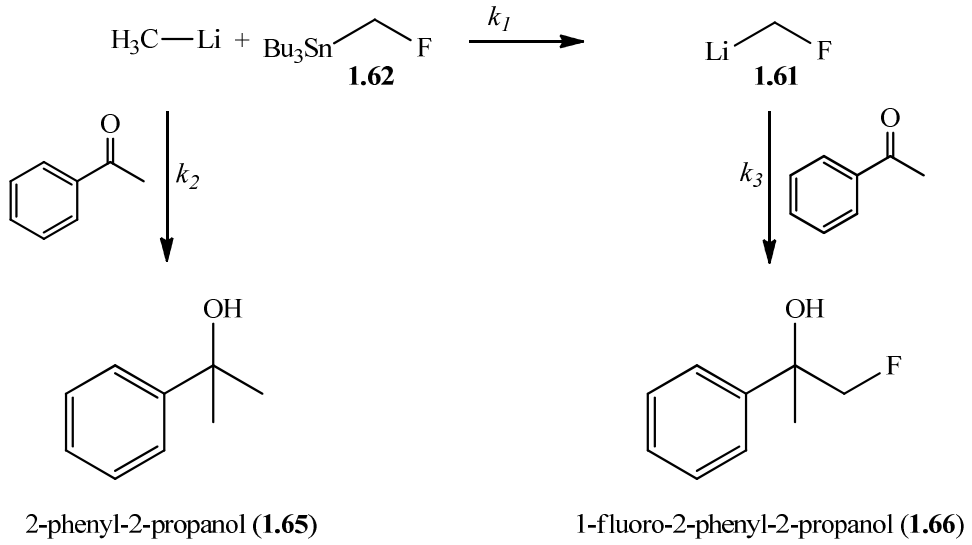

Scheme 1.15 - Preliminary experiments with the unlabeled fluoromethyllithium

The fluoromethylstannane was prepared in 66% yield according to the method developed by Kapeller (Scheme 1.16).[15]

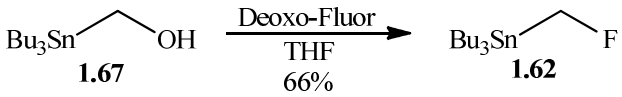

Scheme 1.16 - Preliminary experiments of fluoromethylstannane **1.62**

To test whether fluoromethylstannane does or does not react with the lithium salt of (*R*)-1-(2-naphthyl)ethylthiol, the reaction in Scheme 1.17 was carried out. Surprisingly, fluoride was replaced by the thiol (S_N2 reaction) to give sulfide (*R*)-**1.69** which can be used in the labeled

series to determine the enantiomeric excess. However, the reaction rate of fluoromethylstannane was much slower than that of chlormethylstannane (18 h, 2.5 h respectively).

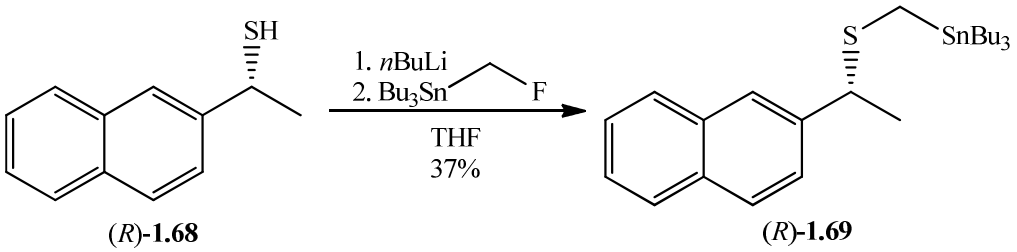

(*R*)-**1.68** (*R*)-**1.69**

Scheme 1.17 - Alkylation of (*R*)-1-(2-naphthyl)ethylthiol with fluoromethyllithium

The first preliminary experiment to evaluate acetophenone as electrophile for the determination of the microscopic configurational stability of chiral fluoromethyllithium was performed at -95˚C. Fluoromethylstannane (1 equiv.) and acetophenone (2 equiv.) in dry THF were used and MeLi (2 equiv., 1M, in THF/diethoxymethane, prepared from 3M in diethoxymethane by dilution with dry THF) was added drop wise (one drop every 5 s). After the addition of the last drop of MeLi, stirring was continued for 5 min before work up (addition of 2M CF_3CO_2H in CH_2Cl_2). The crude product was a mixture of the starting material [tributyl(fluoromethyl)stannane, (**1.62**)], the desired product [1-fluoro-2-phenyl-2-propanol (**1.66**)], the product of addition of MeLi to acetophenone [2-phenyl-2-propanol (**1.65**)], and tributylmethylstannane (used as internal standard in the ^{1}H NMR spectrum) in a molar ratio of 1.16:1.03:1.09:1.00, respectively. Flash chromatography furnished an inseparable mixture (82%, containing a small amount of an impurity) of racemic 1-fluoro-2-phenyl-2-propanol and 2-phenyl-2-propanol in a molar ratio of 1.00:0.80, respectively. When the experiment was repeated at -78˚C, the ratio of compounds in the crude product changed to 2.56:1.13:2.39:1.00. The diastereomeric (*R*)-Mosher esters of the tertiary **1.65** and racemic alcohol 1-fluoro-2-phenyl-2-propanol (**1.66**) were prepared as well, to see whether it could be derivatized to determine the enantiomeric excess in the labeled series (Scheme 1.18).

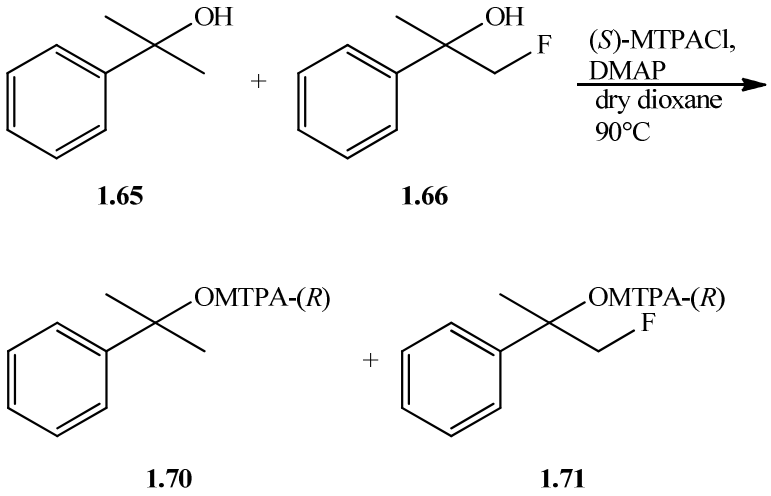

Scheme 1.18 - Derivatization of the mixture of tertiary alcohols with (*S*)-MTPACl

The esterification had to be performed under forcing conditions (DMAP, 50 °C, 9 h) The combined yield of the diastereomeric esters **1.71** was 44% and their ratio was 3.00:1.88, caused by kinetic resolution. The ^{1}H NMR spectrum displayed two AB systems (coupling with fluorine) for the CH_2F groups (Figure 1.14).

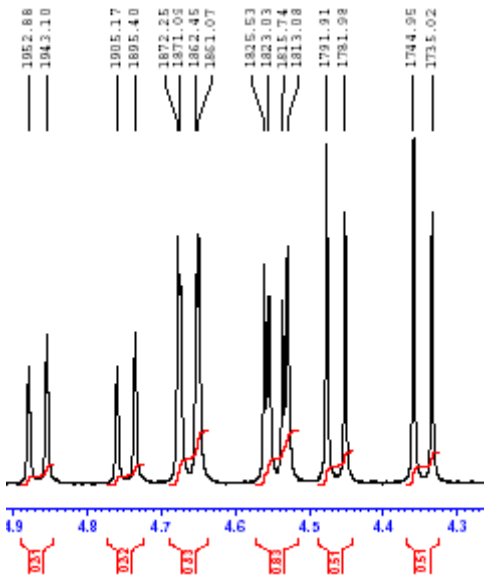

Figure 1.14 - Partially overlapping AB-systems of the CH_2F groups in the ^{1}H NMR spectrum (400.27 MHz, $CDCl_3$) of **1.71**

These two experiments show that the fluoromethyllithium is long-lived enough to be intercepted by acetophenone instead of benzaldehyde. For the generated tributyl(methyl)stannane an equivalent amount of FCH_2Li was formed and added to acetophenone. Chemical instability of

FCH_2Li does not seem to account for losses of product, contrary to the results of Kapeller. I would have expected decomposition to a larger extent. As the rate for the addition of fluoromethyllithium to acetophenone should be slower than that for the addition to benzaldehyde, the increased half-life should increase decomposition. Furthermore, still only about one half of the starting material was consumed at -95 °C (about 30% at -78 °C). Consequently, an even more hindered ketone than acetophenone has to be used as electrophile to secure full conversion of starting material by transmetalation. It is possible that at temperatures lower than -95 °C even the macroscopic configurational stability of fluoromethyllithium can be addressed. More experiments in the labeled and unlabeled series are necessary to clarify the open questions.

2 Stille Reaction

The Stille reaction is a cross-coupling reaction between organostannanes and halides in presence of a Pd^0 catalyst with various ligands on it (Scheme 2.1).[7]

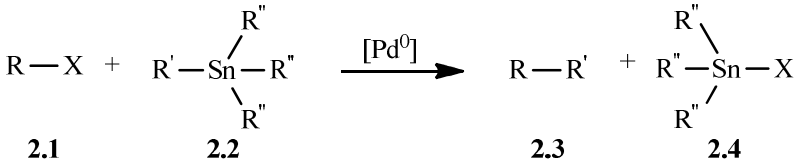

Scheme 2.1 - Stille coupling with a halide and an organostannane

It is very popular because organostannanes are relatively stable and readily available with many functional groups.[26] The first successful experiments were published in 1976 by Eaborn[27, 28] but Stille and his group[29] made it to a standard method that is widely used today. Stille reaction is a very versatile method of coupling that can be done under relatively mild conditions.[30]

The coupling is influenced by the ligands on palladium, the solvent, the additives and by the substrates themselves. Various groups can be transferred from the tin with different effectiveness (Figure 2.1).[31]

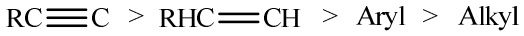

Figure 2.1 - Order of decreasing effectiveness of the group transfer

The reaction consists of 3 steps that can all be rate-determining and depend on the reaction conditions and substrates (Figure 2.2).[7]

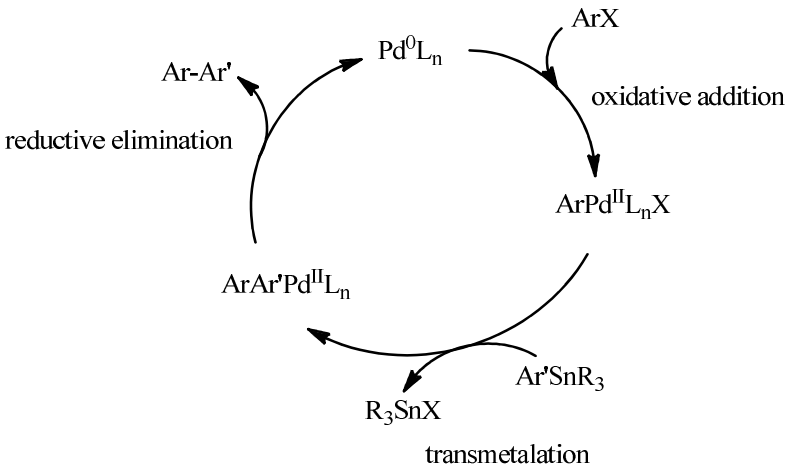

Figure 2.2 - Catalytic cycle of the Stille coupling

The first step is the oxidative addition of the electrophile (halides in my case) to a Pd^0 complex. At first, a cis complex **2.8** is formed which isomerizes to a more stable and thermodynamically favored trans complex (phosphane ligand and R group are trans)[26] unless there is a destabilizing interaction between the ligands, transphobia (Scheme 2.2).[32]

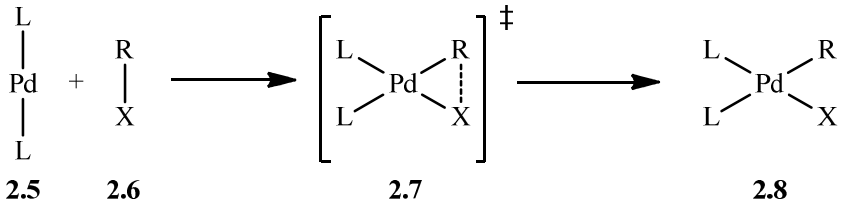

Scheme 2.2 - Cis complex formed during the oxidative addition of the electrophile

If anionic ligands (halides, acetate) are present in the reaction mixture, the electrophile does not add to the neutral Pd complex, but to an anionic one of structure $[Pd^0XL_2]^-$.[33] The oxidative addition goes then through a five-coordinated intermediate **2.10** (Scheme 2.3).[34]

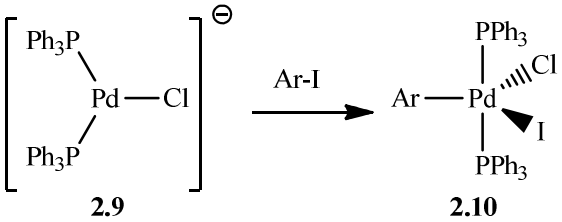

Scheme 2.3 - Five-coordinate intermediated formed from an anionic complex

The second step in the Stille coupling is the transmetalation. Its mechanism is influenced by the polarity of the nucleophile (low in case of alkyl organotin reagents).[26] The process is a ligand substitution on the Pd^{II} complex[35] that can go through two pathways[26, 36, 37]: associative through an 18-electron trigonal bipyramidal complex **2.12** and **2.13** and dissociative through a 14-electron T-shaped intermediate **2.14**. The substitution takes place trans to the ligand with the greatest trans effect (Scheme 2.4).

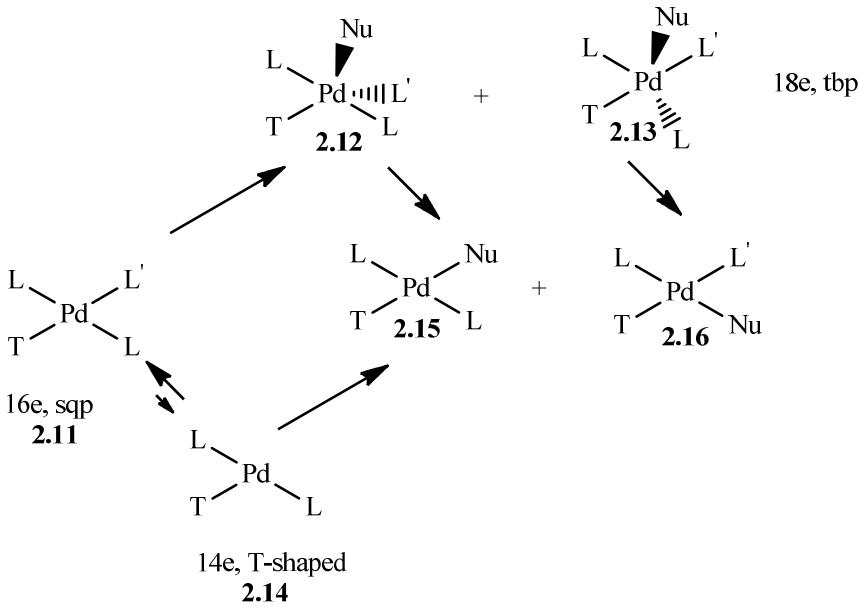

Scheme 2.4 - Associative and dissociative pathway for the ligand substitution

It seems more likely that most of the substitutions go through the associative pathway either through direct substitution or through solvent-assisted substitution (Scheme 2.5).[26] The reason is that it is unlikely that this unsaturated 14-electron species could have a long lifetime in a condensed state.[35]

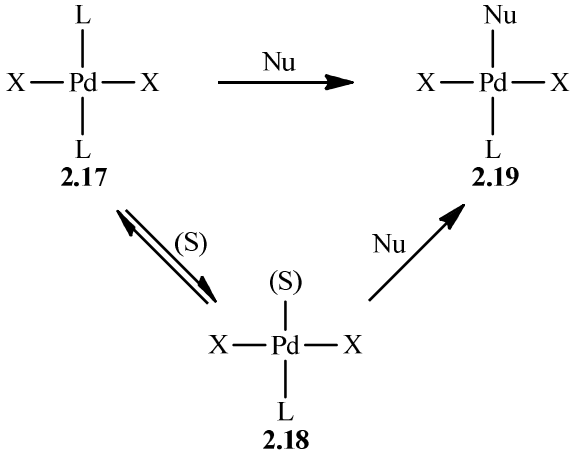

Scheme 2.5 - Two substitution mechanisms for the associative pathway where (S) stands for solvent

Transmetalation can follow a retentive or invertive course. Due to this fact, two different mechanisms, containing an acyclic transition state **2.20** (proceeds through inversion) or a cyclic transition state **2.21** (proceeds through retention), have been proposed by Espinet and Casado (Figure 2.3).[38, 39]

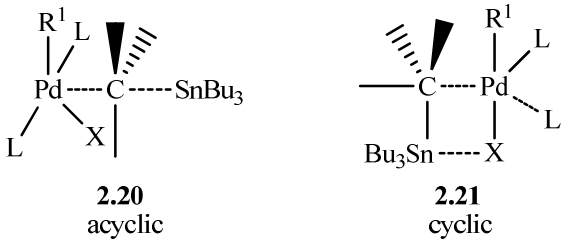

Figure 2.3 - Acyclic and cyclic transition states for transmetalation

The third and last step is the reductive elimination. The simplest mechanism occurs directly from the cis derivative without ligand dissociation or association - unassisted mechanism. Another mechanism is more difficult because the cis complex loses one ligand which makes the alkane elimination very favorable - dissociative mechanism (Scheme 2.6).[40]

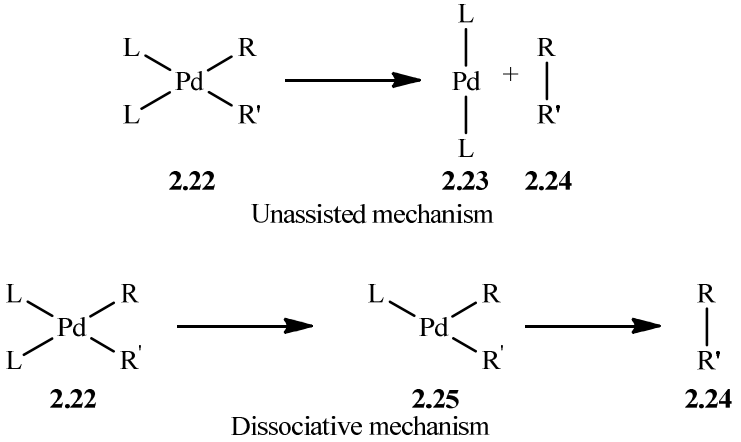

Scheme 2.6 - Two possible mechanisms for the reductive elimination

After everything has been put together, the following mechanism should represent the entire catalytic cycle of the Stille coupling (Scheme 2.7).[38]

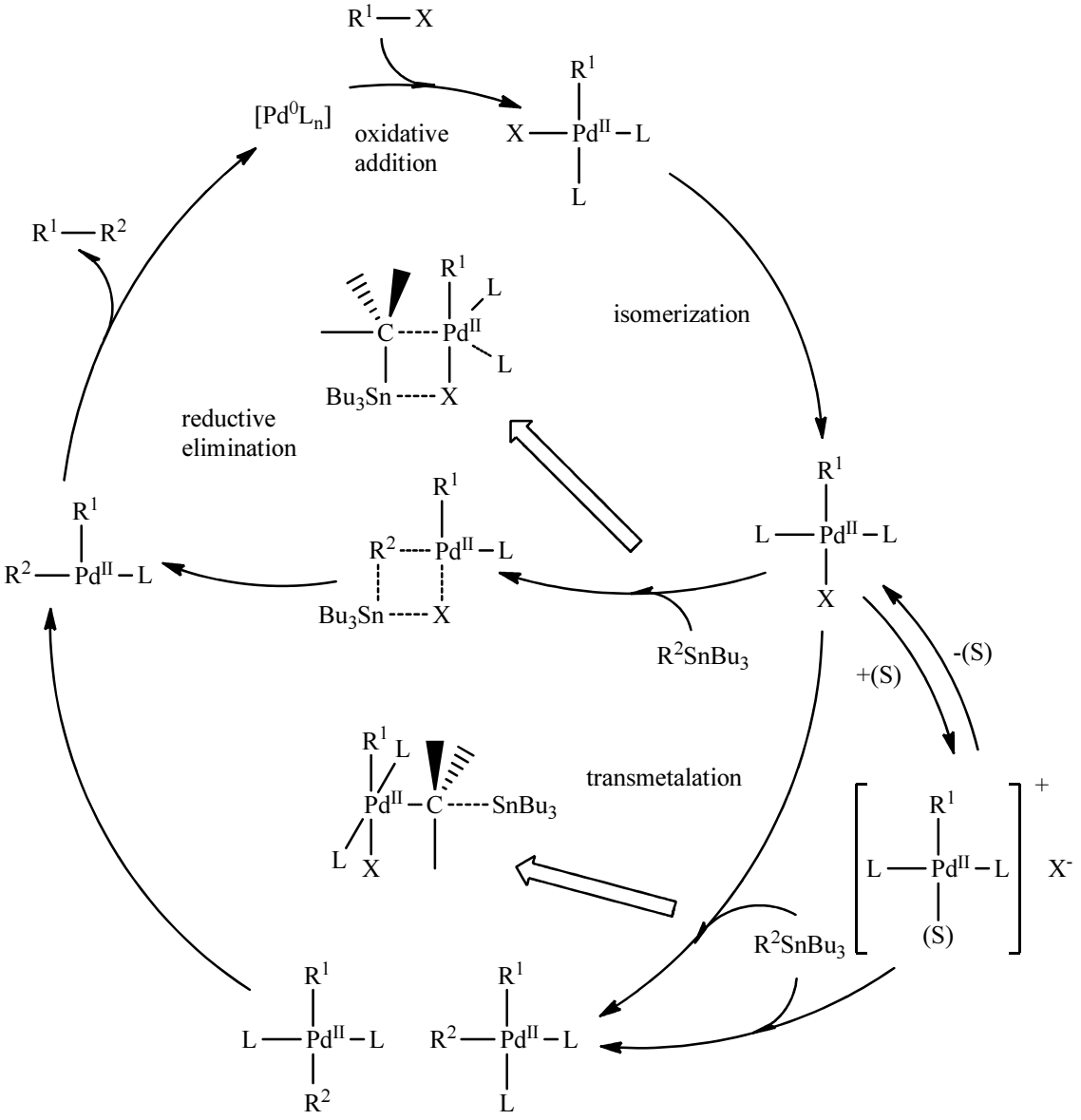

Scheme 2.7 - The entire catalytic cycle for the Stille coupling

There are a few ways how to accelerate the couplings or force unreactive species to react. One way is to add Cu^{I} salts like CuCN to $[PdL_4]$ catalysts.[41] The "copper effect" consists of two different mechanisms that are both dependent on the ligands and the solvent. If there is a "hard" ligand such as PPh_3 on palladium then Cu^{I} can act as its scavenger when it is released so that it cannot inhibit the transmetalation any more (Scheme 2.8).[42]

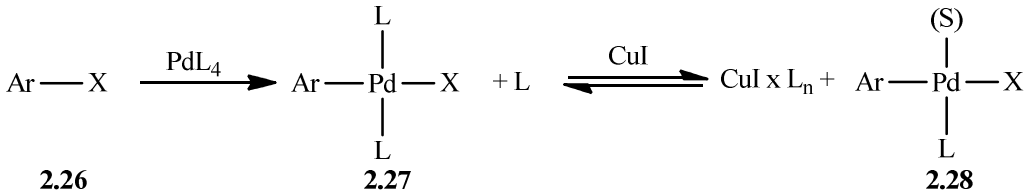

2.26 **2.27** **2.28**

Scheme 2.8 - Copper acting as a scavenger for a "hard" ligand

In a donor solvent like dioxane, transmetalation between Sn and Cu can occur at least partially (Scheme 2.9). This step has a potential to affect the group transfer selectivity.[42]

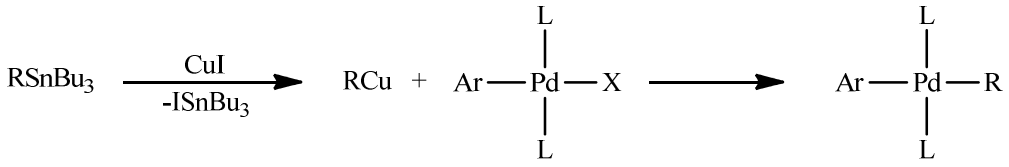

2.29 **2.27** **2.30**

Scheme 2.9 - Transmetalation between tin and copper

Another way to activate the organostannane is to use a fluoride like CsF as an additive. It is postulated that a pentacoordinated tin species containing fluoride as ligand forms. This species is more reactive towards transmetalation.[26, 43]

2.1 Configurational stability of chiral methylpalladium complexes formed during the Stille coupling

Chiral methyllithiums cover a wide range of configurational stabilities, depending mainly on its heteroatom-substituent and the reaction temperature. They add to aldehydes and ketones to give alcohols. To expand the scope of the reactions with chiral methylmetals, Stille couplings were performed with various stannanes as precursors. As these reactions are normally done at temperatures between room temperature and 100 °C, the configurational stability of the intermediate chiral methylpalladium complexes is of critical importance. Before doing a reaction with the chirally labeled methylpalladium species, it was tested first with the unlabeled compound.

2.1.1 Stille coupling with tributylstannylmethanol - microscopic configurational stability of chiral hydroxymethylpalladium complexes

First, I wanted to examine the microscopic configurational stability of hydroxymethylpalladium complexes **2.31** that form during the direct transformation of bromobenzene and tributylstannylmethanol using the Stille coupling (Figure 2.4).

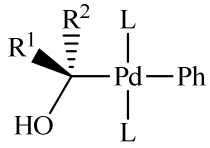

2.31: $R^1 = R^2 = H$
(*R*)-[D_1]**2.31**: $R^1 = D$, $R^2 = H$

Figure 2.4 - Hydroxymethylpalladium complexes

It was not necessary to derivatize tributylstannylmethanol, a well known precursor in our group,[15] because it was used for the coupling. As this Stille reaction with tributylstannylmethanol has already been performed by Japanese researchers in 1985, I could simply repeat these experiments with tributylstannylmethanol and (*S*)-tributylstannyl-[D_1]methanol at 80 °C for 18 h.[44] The low yield was of no major concern in the first place (Scheme 2.10).

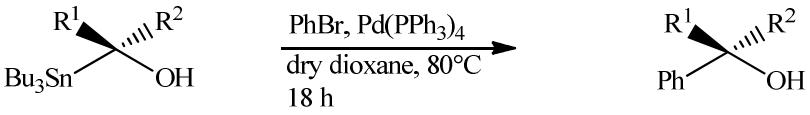

1.67: $R^1 = R^2 = H$
(*S*)-[D_1]**1.67**: $R^1 = D$, $R^2 = H$

2.32: $R^1 = R^2 = H$, 57%
(*R*)-[D_1]**2.32**: $R^1 = D$, $R^2 = H$, 38%

Scheme 2.10 - Stille coupling with unlabeled and labeled tributylstannylmethanol and bromobenzene

The only necessary step after the coupling was esterification of the labeled phenylmethanol **2.32** with (*S*)-MTPACl to determine its configuration and enantiomeric excess (Scheme 2.11).

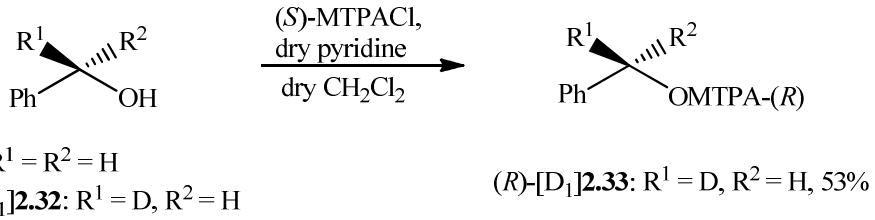

2.32: $R^1 = R^2 = H$
(*R*)-[D_1]**2.32**: $R^1 = D$, $R^2 = H$

(*R*)-[D_1]**2.33**: $R^1 = D$, $R^2 = H$, 53%

Scheme 2.11 - Esterification of labeled phenylmethanol with (*S*)-MTPACl

The ^{1}H NMR spectra of the (*R*)-Moser esters of (*R*)- and (*S*)- phenyl-[D_1]methanol were recorded some time ago so they were used as reference spectra. The segment of the ^{1}H NMR spectrum displaying the CHD group shows that the phenyl-[D_1]methanol derived from (*S*)-tributylstannyl-[D_1]methanol is (*R*)-configured and has an enantiomeric excess of 99% (Figure 2.5).

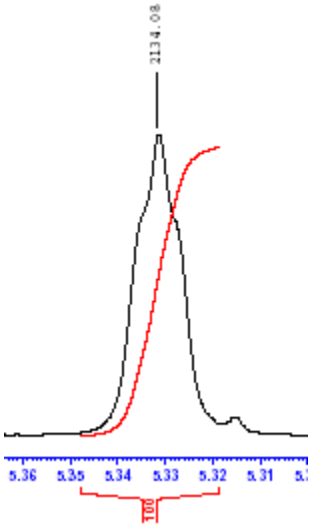

Figure 2.5 - Signal of CHD group of (*R*)-phenyl-[D_1]methanol from ^{1}H NMR spectrum

Therefore, the Stille coupling proceeds with net retention of configuration. Consequently, transmetalation and reductive elimination have to proceed either by retention or inversion. As the enantiomeric excess of the phenyl-[D_1]methanol underlaying the (*R*)-Mosher ester was greater than 99%, the various palladium complexes formed during the Stille coupling are microscopically configurationally stable until reductive elimination of the product.

2.1.2 Stille coupling with tributylstannylmethyl benzoate – microscopic configurational stability of chiral benzoyloxymethylpalladium complexes

In this part of my practical work I wanted to examine the microscopic configurational stability of palladium complexes **2.34** derived from (*R*)- or (*S*)-1-tributylstannyl[D_1]methyl benzoate and benzoyl chloride during the Stille coupling (Figure 2.6).

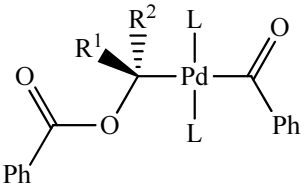

(*R*)-[D_1]**2.34**: R^1 = H, R^2 = D
(*S*)-[D_1]**2.34**: R^1 = D, R^2 = H

Figure 2.6 - Chiral methylpalladium complexes formed during the Stille coupling

I first performed all of the reactions with the unlabeled species to determine whether they could be done in reasonable yields and to see if it was possible to spectroscopically determine the configuration of the product and its enantiomeric excess.
In order to do the coupling I had to prepare the precursor **2.35** by a simple esterification of tributylstannylmethanol (**1.67**) with benzoyl chloride (Scheme 2.12).

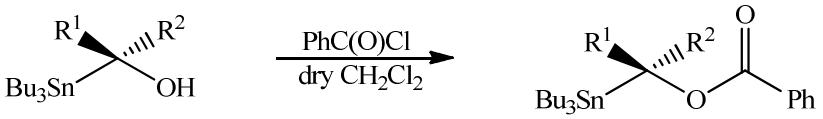

1.67: $R^1 = R^2$ = H
(*R*)-[D_1]**1.67**: R^1 = H, R^2 = D
(*S*)-[D_1]**1.67**: R^1 = D, R^2 = H

2.35: $R^1 = R^2$ = H, 84 %
(*R*)-[D_1]**2.35**: R^1 = H, R^2 = D, 82%
(*S*)-[D_1]**2.35**: R^1 = D, R^2 = H, 90 %

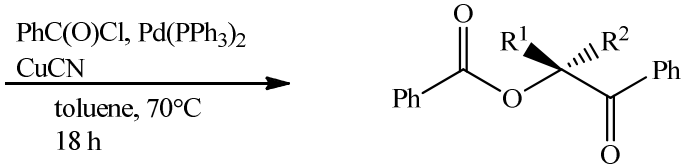

2.36: $R^1 = R^2$ = H, 67%
(*S*)-[D_1]**2.36**: R^1 = D, R^2 = H, 53%
(*R*)-[D_1]**2.36**: R^1 = H, R^2 = D, 94%

Scheme 2.12 - Preparation of the precursors and the Stille couplings

For the coupling I used the procedure reported by Stille et al. for the coupling of α-tributylstannylalkyl benzoates with benzoyl chloride.[41]

Since it was impossible to spectroscopically determine the enantiomeric excess of the product of this reaction directly, two further transformations were necessary (Scheme 2.13).

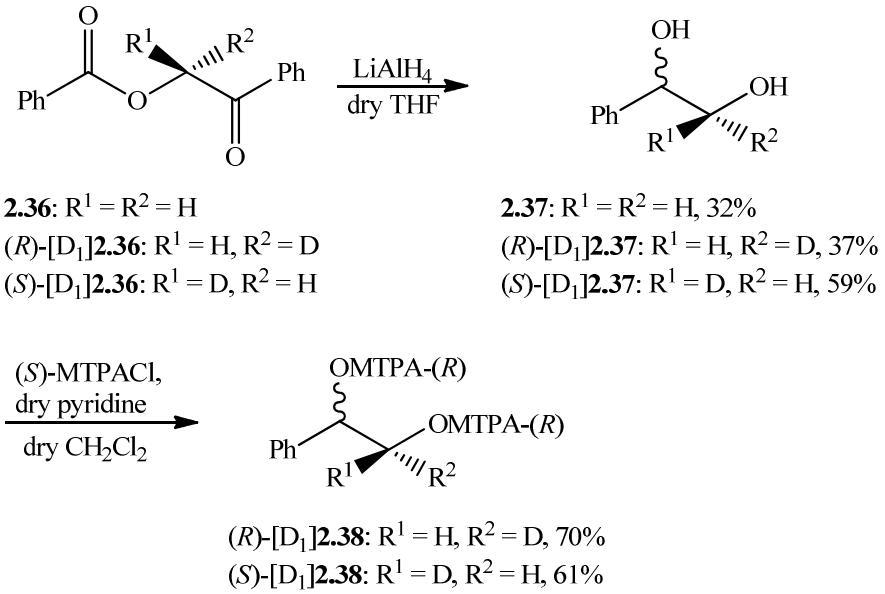

2.36: $R^1 = R^2 = H$

(*R*)-[D_1]**2.36**: $R^1 = H$, $R^2 = D$

(*S*)-[D_1]**2.36**: $R^1 = D$, $R^2 = H$

2.37: $R^1 = R^2 = H$, 32%

(*R*)-[D_1]**2.37**: $R^1 = H$, $R^2 = D$, 37%

(*S*)-[D_1]**2.37**: $R^1 = D$, $R^2 = H$, 59%

(*R*)-[D_1]**2.38**: $R^1 = H$, $R^2 = D$, 70%

(*S*)-[D_1]**2.38**: $R^1 = D$, $R^2 = H$, 61%

Scheme 2.13 - Derivatization of the product of the Stille coupling

The resulting benzoates **2.36** were reduced with $LiALH_4$ to give a mixture of a racemic diol **2.37** in the unlabeled series and a mixture of diastereomeric diols in the labeled series beside phenylmethanol derived from the benzoyl group. The configuration of the labeled carbon atom did not change. The last step was the esterification of the diols with (*S*)-MTPACl to give two diastereomeric (*R*)-Mosher esters **2.38**, which was only done with the labeled species because reference spectra of the unlabeled esters were known.

The ^1H NMR spectra were compared to the reference spectra recorded by Kapeller to determine the absolute configuration and the enantiomeric excess at the labeled carbon atom of the ester. Since all of the steps before and after the coupling followed a retentive course, I proved that the coupling proceeded with net retention of configuration. This means that the transmetalation and reductive elimination both go through either retention or inversion, but the retentive mechanism is the more feasible one. It was further proven that the palladium complexes **2.34** derived from (*R*)- or (*S*)-tributylstannyl-[D_1]methyl benzoate and benzoyl chloride are microscopically configurationally stable during the Stille coupling at 70 °C, because the enantiomeric excess of the labeled carbon atom in each case was equal to or greater than 99% (Figure 2.7).

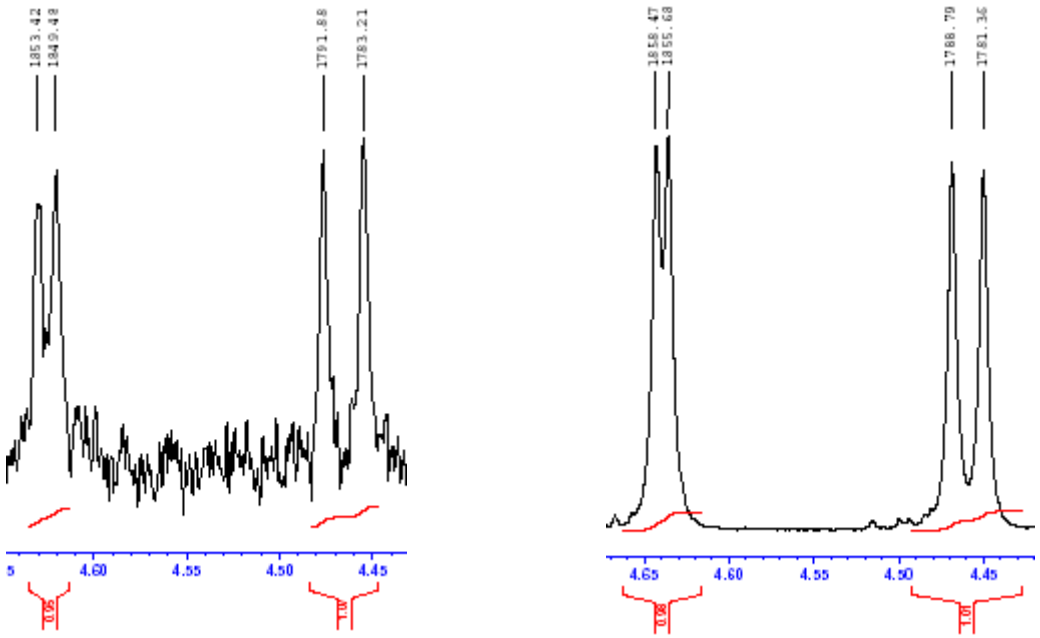

(R) (*S*)

Figure 2.7 - Signals of CHD groups of the (*R*)-Mosher esters of labeled diols **2.37** in ^{1}H NMR spectra (400.27 MHz, $CDCl_3$)

Furthermore, the Stille coupling has to go through a closed transition state **2.39** here to account for net retention of configuration for the coupling step (Figure 2.8).

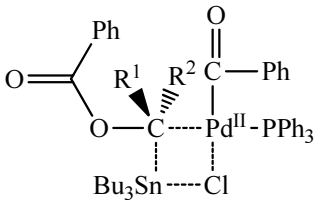

2.39: $R^1 = R^2 = H$
(*R*)-[D_1]**2.39**: $R^1 = D$, $R^2 = H$
(*S*)-[D_1]**2.39**: $R^1 = H$, $R^2 = D$

Figure 2.8 - Closed transition state of the Stille coupling

2.1.3 Stille coupling with (benzylthiomethyl)tributylstannane and (*S*)-tributylstannylmethyl thioacetate - Microscopic configurational stability of chiral thiomethylpalladium complexes

The biggest challenge of my practical work turned out to be the preparation and determination of the configurational stability of various palladium complexes containing sulfur (Figure 2.9).

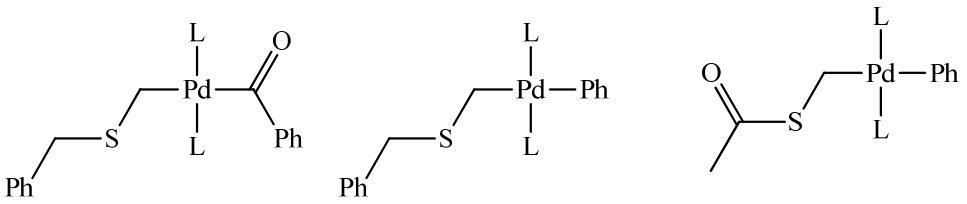

Figure 2.9 - Palladium complexes that were studied

In principle, everything was supposed to work great and the steps that had to be performed after the coupling in order to determine the enantiomeric excess were well established. Preliminary experiments for the determination of the enantiomeric excess of the labeled α-benzylthio-acetophenone were performed with the unlabeled compound **2.42a** accessed from phenylmethanthiol and α-bromoacetophenone by a literature procedure.[45] Reduction with $LiAlH_4$ in dry THF furnished the desired alcohol **2.43** in 96% yield. Esterification with (*S*)-MTPACl was not performed but was expected to furnish a mixture of diastereomeric Mosher esters **2.44** (Scheme 2.14).

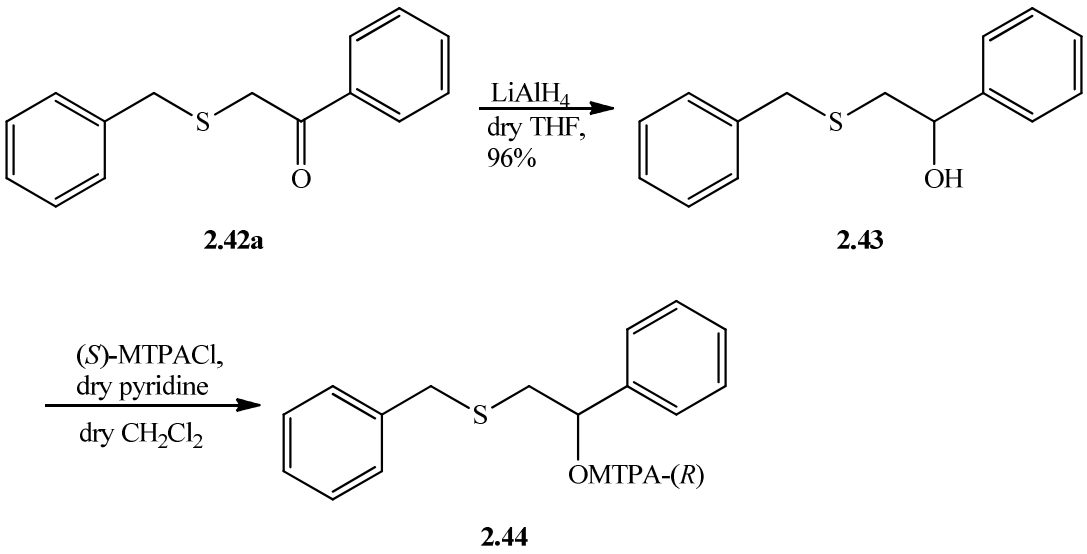

Scheme 2.14 - Derivatization of the ketone **2.42a** obtained from the Stille coupling

The problems turned up when I tried to do the Stille coupling of the unlabeled (benzylthiomethyl)tributylstannane (**2.45a**) and later with the labeled species, because I ran out of the unlabeled material, with benzoyl chloride or bromobenzene. Finally, the benzyl group in the stannane was replaced by an acetyl group as protecting group (Scheme 2.15).

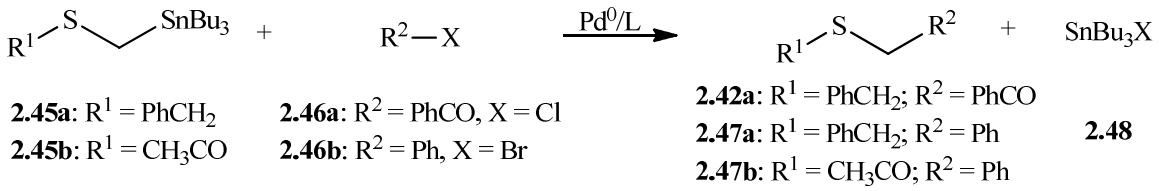

2.45a: $R^1 = PhCH_2$ **2.46a**: $R^2 = PhCO$, X = Cl **2.42a**: $R^1 = PhCH_2$; $R^2 = PhCO$
2.45b: $R^1 = CH_3CO$ **2.46b**: $R^2 = Ph$, X = Br **2.47a**: $R^1 = PhCH_2$; $R^2 = Ph$ **2.48**
2.47b: $R^1 = CH_3CO$; $R^2 = Ph$

Scheme 2.15 - Stille coupling of the benzoyl chloride or bromobenzene and the stannane

I tried various solvents, Pd catalysts and ligands, known from the literature.[41, 44, 46, 47] However, none of them were tried on compounds containing sulfur in the α-position to the carbon that was to be coupled (Table 2.1).

Entry	R^1 in 2.45	R^2 in 2.46	Catalyst	Conditions	Yield
1	**a**	**a**	$Pd(PPh_3)_2Cl_2$ (5 mol %), CuCN (10 mol %)	Toluene, 75˚C, 24 h[41]	product gone
2			$Pd(PPh_3)_2Cl_2$ (5 mol %), CuCN (10 mol %)	Toluene, RT→40→75˚C, 2→2→3 h[41]	n.r.*
3		**b**	$Pd(PPh_3)_4$ (5 mol %)	Dioxane, 80˚C, 18 h[44]	n.r.*
4			$Pd(PPh_3)_2Cl_2$ (5 mol %)	HMPA, 80˚C, 18 h[47]	n.r.*
5			$Pd(P(tBu)_3)_2$ (3 mol %), CsF (2.2 eq)	Dioxane, 90˚C, 25 h[46]	wrong product
6	**a**[a]	**b**	$Pd(P(tBu)_3)_2$ (3 mol %)	Dioxane, 40→70→100˚C, 3→4→18 h[46]	n.r.*
7	**b**	**b**	$Pd(PPh_3)_4$ (5 mol %)	Dioxane, RT→80→100˚C, 2→22→3 h[44]	n.r.*
8			$Pd(P(tBu)_3)_2$ (3 mol %)	Dioxane, RT→50→100˚C, 4→3→18 h[46]	n.r.*

* no reaction, [a](*S*)-[D_1]**2.45a**

Table 2.1 - Overview of all of the experiments performed according to Scheme 2.15 and their results

As can be seen from the table the desired product never formed. Only in the first experiment (Entry 1) was the starting material consumed, but no coupling product could be detected. It seemed that the product was formed, but underwent self-condensation under these reaction conditions. Therefore, the Stille coupling was repeated starting from room temperature (Entry 2). The progress of the reaction was monitored by TLC and reference sample **2.42a** was also applied to the plate. Unfortunately, no coupling product formed and the starting material did not disappear at all this time even though the temperature was raised to the same temperature as in the previous experiment.

At that point it was decided to try the coupling with bromobenzene using different catalysts to see if this would result in the desired product **2.47a**. The reference sample was prepared according to literature (Scheme 2.16).[48]

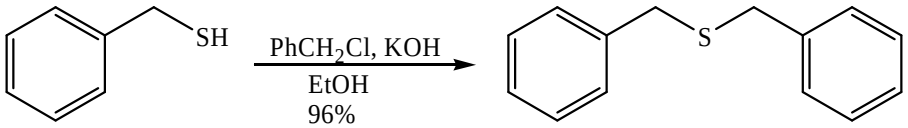

2.49 **2.47a**

Scheme 2.16 - Preparation of the product of the Stille coupling by an independent method

The conditions that I tried next – addition of excess CsF (Entry 5) - were very promising as they were successfully used on many unreactive organotin reagents and aryl halides. This time, a product was formed that on first sight looked great, but integration in the ^{1}H NMR spectrum showed, that it was not the desired disulfide **2.47a**, but one which was evidently formed by a sulfur-carbon coupling (Figure 2.16).

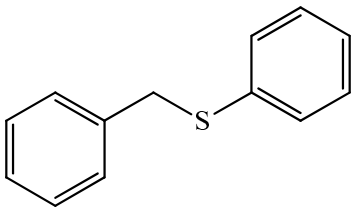

2.50

Figure 2.16 - Product of sulfur-carbon coupling

It is possible that the fluoride additive caused the formation of a phenylmethylthiol which got coupled with the bromobenzene so I tried the reaction once more time without CsF but unfortunately this did not result in the desired product either (Entry 6).

I decided to give the Stille coupling with a thiomethylstannane two last tries with an acetyl protecting group on the sulfur atom. The precursor was made from tributylstannylmethanol and thioacetic acid by a Mitsunobu reaction (Scheme 2.17)[49].

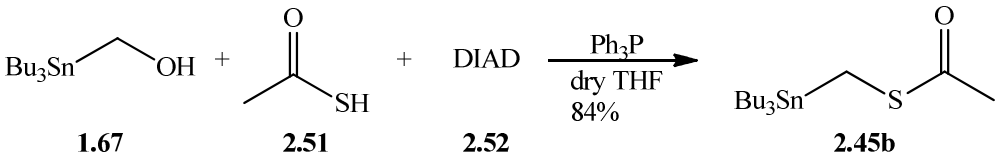

1.67 **2.51** **2.52** **2.45b**

Scheme 2.17 - Preparation of the thioacetate **2.45b**

However, even this precursor was not to be coupled with bromobenzene. It was not reactive enough to be consumed.

2.1.4 Stille coupling with *N*-protected tributylstannylmethylamines – Microscopic configurational stability of chiral aminomethylpalladium complexes

At last, the microscopic configurational stability of *N*-protected aminomethylpalladium complexes derived from (*R*)-*N*-tributylstannyl-[D_1]methylphthalimide and benzoyl chloride was addressed (Figure 2.17).

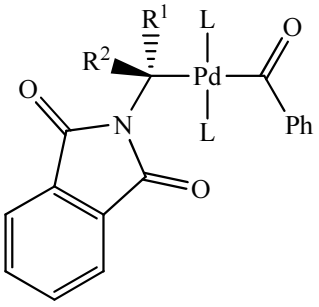

2.53: R^1 = H, R^2 = H
(*R*)-[D_1]**2.53**: R^1 = H, R^2 = D

Figure 2.17 - Studied aminomethylpalladium complexes

As in all other cases, the labeled and unlabeled precursors were made by a simple Mitsunobu reaction[49] between unlabeled and labeled tributylstannylmethanol (**1.67**) and phthalimide which proceeded with inversion of configuration (S_N2) (Scheme 2.18).

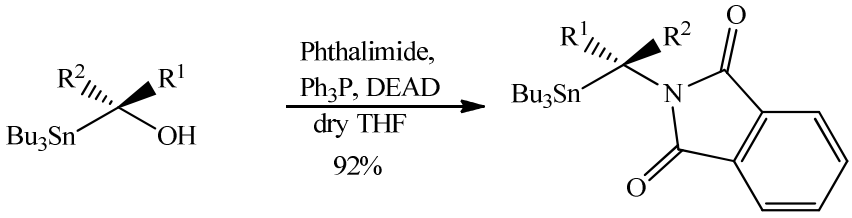

1.67: R^1 = R^2 = H
(*S*)-[D_1]**1.67**: R^1 = D, R^2 = H

2.54: R^1 = R^2 = H
(*R*)-[D_1]**2.54**: R^1 = D, R^2 = H

Scheme 2.18 - Preparation of the phthalimide **2.54**

The conditions used for the Stille coupling were the same as used for simiral substrates, which were also coupled with benzoyl chloride (Scheme 2.19)[1]

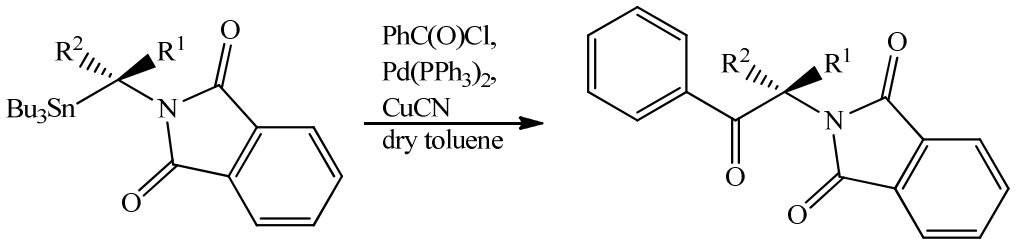

2.54: $R^1 = R^2 = H$
(*R*)-[D_1]**2.54**: $R^1 = H$, $R^2 = D$

2.55: $R^1 = R^2 = H$, 78%
(*S*)-[D_1]**2.55**: $R^1 = H$, $R^2 = D$, 77%

Scheme 2.19 - Stille coupling of phthalimide **2.54** with benzoyl chloride

The yields for the reactions performed in the presence of CuCN were virtually the same, 77% and 78%, for the labeled and unlabeled substrate. The reaction was monitored by TLC, using the literature known compound **2.55** as a reference sample.[50]

In order to determine the enantiomeric excess of the labeled product two easy steps were necessary (Scheme 2.20).

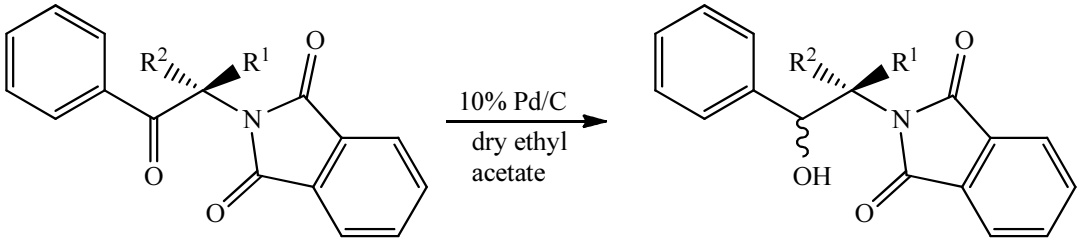

2.55: $R^1 = R^2 = H$
(*S*)-[2-D_1]**2.55**: $R^1 = H$, $R^2 = D$

2.56: $R^1 = R^2 = H$, 77%
(*2S*)-[2-D_1]**2.56**: $R^1 = H$, $R^2 = D$, 41%

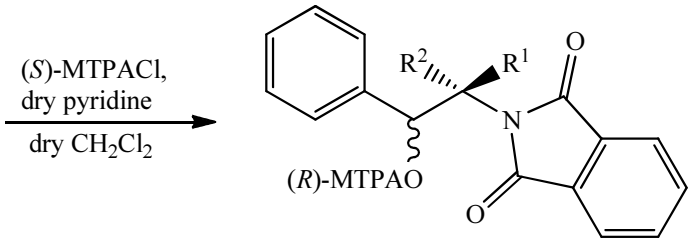

2.57: $R^1 = R^2 = H$, 91%
(*2S*)-[2-D_1]**2.57**: $R^1 = H$, $R^2 = D$, 71%

Scheme 2.20 - Derivatization of the product of Stille coupling to determine its enantiomeric excess

The ketone **2.55** was catalytically reduced to the alcohol **2.56** with a large amount of catalyst in a Parr apparatus.[51] Although the yields suffered from low reproducibility, even the low ones were acceptable, because only about 10 mg were sufficient for the next step, the esterification with (*S*)-MTPACl, resulting in a mixture of diastereomers. The enantiomeric excess was greater than 98% as determined by ^{1}H NMR spectroscopy (Figure 2.18). Therefore, the intermediate palladium complexes **2.53** of the Stille coupling, formed from a Pd^0 complex and (*R*)-*N*-tributylstannyl-[D_1]methylphthalimide and benzoyl chloride are microscopically configurationally stable at 75°C. As there was no reference sample available, it was not possible to determine the absolute configuration at the nitrogen bearing carbon atom.

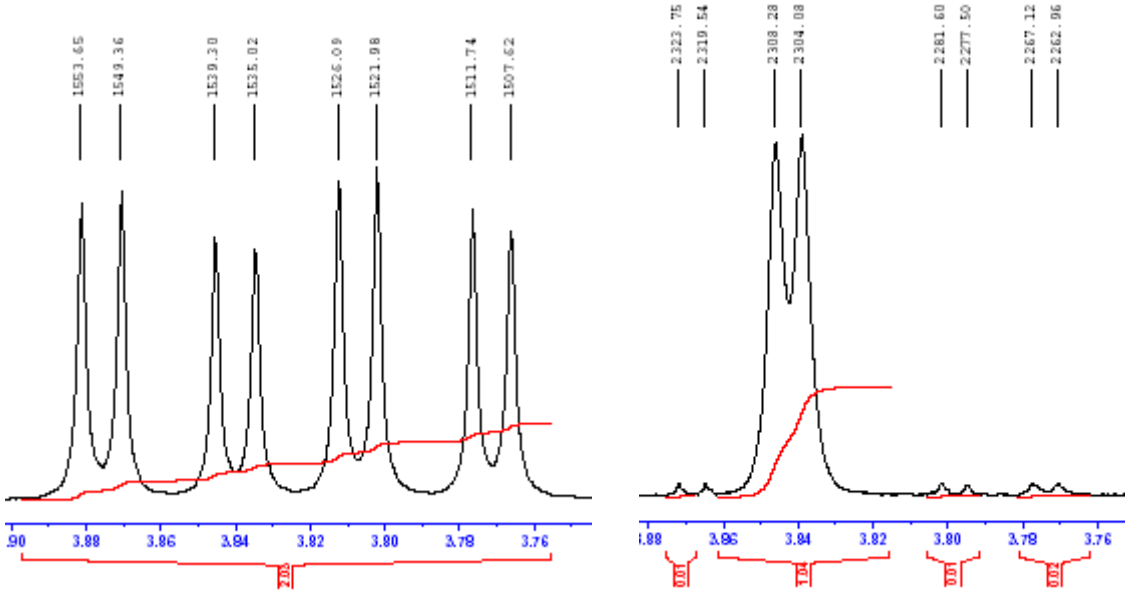

a) b)

Figure 2.18 - Segments of ^{1}H NMR spectra (400.27 MHz, $CDCl_3$) of (*R*)-Mosher esters: a) CH_2N group of unlabled species; b) CHDN group of labeled species derived from (*S*)-*N*-tributylstannyl-[D_1]methylphthalimide

In order to determine the absolute configuration, I decided to use the analogous palladium complexes **2.58**, assuming that the Stille coupling with benzoyl chloride and bromobenzene follows the same stereochemical course (Figure 2.19).

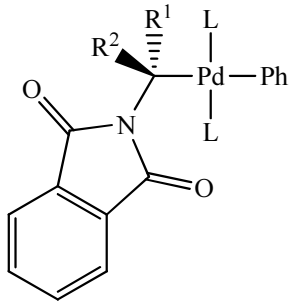

2.58: $R^1 = H$, $R^2 = H$
(*R*)-[D_1]**2.58**: $R^1 = H$, $R^2 = D$
(*S*)-[D_1]**2.58**: $R^1 = D$, $R^2 = H$

Figure 2.19 - Palladium complex analogous to complex **2.53**

These complexes were generated from unlabeled and labeled **2.54** and bromobenzene to prepare the phthalimide **2.59** (Scheme 2.21).

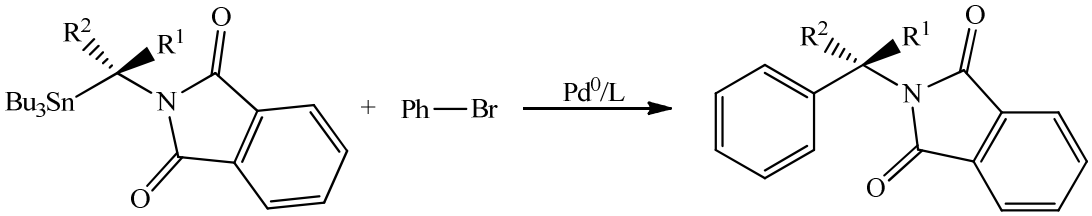

2.54: $R^1 = R^2 = H$
(*R*)-[D_1]**2.54**: $R^1 = H$, $R^2 = D$
(*S*)-[D_1]**2.54**: $R^1 = D$, $R^2 = H$

2.59: $R^1 = R^2 = D$
(*S*)-[D_1]**2.59**: $R^1 = H$, $R^2 = D$
(*R*)-[D_1]**2.59**: $R^1 = D$, $R^2 = H$

Scheme 2.21 - Stille coupling of **2.54** and bromobenzene

This Stille coupling was much more sluggish that the one with benzoyl chloride and the results are compiled in Table 2.2. Despite the low yields in the unlabelled series, the reaction in the labeled series was performed with both enantiomers of the amino-[D_1]methylstannane in dry toluene and dioxane, to study the influence of different solvents. The configuration of the labeled products could be determined by chemical correlation.

The reference sample of known configuration was prepared from (*R*)-phenyl-[D_1]methanol by the Mitsunobu reaction[49] that proceeded with inversion of configuration (Scheme 2.22).

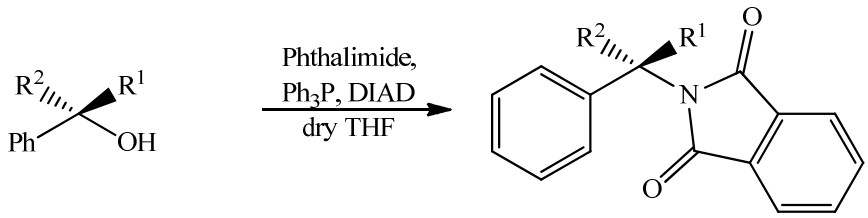

(*R*)-[D_1]**2.60**: R^1 = D, R^2 = H (*S*)-[D_1]**2.59**: R^1 = H, R^2 = D, 72%

Scheme 2.22 - Preparation of the labeled phthalimide **2.59** of known configuration

The *N*-substituted phthalimide was then deblocked and converted to the (*R*)-Mosher amide in the same way as the product of the Stille coupling.

Various conditions for the Stille coupling were tried[41, 44, 46] to find the one that produced the best yield. In summary, this coupling did not work as well as the one with benzoyl chloride. However, the yield was good enough so that I could determine the configuration and the enantiomeric excess of the product.

Entry	Stannane	Halide	Catalyst	Conditions	Yield
1	**2.54**	PhBr	$Pd(PPh_3)_2Cl_2$ (4 mol %), CuCN (8 mol %)	Toluene,80˚C, 20 h[41]	13%
2			$(PPh_3)_4Pd$ (5 mol %)	Dioxane,80˚C, 20 h[44]	14%
3			$Pd(P(tBu)_3)_2$ (3 mol %), CsF (2.2 eq)	Dioxane, 80→100˚C, 23→3 h[46]	n.r.*
4			$Pd(P(tBu)_3)_2$ (3 mol %)	Dioxane, 80˚C, 20 h[46]	n.r.*
5			$Pd(PPh_3)_2Cl_2$ (8 mol %), CuCN (16 mol %)	Toluene, 110˚C, 6 h[41]	37%
6			$Pd(PPh_3)_2Cl_2$ (8 mol %), CuCN (16 mol %)	Dioxane,100˚C, 6 h[41]	37%
7	(*R*)-[D_1]**2.54** (*S*)-[D_1]**2.54**	PhBr	$Pd(PPh_3)_2Cl_2$ (8 mol %), CuCN (16 mol %)	Toluene, 90˚C, 3 h[41]	53%
8			$Pd(PPh_3)_2Cl_2$ (8 mol %), CuCN (16 mol %)	Dioxane, 90˚C, 3 h[41]	29%

***** no reaction

Table 2.2 - Overview of all of the experiments performed according to Scheme 2.18 and their results

The best conditions as found with unlabeled substrate turned out to be $Pd(PPh_3)_2Cl_2$ (8 mol %), CuCN (16 mol %) in toluene or dioxane at 100 °C (Entries 5 and 6). The enantiomers of labeled phthalimides **2.54** were coupled in toluene and dioxane (Entries 7 and 8).

To determine the absolute configuration of the *N*-phenyl-[D_1]methylphthalimides and their enantiomeric excesses, the phthalimides **2.59** were deprotected and transformed into (*R*)-Mosher amides (Scheme 2.23). The sequence was optimized with the unlabeled phthalimide **2.59**.

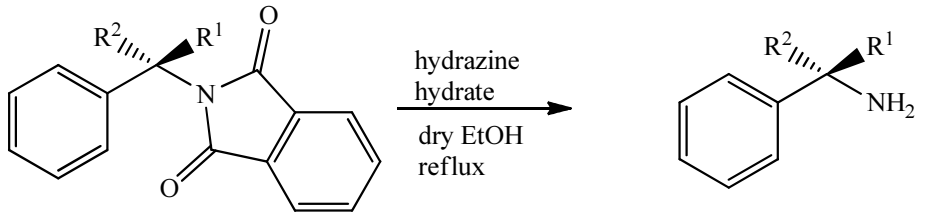

2.59: $R^1 = R^2 = H$
(*R*)-[D_1]**2.59**: $R^1 = D$, $R^2 = H$
(*S*)-[D_1]**2.59**: $R^1 = H$, $R^2 = D$

2.61: $R^1 = R^2 = H$, 21%
(*R*)-[D_1]**2.61**: $R^1 = D$, $R^2 = H$, 55%
(*S*)-[D_1]**2.61**: $R^1 = H$, $R^2 = D$, 100%

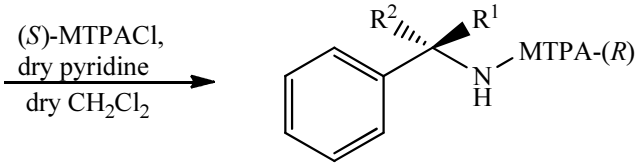

2.62: $R^1 = R^2 = H$, 61%
(*R*)-[D_1]**2.62**: $R^1 = D$, $R^2 = H$, 65%
(*S*)-[D_1]**2.62**: $R^1 = H$, $R^2 = D$, 13%

Scheme 2.23 - Conversion of phthalimides **2.59** to (*R*)-Mosher amides

The isolation of the small amounts of phenylmethylamine after deprotection of the amino group with hydrazine hydrate proved to be rather tricky. As the amine was also soluble in water, it took many tries and modifications of the literature known work-up[52] to remove the hydrazide of phthalic acid and hydrazine hydrate that was used in excess for the deprotection. Once I managed to do that, even though I could not completely remove the hydrazine hydrate, the conversion to the (*R*)-Mosher amide **2.62** was easy. Both of these steps did not touch the absolute configuration. The ^{1}H NMR spectrum of (*R*)-Mosher amide **2.62** derived from (*R*)-*N*-tributylstannyl-[D_1]methylphthalimide and bromobenzene was compared to the spectra of the amides derived from phenylmethylamine and (*R*)-phenyl-[D_1]methanol. It was found that the (*R*)-Mosher amide obtained by the Stille coupling was a mixture of diastereomers (enantiomeric excess of underlying amine 52%), the major one having (*S*) configuration. This implies that the Stille coupling follows a predominantly retentive course (Figure 2.20).

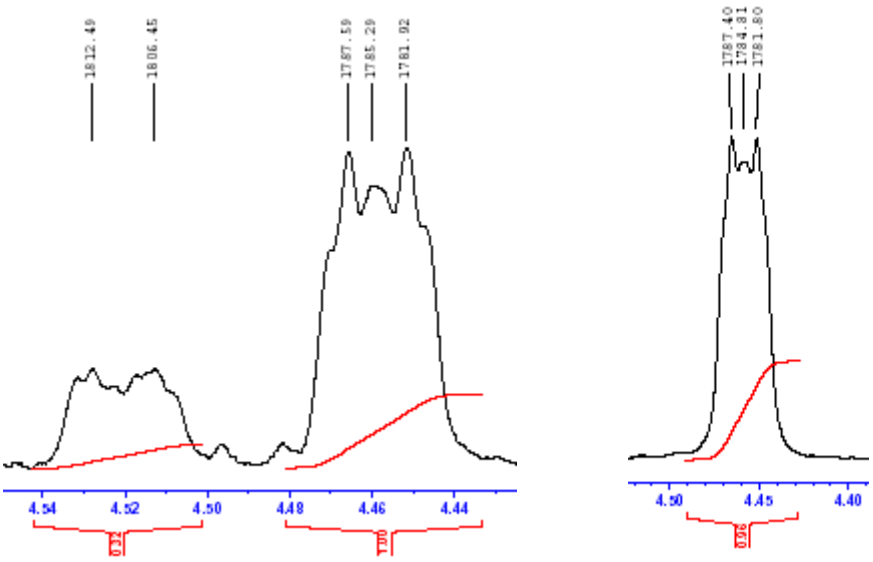

a) b)

Figure 2.20 - Signals of the CHD group in ^{1}H NMR spectra (400.27 MHz, $CDCl_3$) of (R)-Mosher amides a) (*S*)-[D_1]**2.62** derived from the product of the Stille coupling and b) (*S*)-[D_1]**2.62** derived from (*R*)-phenyl-[D_1]methanol

Analogously, I assume that the previous Stille coupling between the (*R*)-*N*-tributylstannyl-[D_1]methylphthalimide (**2.54**) and benzoyl chloride also proceeds with net retention of configuration, but exclusively.

The two differences with the previous Stille coupling were the solvent used and replacing benzoyl chloride by bromobenzene. To figure out whether the partial racemization has to be attributed to the dioxane used as a solvent, the phthalimide (*S*)-[D_1]**2.54** was Stille coupled similarly to the (*R*)-enantiomer, except that toluene replaced dioxane. The result was not significantly different. The coupling proceeded predominantly with retention of configuration and the enantiomeric excess of the product increased to 69% (Figure 2.21).

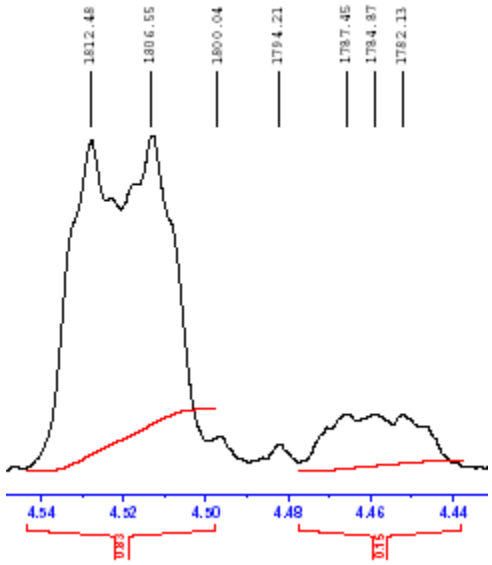

Figure 2.21 - Signal of CHD group in ^{1}H NMR spectrum (400.27 MHz, $CDCl_3$) of the (*R*)-Mosher amide derived from (*R*)-[D_1]**2.61**

Therefore, the main factor for partial enantiomerization does not seem to be the solvent. There are two options left to explain it:

Either the intermediate *N*-protected chiral aminomethylpalladium complexes **2.58** are microscopically configurationally labile or transmetalation proceeds by a combination of a predominating closed transition state **2.64** (with retention of configuration) and a minor open transition state **2.63** (with inversion of configuration) (Figure 2.22). The overall stereochemistry is therefore net retention of configuration.

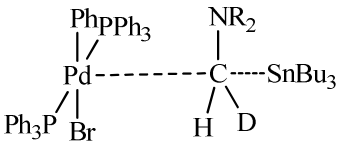

2.63

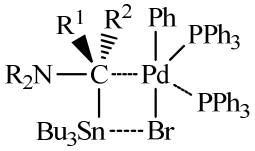

(*R*)-[D_1]**2.64**: R^1 = D, R^2 = H
(*S*)-[D_1]**2.64**: R^1 = H, R^2 = D

Figure 2.22 - Two possible transition states for the transmetalation during Stille coupling

To see if yields for the Stille coupling with stannylmethylamines could be improved by using a different protecting group for the amino group, the Boc protecting group was tested as an alternative to the phthalimide group (Table 2.3).

Entry	Stannane	Halide	Catalyst	Conditions	Yield
1	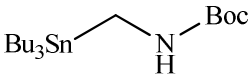 **2.65**	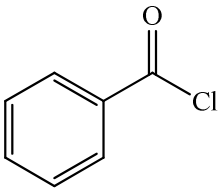	$Pd(PPh_3)_2Cl_2$ (8 mol %), CuCN (16 mol %)	Toluene, 80˚C, 3 h[41]	wrong product
2			$Pd(PPh_3)_2Cl_2$ (8 mol %), CuCN (16 mol %)	Toluene, RT→50˚C, 4→20 h[41]	wrong product
3	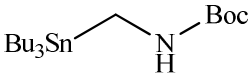 **2.65**	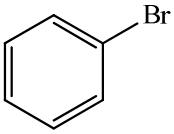	$Pd(PPh_3)_2Cl_2$ (8 mol %), CuCN (16 mol %)	Toluene, 80˚C, 3 h[41]	wrong product
4			$Pd(PPh_3)_2Cl_2$ (8 mol %), CuCN (16 mol %)	Toluene, RT→50˚C, 4→20 h[41]	wrong product

Table 2.3 - Overview of the performed experiments with nitrogen protected by a Boc group

The first experiment did not yield the desired product, but one that was identical with the starting material, except that it had lost one butyl group (Entry 1). Hoping that this side reaction could be suppressed, the experiment was repeated, but starting it at room temperature and then increasing the temperature to 50˚C. The result was basically the same as before.

This same side reaction was also noticed in Stille couplings with the phthalimide protecting group, but always to a much lesser extent. It is possible that the carbonyl oxygen from the Boc group coordinates to the tin atom thus making the transfer of a butyl group more favorable than that of the protected aminomethyl group. The reason why it was not observed so much with the phthalimide group could be that coordination of tin to the oxygen atom is less favorable than in the Boc-protected precursor (Figure 2.23).

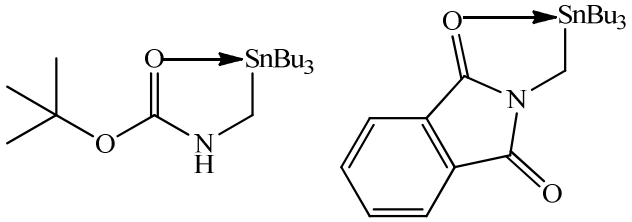

2.66 **2.67**

Figure 2.23 - Coordination of tin to the oxygen atom in Boc and phthalimide protected tributylstannylmethylamine

3 Phosphonic and phosphinic acids

Phosphonic acids contain one P-C bond and phosphinic ones two in place of P-O bonds.[53] Phosphonic acids are widely distributed in nature; 20% to 30% of all of the available phosphorus in the oceans is stored in 2-aminoethylphoshonic acid (AEP).[54] Phosphonates can be found in lipids, polysaccharides, proteins, and phosphonoglycans. Their functions in living organisms have not been determined yet but it was suggested that they may be involved in cell-cell signaling and phosphorus storage.[53]

Naturally occurring phosphonic and phosphinic acids are bioactive compounds. Two of them, fosfomycin (**3.1**) and phosphinothricin (**3.2**), are of commercial importance (Figure 3.1).

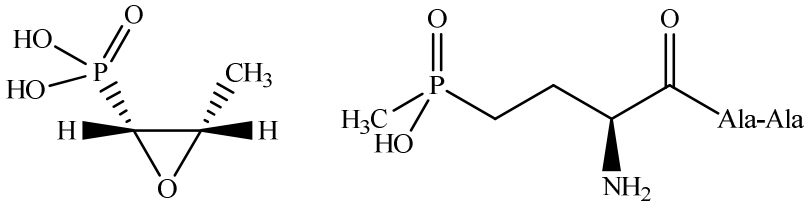

3.1 **3.2**

Figure 3.1 - Commercially important natural products containing a P-C bond

Fosfomycin is a clinically used antibiotic that blocks the first step in the biosynthesis of the bacterial cell wall. Phosphinothricin and the tripeptide bialaphos containing it are marketed as herbicides for agriculture.[53]

Because small phosphonic and phosphinic acids are structurally similar to various carboxylic acids and phosphate esters which are substrates for different enzymes they can act as enzyme inhibitors. Fosfomycin is an example of an irreversible inhibitor of the UDPGlcNAc carboxyvinyltransferase.[55]

2-Aminoethylphosphonic acid (AEP, **3.3**), the first known natural phosphonic acid, was isolated in 1959 by Horiguchi and Kandatsu.[56] It is a β-aminophosphonic acid. This aminophosphonic acid is found in a large number of lower organisms (Figure 3.2).

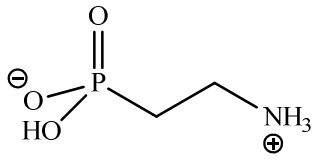

3.3

Figure 3.2 - 2-Aminoethylphosphonic acid (AEP)

Aminophosphonic acids are structural analogs of aminocarboxylic acids and present low toxicity against mammals.[57]

It was postulated that phosphonic acids were present before phosphates as the first forms of life evolved. They were even discovered in the Murchinson meteorite[58] found near the town Murchinson in Victoria, Australia on September 28th, 1969.

3.1 Biosynthesis of natural products containing a P-C bond

All of the biosyntheses of phosphonic and phosphinic acids start with the same initial steps that lead to 2-aminoethylphosphonate (AEP) (Scheme 3.1).[53]

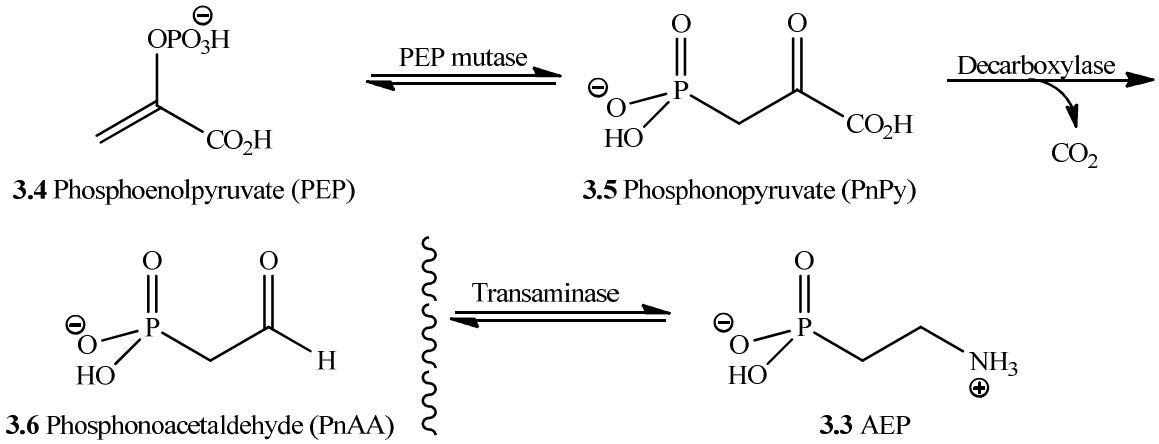

3.4 Phosphoenolpyruvate (PEP) **3.5** Phosphonopyruvate (PnPy)

3.6 Phosphonoacetaldehyde (PnAA) **3.3** AEP

Scheme 3.1 - Initial steps that lead to AEP

The carbon-phosphorus bond is formed by an intramolecular rearrangement of phosphoenolpyruvate (PEP) by PEP mutase giving phoshonopyruvic acid **3.5** (Scheme 3.2).[57]

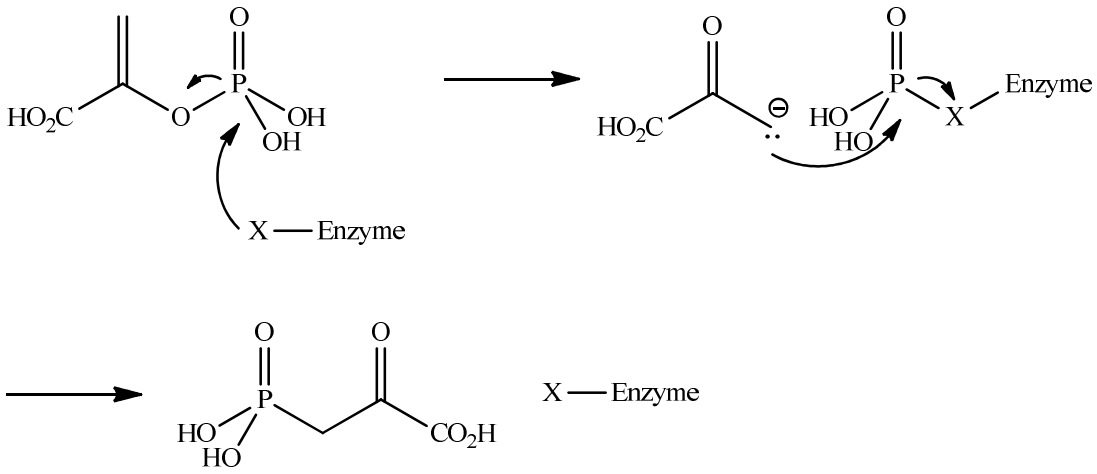

Scheme 3.2 - Formation of the carbon-phosphorus bond

3.2 Phosphinothricin

Phosphinothricin is a non-proteinogenic α-amino acid with a phosphinic acid group in the side chain (Figure 3.3).[59]

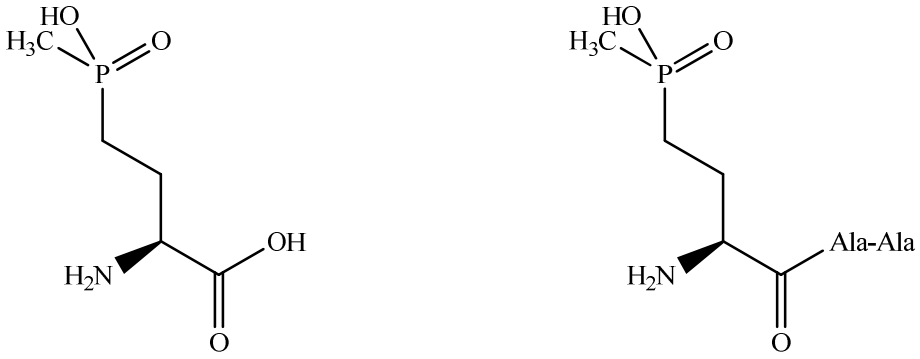

Phosphinothricin (**3.7**) Bialaphos (**3.2**)

Figure 3.3 - Structure of phosphinothricin and its tripeptide bialaphos

It is produced and coupled with two L-alanines by *Streptomyces hygroscopicus* and *Streptomyces viridochromogenes*. The tripeptide formed is called bialphos and is sold as a herbicide. Synthetic phosphinothricin is the active ingredient in a variety of commercial herbicides like Basta and Liberty that are used with transgenic plants like corn, cotton and canola.[60]

3.2.1 Mechanism for inhibition of glutamine synthetase by phosphinothricin

Phosphinothricin is a structural analog of glutamate, which inhibits glutamine synthetase. Glutamine synthetase is an important enzyme responsible for the binding of ammonia in plants. If the concentration of ammonia increases, the plant dies. Bialaphos is taken up by plants and hydrolysed by cytoplasmatic peptidases to release phosphinothricin, the actual inhibitor. The tripetide is a "Trojan Horse" for phosphinothricin.[53] The biosynthesis of glutamine is given in Scheme 3.3.

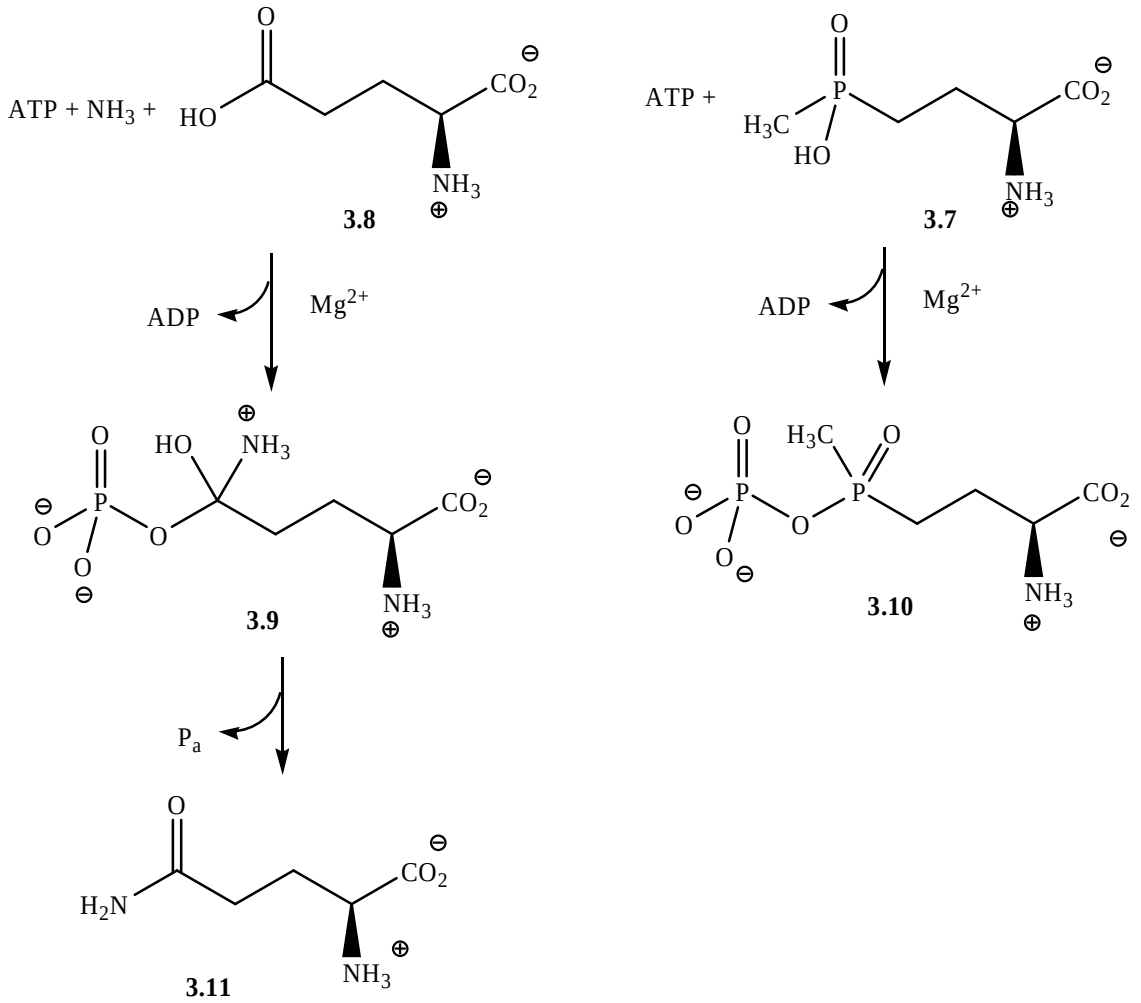

Scheme 3.3 - Mechanism for inhibition of glutamine synthetase by phosphinothricin

Glutamate (**3.8**) is activated with ATP at the γ carboxyl group to generate a mixed anhydride, which is attacked by ammonia. The tetrahedral intermediate **3.9** formed collapses and yields glutamine **3.11** and inorganic phosphate. However, phosphinothricin is phosphorylated, but cannot be attacked by ammonia. The phosphorylated species **3.10** mimics the tetrahedral intermediate **3.9** and remains bound to glutamine synthase, which is blocked.[61]

Certain transgenic plants are resistent to phosphinothricin, because they contain a gene that encodes an acetyltransferase that acetylates the amino group of phosphinothricin and so deactivates it (Scheme 3.4).

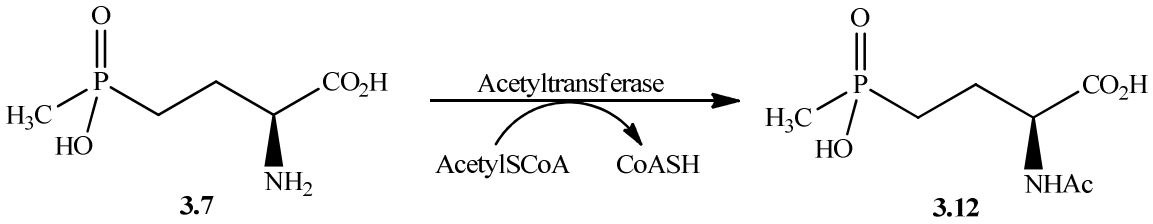

Scheme 3.4 - Deactivation of phosphinothricin

3.2.2 Biosynthesis of phosphinothricin

The biosynthesis of phosphinothricin starts with the same two steps giving phosponoacetaldehyde as in the already mentioned biosynthesis of AEP. The aldehyde **3.6** is reduced by a dehydrogenase to 2-hydroxyethylphosphonate (HEP, **3.13**), which is degraded by 2-hydroxyethylphosphonate dioxygenase (HEPD) to give hydroxymethylphosphonate (HMP, **3.14**) and formic acid. This transformation is mechanistically very interesting. Without going into details, the hydroxymethylphoshonate is further metabolized to finally yield phosphinothricin (**3.7**), whereby only the phosphorous atom ends up in the end product (Scheme 3.5).[53]

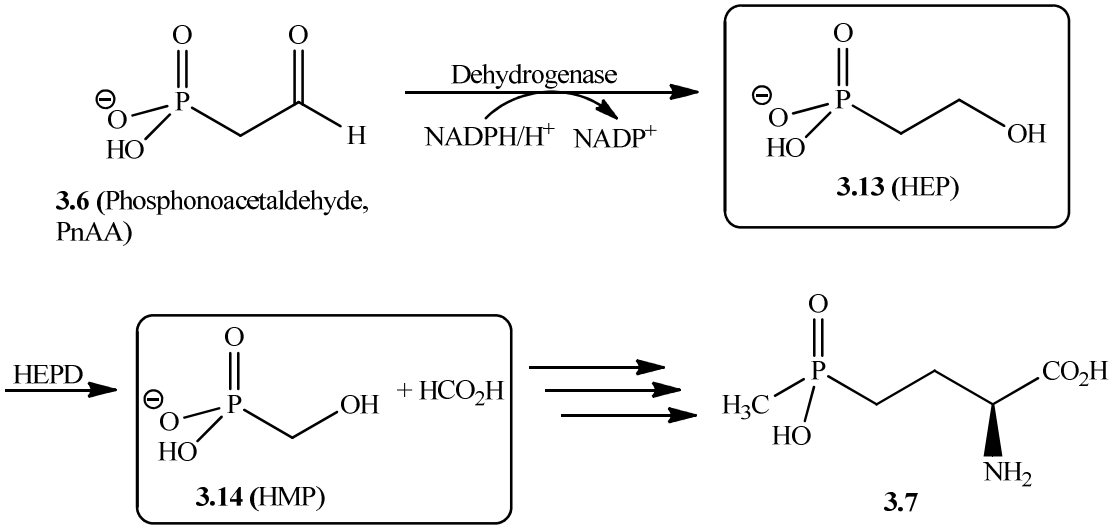

Scheme 3.5 - First steps in the biosynthesis of phosphinothricin, including the HEPD-catalyzed reaction

3.2.3 2-Hydroxyethylphosphonate dioxygenase (HEPD)

2-Hydroxyethylphosphonate dioxygenase (HEPD) is a product of the *phpD* gene isolated from *Streptomyces viridochromogenes*.[53] It belongs to a group of dioxygenases which are redox-enzymes that incorporate both oxygen atoms of O_2 into the substrate (Scheme 3.6).[62]

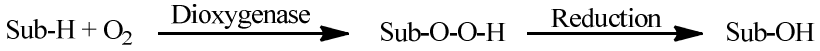

Scheme 3.6 - Typical reaction catalyzed by a dioxygenase

In a typical reaction a highly reactive peroxide species is formed that can then be either reduced to an alcohol or can react further to form other products. In case of HEPD, the mechanism is still unknown and the result of the reaction is the shortening of the HEP chain with the release of formic acid and hydroxymethylphosphonate (HMP). Experiments that have been performed with labeled O_2 and with labeled carbons of HEP[63] show that C-1 of HEP remains the C-1 of HMP and C-2 ends up as formic acid. One oxygen atoms of the O_2 molecule is found in HMP, the other one in formic acid (Scheme 3.7).[53]

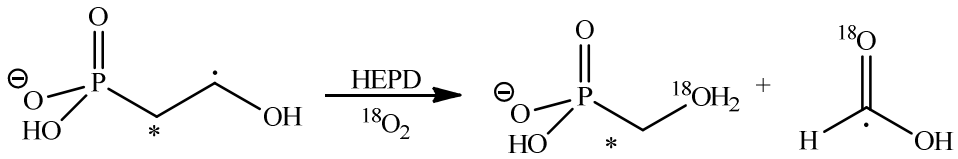

3.13 (HEP) **3.14** (HMP) **3.15**

Scheme 3.7 - Degradation of HEP to HMP and formic acid by HEPD

HEPD needs besides Fe(II) and O_2 as co-substrate no other cofactors to perform its function. It is a non-haem iron protein that contains Fe(II) tightly bound to the side chains of two histidines and one glutamate (Figure 3.4).

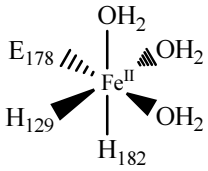

E = Glutamate
H = Histidine

Figure 3.4 - Amino acids from HEPD and water act as ligands for the Fe(II) at the active site of the enzyme

The crystal structure solved by Higgins et al.[64] shows that its active site and tertiary structure are similar to 2-hydroxypropylphosphonate epoxidase (HppE) that is involved in the biosynthesis of the antibiotic fosfomycin.[65]

Two different mechanisms have been proposed for the action of HEPD.[59] First, substrate and the O_2 are bound to the octahedrally coordinated Fe(II) by replacing three water molecules. Both of the mechanisms start with the same two steps in which a radical complex is formed and Fe(II) is oxidized to Fe(III) (Scheme 3.7).

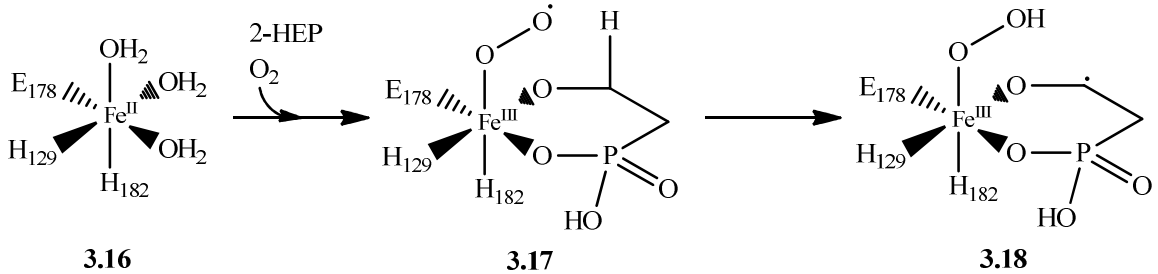

3.16 **3.17** **3.18**

Scheme 3.7 - First two steps of the proposed mechanisms

The first contains an oxygen-centered radical that stereospecifically abstracts a hydrogen atom from C-2 of HEP, generating a carbon-centered radical and a hydroperoxide ligand at Fe(III).
It is proposed that afterwards an alkylhydroperoxide is formed and Fe(III) is reduced to Fe(II) again in the next step. Complex **3.19** undergoes a Bayer-Villiger type reaction yielding an *O*-formyl-HMP bound to Fe(II). Cleavage of the formate gives HMP and formic acid. Surprisingly, it has been postulated that a hydroxide ion replaces the formate group with inversion of configuration (S_N2 reaction). The chemical Bayer-Villiger oxidation follows a retentive course. If this is also true for this enzymatic version here remains to be determined (Scheme 3.8).

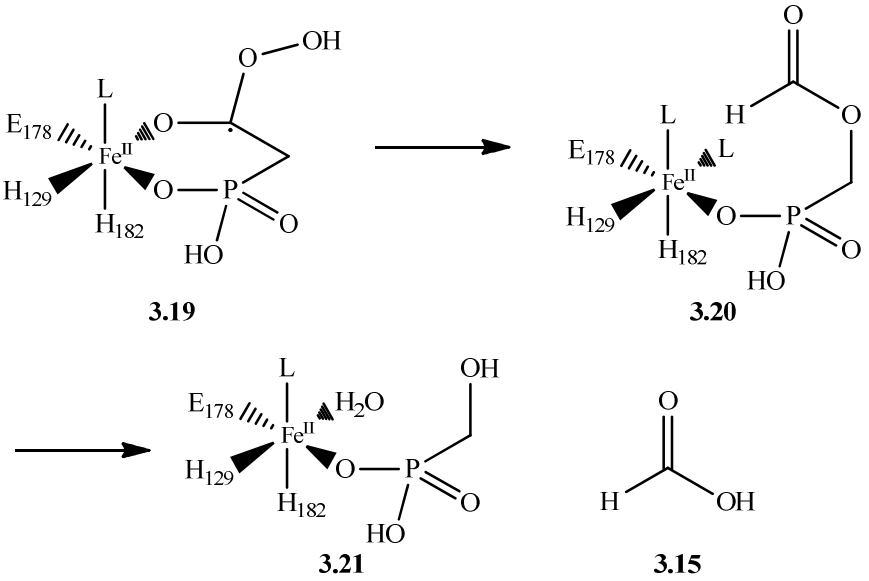

Scheme 3.8 - Proposed formation of an alkylhydroperoxide and Bayer-Villiger oxidation in the first mechanism

The second mechanism outlined in Scheme 3.9 involves a Fe(IV)=O species containing an oxy anion, which is assumed to fragment to formic acid and a carbanion attacking the electrophilic oxygen of Fe(IV)=O. The HMP bound to Fe(II) is replaced by water molecules as ligands.

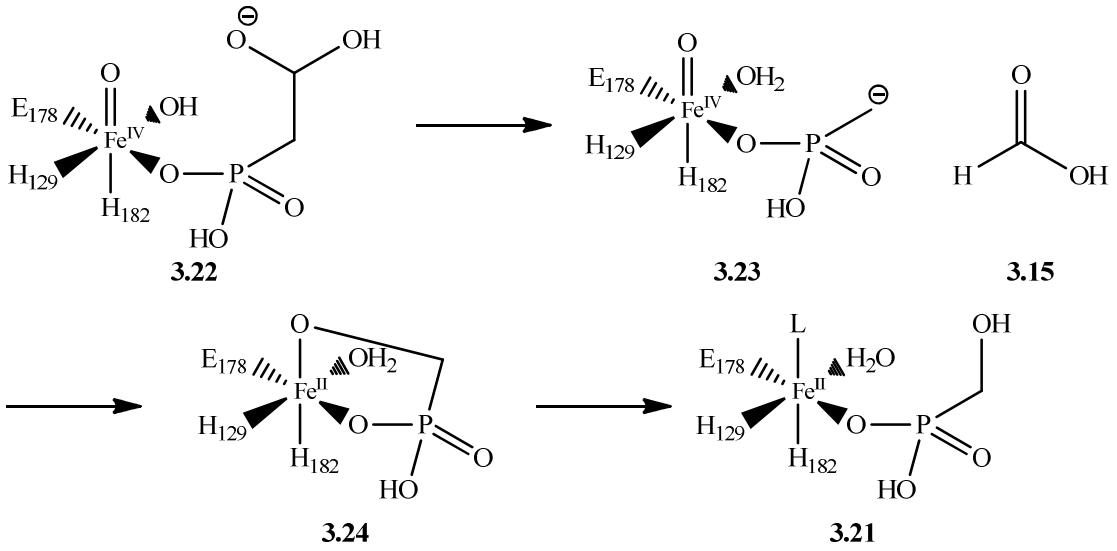

Scheme 3.9 - Alternative mechanism that goes through a putative Fe(IV)=O intermediate

3.2.4 Aminomethylphosphonic acid (AMPA)

Aminomethylphosphonic acid (AMPA, **3.26**) along with glyoxalate (**3.27**) is a major metabolite of the biodegradation of *N*-phosphonomethylglycine (**3.25**), a broad spectrum herbicide called Glyphosate (Scheme 3.10).[57] It was also found that it inhibits the growth of tobacco rootlets.[66]

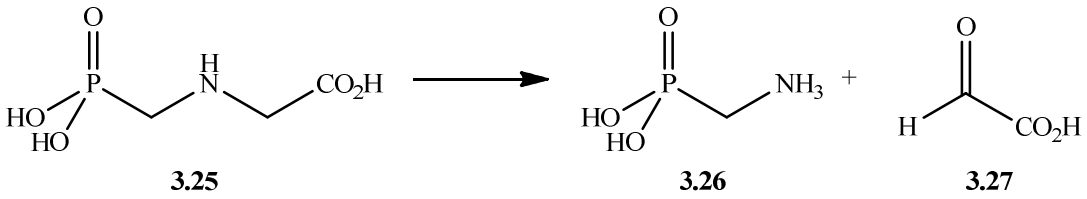

Scheme 3.10 - Biodegradation of Glyphosate

Furthermore, it was produced as a shunt metabolite by a strain of *Streptomyces viridochromogenes* containing a mutated *ΔphpJ* gene. As it codes for the aldehyde dehydrogenase that converts phosphonoformaldehyde (**3.28**) to phosphonoformic acid (**3.39**), the aldehyde is accumulated and transformed into the amine by an aminotransferase (Scheme 3.11).[60]

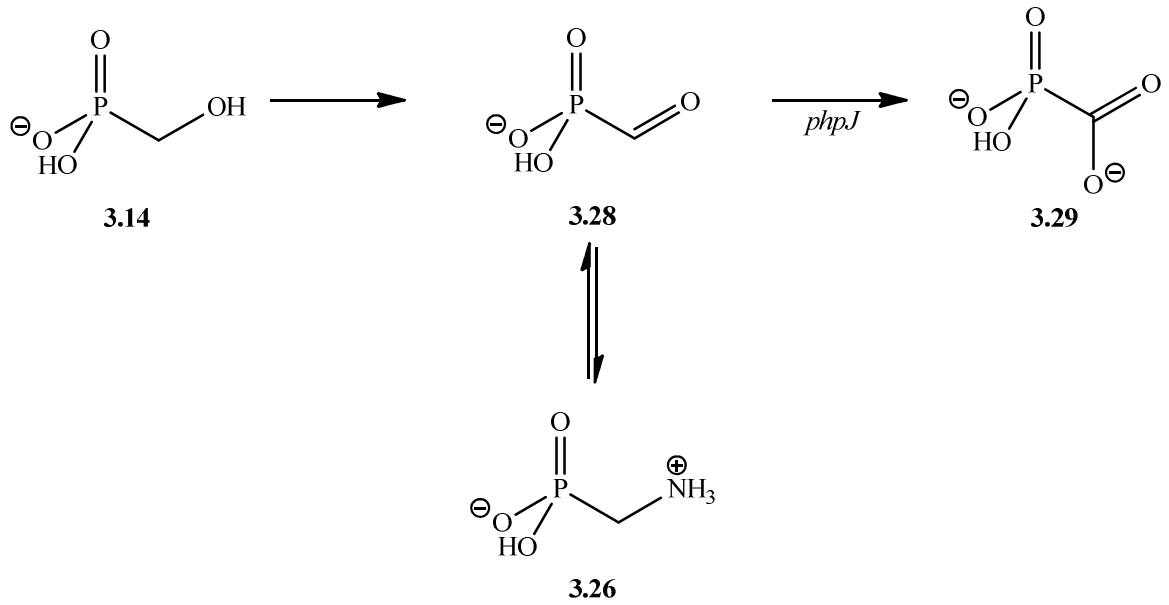

Scheme 3.11 - Production of AMPA by *Streptomyces viridochromogenes* containing a mutated *ΔphpJ* gene

3.2.5 Synthesis of the (*R*)- and (*S*)-hydroxy-[D_1]methylphosphonic acids

In order to be able to determine the mechanism of HEPD, both enantiomerically pure (*R*)- and (*S*)-hydroxy-[D_1]methylphosphonic acids had to be prepared as reference samples. Their synthesis was based on previous work in our group. The acids could then be compared to the labeled HMP obtained from the enantiomers of 2-hydroxy-[1-D_1]ethylphosphonic acid by the action of HEPD. I first started with the synthesis of the unlabeled species so that all of the steps were optimized and only when that was done I moved on to the labeled compounds (Scheme 3.12).

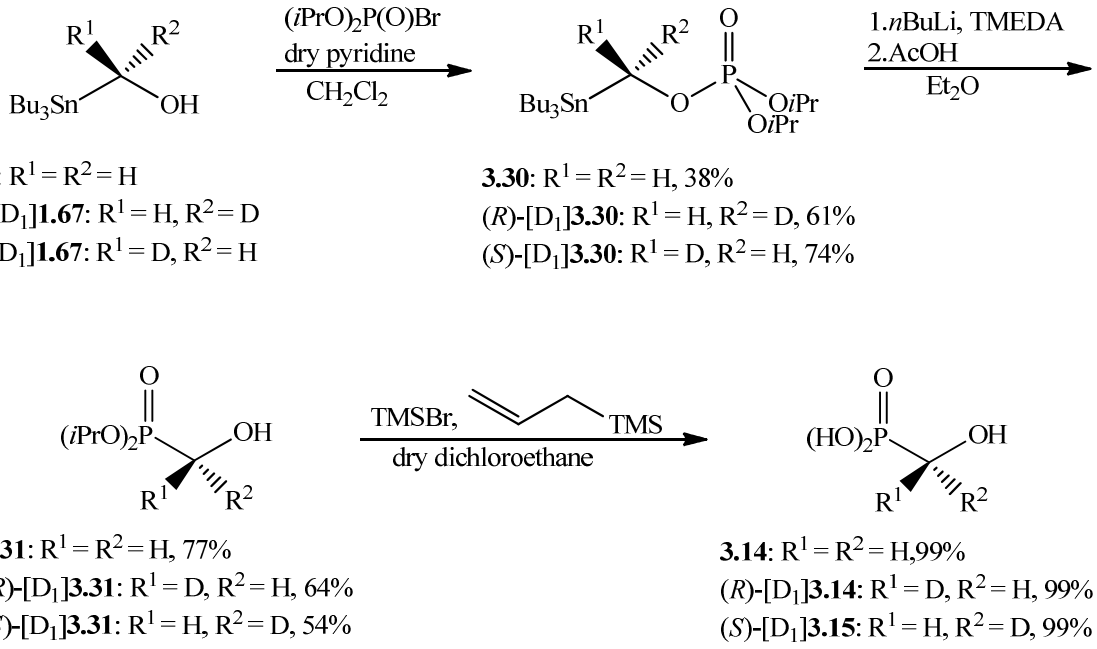

1.67: $R^1 = R^2 = H$
(*R*)-[D_1]**1.67**: $R^1 = H$, $R^2 = D$
(*S*)-[D_1]**1.67**: $R^1 = D$, $R^2 = H$

3.30: $R^1 = R^2 = H$, 38%
(*R*)-[D_1]**3.30**: $R^1 = H$, $R^2 = D$, 61%
(*S*)-[D_1]**3.30**: $R^1 = D$, $R^2 = H$, 74%

3.31: $R^1 = R^2 = H$, 77%
(*R*)-[D_1]**3.31**: $R^1 = D$, $R^2 = H$, 64%
(*S*)-[D_1]**3.31**: $R^1 = H$, $R^2 = D$, 54%

3.14: $R^1 = R^2 = H$,99%
(*R*)-[D_1]**3.14**: $R^1 = D$, $R^2 = H$, 99%
(*S*)-[D_1]**3.15**: $R^1 = H$, $R^2 = D$, 99%

Scheme 3.12 - Preparation of unlabeled and labeled HMP

The first step of the synthesis was the phosphorylation of tributylstannylmethanol with diisopropyl bromophosphate that was formed from triisopropyl phosphite and a solution of bromine in dry dichloromethane.[67] Phosphate **3.30** was treated with BuLi/TMEDA in Et_2O at -78 °C to induce a phosphate-phosphonate rearrangement that resulted in the diisopropyl hydroxymethylphosphonate. At first, transmetalation generated dipole-stabilized oxymethyllithium **3.32** that rearranged to the lithiated hydroxymethylphosphonate **3.33** that was hydrolyzed to the desired product **3.31** during work up. The rearrangement was proven to proceed with retention of configuration (Scheme 3.13).[24]

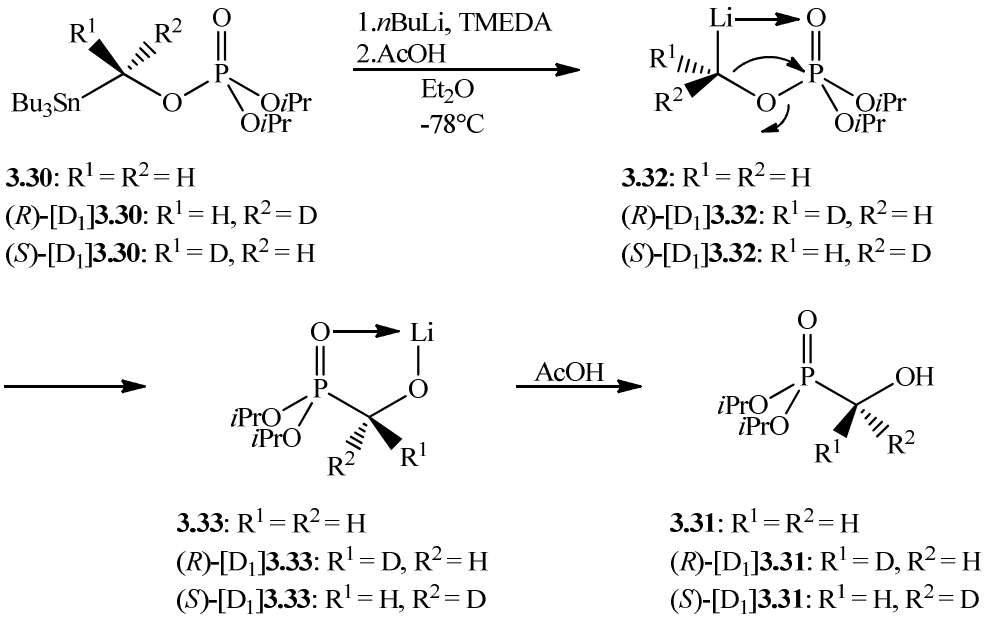

3.30: $R^1 = R^2 = H$
(*R*)-[D_1]**3.30**: $R^1 = H, R^2 = D$
(*S*)-[D_1]**3.30**: $R^1 = D, R^2 = H$

3.32: $R^1 = R^2 = H$
(*R*)-[D_1]**3.32**: $R^1 = D, R^2 = H$
(*S*)-[D_1]**3.32**: $R^1 = H, R^2 = D$

3.33: $R^1 = R^2 = H$
(*R*)-[D_1]**3.33**: $R^1 = D, R^2 = H$
(*S*)-[D_1]**3.33**: $R^1 = H, R^2 = D$

3.31: $R^1 = R^2 = H$
(*R*)-[D_1]**3.31**: $R^1 = D, R^2 = H$
(*S*)-[D_1]**3.31**: $R^1 = H, R^2 = D$

Scheme 3.13 - Mechanism of the phosphate-phosphonate rearrangement

The only thing left to do to obtain the desired hydroxymethylphosphonic acid was the removal of the isopropyl groups from the ester with bromotrimethylsilane and allyltrimethylsilane in dry 1,2-dichloroethane according to a literature procedure.[68] Similarly, the syntheses of the labeled enantiomers were performed, except that (*R*)- and (*S*)-tributylstannyl-[D_1]methanols were used as starting materials (Scheme 3.12).

To determine the enantiomeric excess of the (*R*)- and (*S*)-hydroxy-[D_1]methylphosphonic acids the phosphonic acid group was esterified with a distilled ethereal solution of diazomethane in dry methanol[69] to give the dimethyl ester and as a side product dimethyl methoxymethylphosphonate (6% of the unlabeled and 12% of the labeled species, by ^1H and ^{31}P NMR). It resulted from etherification of the hydroxymethyl group by diazomethane as side reaction. The crude ester was esterified with (*S*)-MTPACl in dry pyridine and dry dichloromethane (Scheme 3.14).

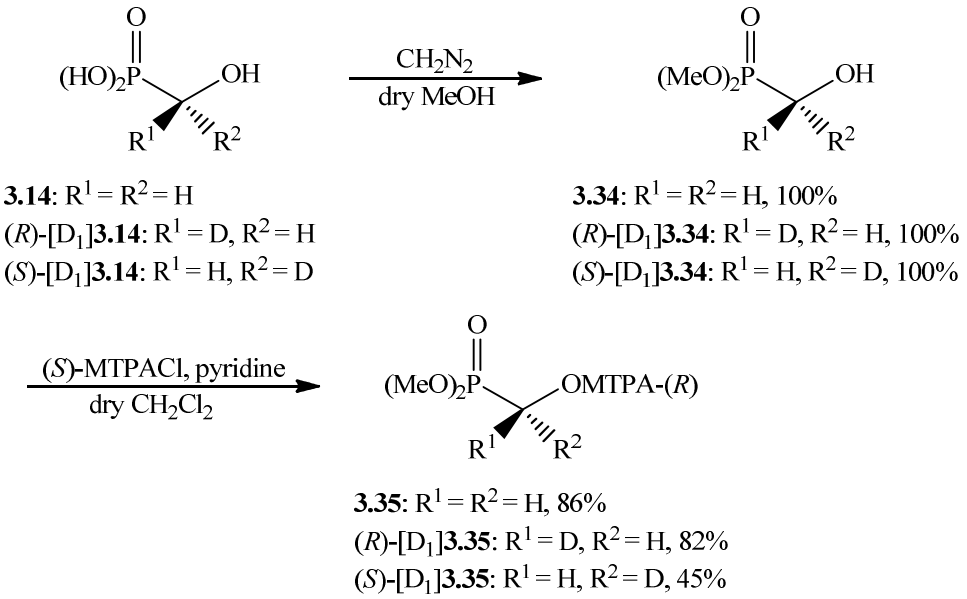

3.14: $R^1 = R^2 = H$
(*R*)-[D_1]**3.14**: $R^1 = D$, $R^2 = H$
(*S*)-[D_1]**3.14**: $R^1 = H$, $R^2 = D$

3.34: $R^1 = R^2 = H$, 100%
(*R*)-[D_1]**3.34**: $R^1 = D$, $R^2 = H$, 100%
(*S*)-[D_1]**3.34**: $R^1 = H$, $R^2 = D$, 100%

3.35: $R^1 = R^2 = H$, 86%
(*R*)-[D_1]**3.35**: $R^1 = D$, $R^2 = H$, 82%
(*S*)-[D_1]**3.35**: $R^1 = H$, $R^2 = D$, 45%

Scheme 3.14 - Derivatization of HMP for the determination of enantiomeric excess

The ^{1}H NMR spectrum of Mosher ester **3.35** displayed a nice AB system coupling with the phosphorous atom for the diastereotopic hydrogen atoms of the PCH_2 group (Figure 3.5). Therefore, the (*R*)-Mosher esters of the labeled compounds are amenable to the determination of the enantiomeric excess by ^{1}H NMR spectroscopy.

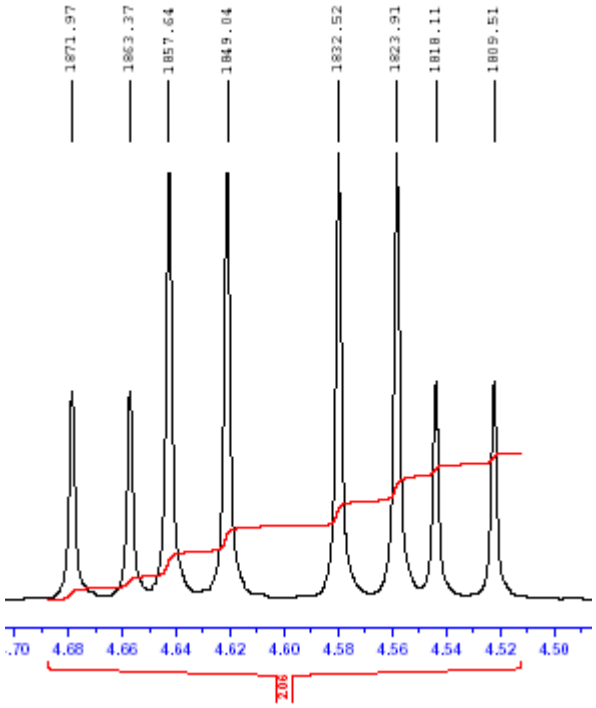

Figure 3.5 - Segment of ^{1}H NMR spectrum (400.13 MHz, $CDCl_3$) of the PCH_2 group of unlabeled (*R*)-Mosher ester **3.35**

If one deuterium atom was present in place of a hydrogen atom sterespecifically, one half of this AB-system would be missing and the enantiomeric excess would be equal to or greater than 99%. As can be seen from the ^{1}H-NMR spectra below, both (*R*)- and (*S*)-hydroxy-[D_1]methylphosphonic acids were synthesized with enantiomeric excesses greater that 99% (Figure 3.6).

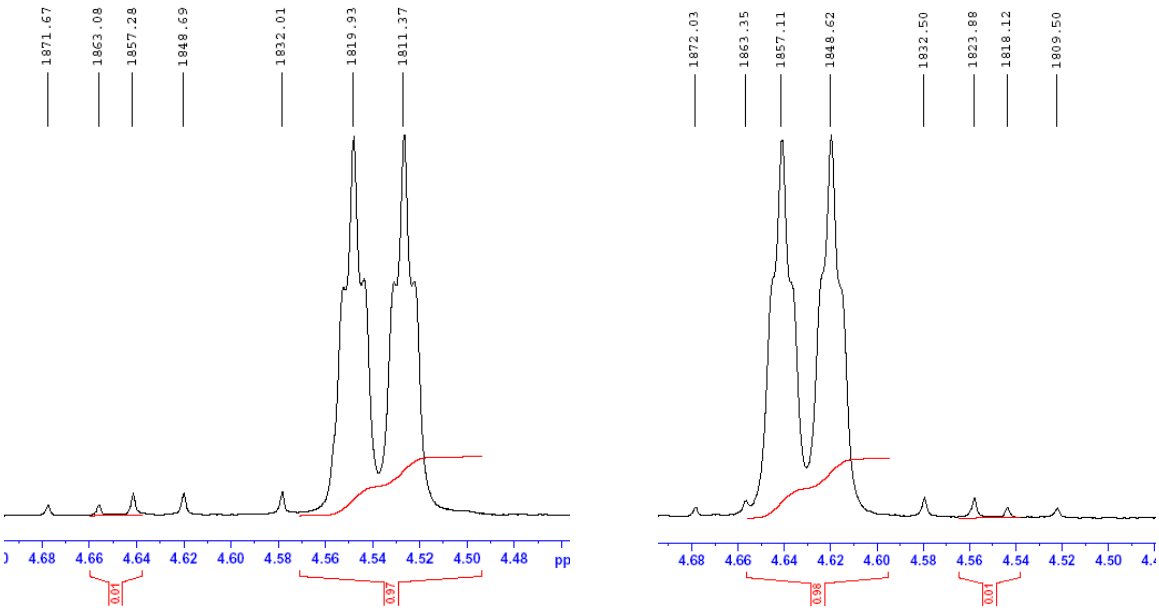

(*R*) (*S*)

Figure 3.6 - Segments of ^{1}H NMR spectra (400.13 MHz, $CDCl_3$) of the PCHD groups of (*R*)-Mosher esters of (*R*)- and (*S*)-hydroxy-[D_1]methylphosphonic acids

They served as reference samples to determine the configurations and the enantiomeric excesses of the labeled HMP derived from (*R*)- and (*S*)-hydroxyl-[1-D_1]ethylphophonic acids by the HEPD catalyzed reaction. Both samples of labeled HMP provided by van der Donk´s group were converted to the (*R*)-Mosher esters of the dimethyl phosphonates. They were purified by preparative thin layer chromatography. It is clear, that both samples are virtually racemic, which is not compatible with an enzymatic version of the Bayer-Villiger oxidation as model reaction for the HEPD catalyzed transformation (Figure 3.7).

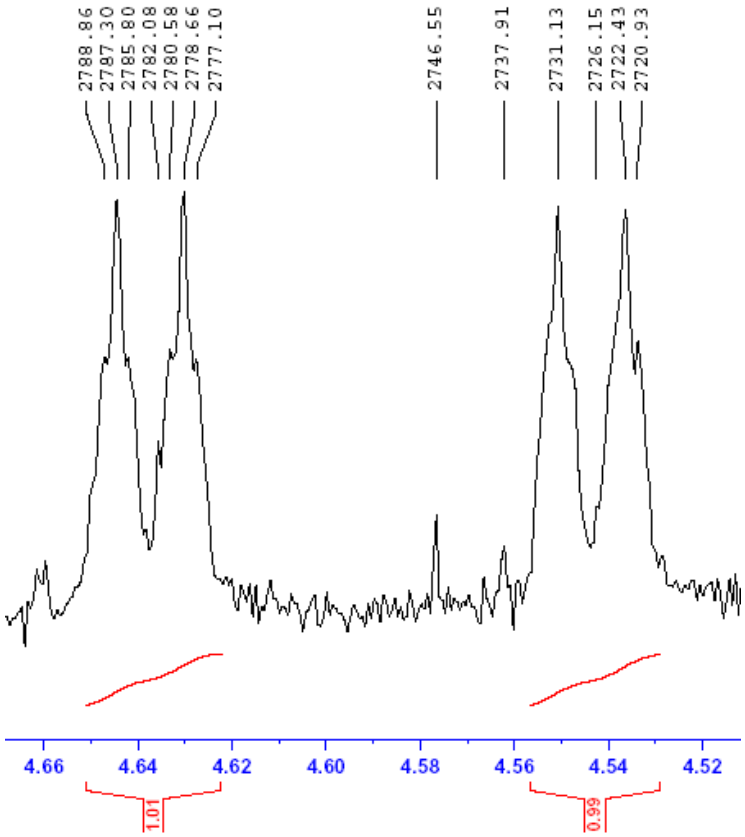

Figure 3.7 - Segment of ^{1}H NMR spectrum (400.13 MHz, $CDCl_3$) of the PCHD group from the derivatized samples from the van der Donk's group

3.2.6 Synthesis of the (*R*)- and (*S*)-amino-[D_1]methylphosphonic acid

Parallel to the synthesis of the (*R*)- and (*S*)-hydroxy-[D_1]methylphosphonic acids based on the previos work in our group, (*R*)- and (*S*)-amino-[D_1]methylphosphonic acids were prepared, which could also be used to elucidate enzyme mechanisms. Again I started with the synthesis of the unlabeled species and then I moved on to the synthesis of the labeled aminophosphonic acids.

The first step of the synthesis was a Mitsunobu reaction[49] (S_N2 reaction) to couple tributylstannylmethanol with a Boc-protected phosphoramidate to obtain *N*-tributylstannylmethyl phosphoramidate in 82% yield (Scheme 3.15).[15]

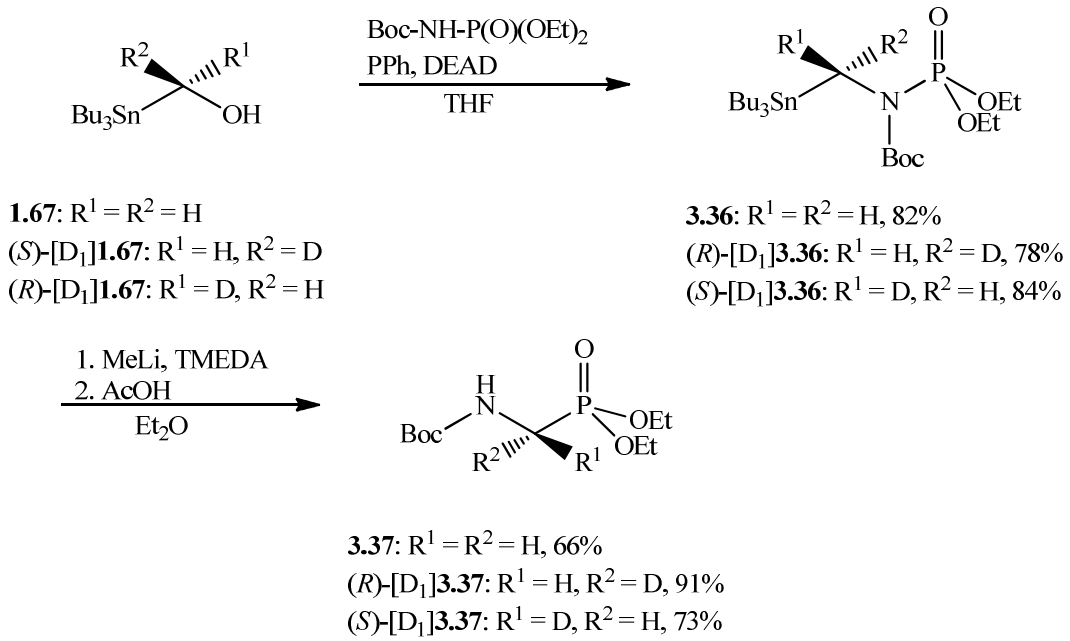

1.67: $R^1 = R^2 = H$
(*S*)-[D_1]**1.67**: $R^1 = H$, $R^2 = D$
(*R*)-[D_1]**1.67**: $R^1 = D$, $R^2 = H$

3.36: $R^1 = R^2 = H$, 82%
(*R*)-[D_1]**3.36**: $R^1 = H$, $R^2 = D$, 78%
(*S*)-[D_1]**3.36**: $R^1 = D$, $R^2 = H$, 84%

3.37: $R^1 = R^2 = H$, 66%
(*R*)-[D_1]**3.37**: $R^1 = H$, $R^2 = D$, 91%
(*S*)-[D_1]**3.37**: $R^1 = D$, $R^2 = H$, 73%

Scheme 3.15 - First three steps of the AMPA synthesis

The phosphoramidate was prepared from diethoxyphosphinyl isocyanate and *t*-butanol by a literature procedure (Scheme 3.16).[70]

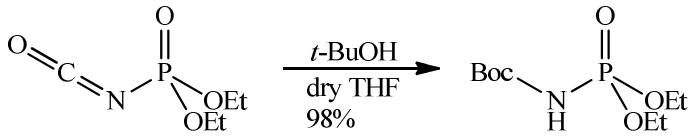

3.38 **3.39**

Scheme 3.16 - Preparation of Boc-protected phosphoramidate **3.39**

The *N*-stannylmethyl phosphoramidate **3.36** was transmetalated with MeLi at low temeperature to generate chemically labile dipole-stabilized aminomethyllithium **3.40**, which isomerized immediately (phosphoramidate-aminophosphonate rearrangement) with retention of configuration. Work up furnished the protected aminomethlyphosphonate **3.38**, which had to be deprotected (Scheme 3.17).[15]

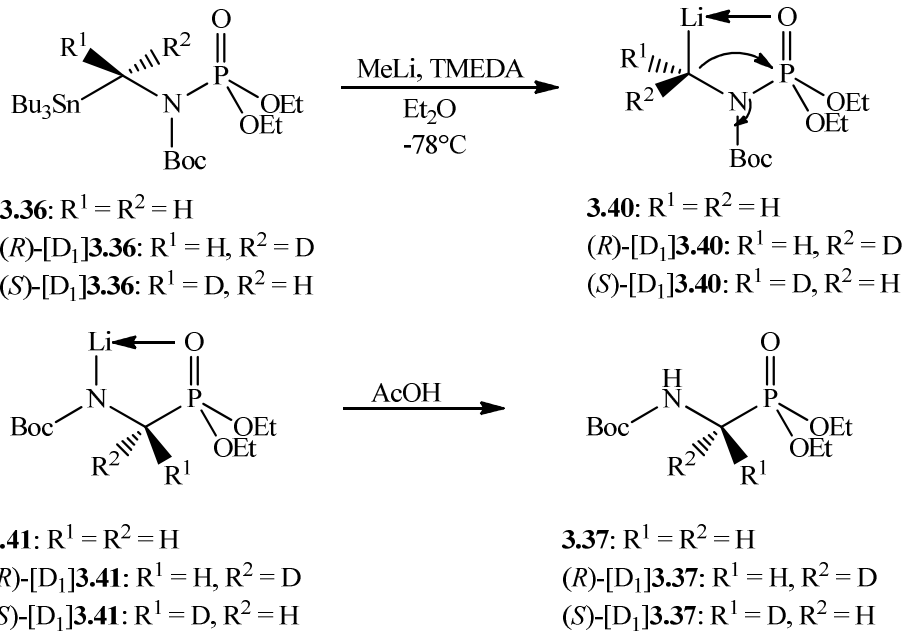

3.36: $R^1 = R^2 = H$
(*R*)-[D_1]**3.36**: $R^1 = H$, $R^2 = D$
(*S*)-[D_1]**3.36**: $R^1 = D$, $R^2 = H$

3.40: $R^1 = R^2 = H$
(*R*)-[D_1]**3.40**: $R^1 = H$, $R^2 = D$
(*S*)-[D_1]**3.40**: $R^1 = D$, $R^2 = H$

3.41: $R^1 = R^2 = H$
(*R*)-[D_1]**3.41**: $R^1 = H$, $R^2 = D$
(*S*)-[D_1]**3.41**: $R^1 = D$, $R^2 = H$

3.37: $R^1 = R^2 = H$
(*R*)-[D_1]**3.37**: $R^1 = H$, $R^2 = D$
(*S*)-[D_1]**3.37**: $R^1 = D$, $R^2 = H$

Scheme 3.17 - Mechanism of the phosphoramidate-aminophosphonate rearrangement

To get an appreciable amount of unlabled aminomethylphosphonic acid, dimethyl *N*-(triphenylmethyl)aminomethylphosphonate (**3.42**) was accessed from tritylamine, formaldehyde and dimethyl phosphit by a literature procedure.[71] It was deprotected by refluxing with 6 M HCl for 6 h. The hydrochloride salt was transformed into the free aminomethylphosphonic acid by ion exchange chromatography (Dowex 50, H^+, water as eluent). The labeled aminomethylphosphonic acids were deprotected and purifed similarly (Scheme 3.18).

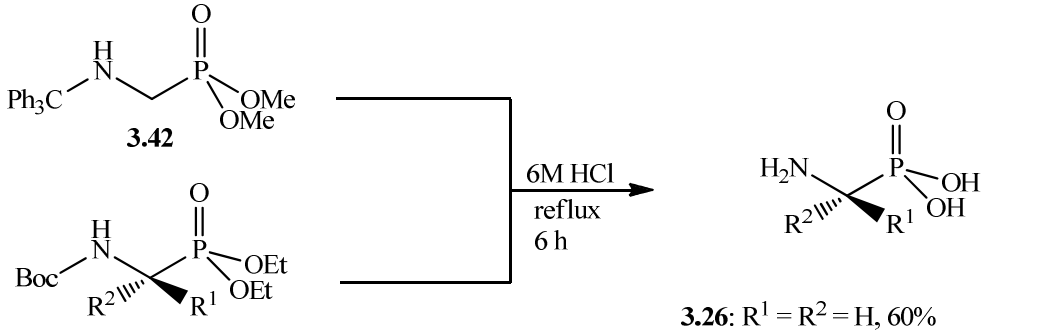

(*R*)-[D_1]**3.37**: $R^1 = H$, $R^2 = D$
(*S*)-[D_1]**3.37**: $R^1 = D$, $R^2 = H$

3.26: $R^1 = R^2 = H$, 60%
(*R*)-[D_1]**3.26**: $R^1 = H$, $R^2 = D$, 41%
(*S*)-[D_1]**3.26**: $R^1 = D$, $R^2 = H$, 20%

Scheme 3.18 - Sequence leading to the free AMPA

As with the hydroxymethylphosphonic acid, it was impossible at this stage to determine the enantiomeric excess without derivatization. The procedure that was used was very similar to the

one used with the hydroxymethylphosphonic acid, but in reverse order of the steps (Scheme 1.19).

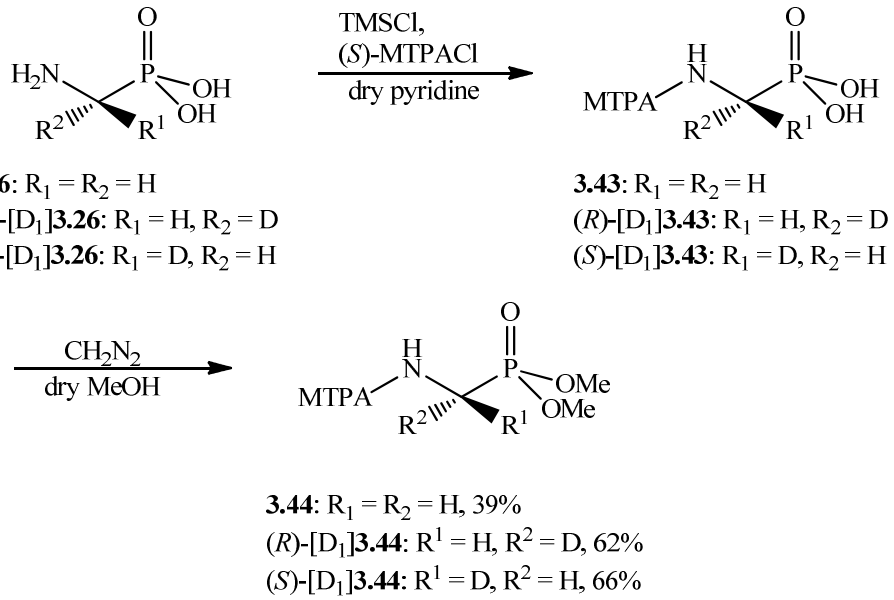

3.26: $R_1 = R_2 = H$
(*R*)-[D_1]**3.26**: $R_1 = H$, $R_2 = D$
(*S*)-[D_1]**3.26**: $R_1 = D$, $R_2 = H$

3.43: $R_1 = R_2 = H$
(*R*)-[D_1]**3.43**: $R_1 = H$, $R_2 = D$
(*S*)-[D_1]**3.43**: $R_1 = D$, $R_2 = H$

3.44: $R_1 = R_2 = H$, 39%
(*R*)-[D_1]**3.44**: $R^1 = H$, $R^2 = D$, 62%
(*S*)-[D_1]**3.44**: $R^1 = D$, $R^2 = H$, 66%

Scheme 3.19 - Derivatization of AMPA for the determination of enantiomeric excess

At first, in pyridine insoluble aminomethyl- and (*R*)-amino-[D_1]methylphosphonic acids, not recrystallized after ion exchange chromatography, were silylated to give the soluble species with TMSCl, which then reacted with (*S*)-MTPACl to (*R*)-Mosher amides. These amides were esterified in dry methanol with a distilled ethereal solution of diazomethane. Similarly, the (*S*)-amino[D_1]methylphosphonic acid was converted to the (*S*)-Mosher amide with (*R*)-MTPACl and finally esterified with diazomethane. The (*S*)-Mosher amide was used here, because the signal of the PCHD group of the (*R*)-Mosher amide overlapped with the resonances of the MeO groups at phosphorous, prohibiting the determination of the enantiomeric excess (Figure 3.8).

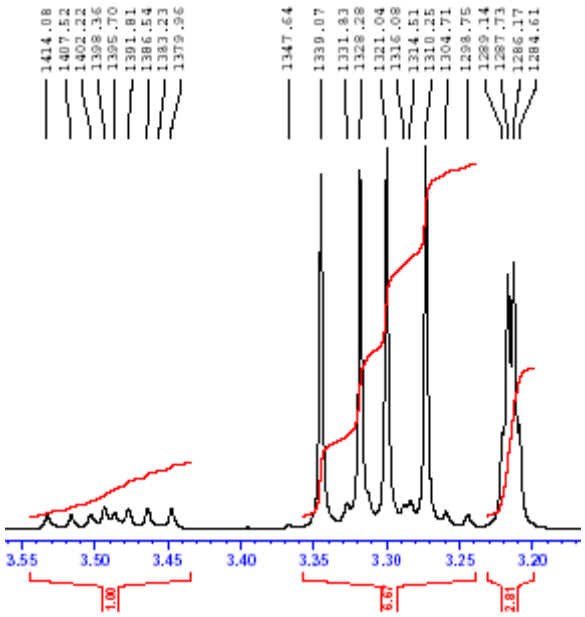

Figure 3.8 - Segment of ^{1}H NMR spectrum (400.13 MHz, toluene-d_8) with the AB-system of the PCH_2 group overlapping with the MeO signal of the (*R*)-Mosher amide derived from AMPA

The enantiomeric excesses of both enantiomers of amino-[D_1]methylphosphonic acids were found to be greater than 94%. The absolute configurations of the enantiomers were assigned on the basis of the known stereochemistry of the involved steps (Figure 3.9).

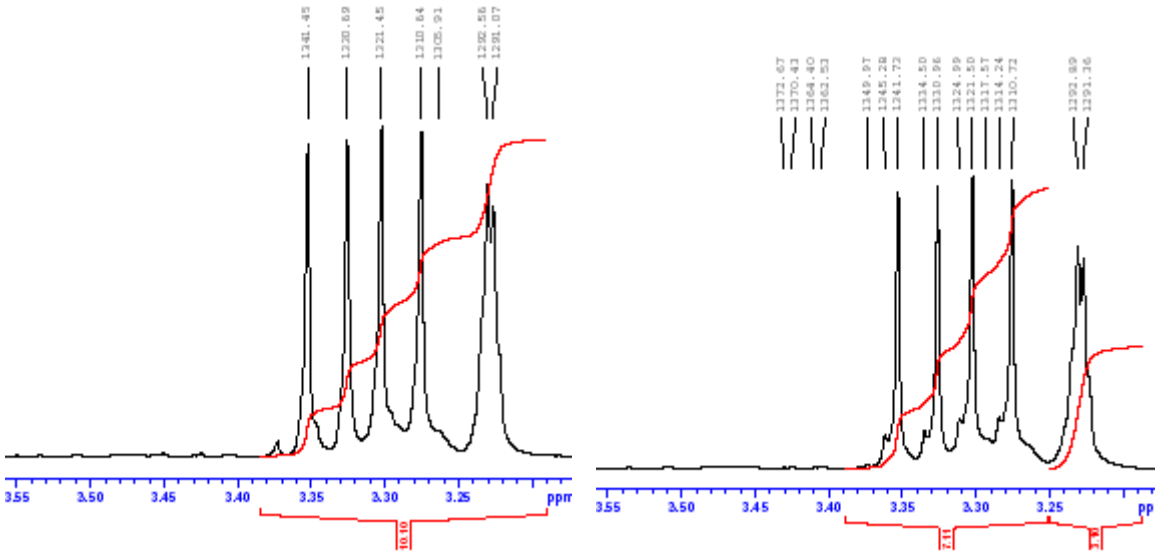

(*R*)-Mosher amide ((*R*)-[D_1]**3.44**) (*S*)-Mosher amide ((*S*)-[D_1]**3.44**)

Figure 3.9 - Segment of ^{1}H NMR (400.13 MHz, Toluene) of PCHD peaks of (*R*)-Mosher amides derived from labeled AMPA

4 Experimental

4.1 General Remarks

Flash chromatography was performed with Merck silica gel 60 (230-400 mesh). Reactions and flash (column) chromatography were monitored by TLC carried out on 0.25 mm thick, silica gel 60, F_{254} Merck plates. The spots were visualized, unless otherwise specified, by UV and/or dipping the plate into a solution of $(NH_4)_6Mo_7O_{24}\cdot 4\ H_2O$ (23.0 g) and $Ce(SO_4)_2\cdot 4\ H_2O$ (1.0 g) in 10% aqueous H_2SO_4 (500 ml) and heating with a heat gun.

$^1H/^{13}C$ NMR spectra were measured at 300 K on Bruker Avance DRX 400 (^1H: 400.13 MHz, ^{13}C: 100.61 MHz, ^{31}P: 161.98 MHz), AV 400 (^1H: 400.27 MHz, ^{13}C: 100.65 MHz, ^{31}P: 162.03 MHz) and DRX 600 (^1H: 600.13 MHz, ^{13}C: 150. 92 MHz, ^{31}P: 242.94 MHz). The spectra were referenced to residual $CHCl_3$ (δ_H = 7.24)/toluene-d_8 (CHD_2: δ_H = 2.09)/HOD (δ_H = 4.80) or $CDCl_3$ (δ_C = 77.00)/toluene-d_8 (CHD_2: δ_C = 21.04).

IR spectra were recorded on a silicon disc (Si) on a Perkin-Elmer 1600 FT-IR spectrometer or by using ATR on a Bruker VERTEX 70 IR spectrometer or Perkin-Elmer Spectrum 2000 FT-IR spectrometer.

Optical rotations were measured at 20°C on a Perkin-Elmer 141 polarimeter in a 1 dm cell.

Melting points were measured with a Reichert Thermovar instrument and are uncorrected.

Dry THF (over K) and Et_2O (over $LiAlH_4$) were used right after distillation. TMEDA was refluxed over CaH_2, distilled and stored over molecular sieves (4 Å).

All of the other chemicals were used as supplied from Aldrich, Fluka, Merck or Acros.

4.2 Chapter 1

Tributyl(fluoromethyl)stannane (1.62)

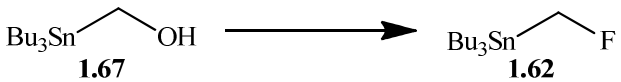

1.67 **1.62**

A solution of bis(2-methoxyethyl)aminosulfur trifluoride (Deoxo-Fluor®, 7.2 mmol, 3.06 ml, ~50% in toluene) and tributylstannylmethanol (**1.67**, 1.173 g, 3.6 mmol) in dry THF (20 ml) was stirred at room temperature for 1 h and concentrated under reduced pressure.[15] The residue was

purified by flash chromatography (hexane, R_f = 0.84) to yield stannane **1.62** (0.770 g, 66%) as a colorless oil.

^{1}H NMR (400.13 MHz, $CDCl_3$): δ = 5.07 (d, J = 47.3 Hz, 2H, FCH_2), 1.60-1.48 (m, 6H, 3x$SnCH_2\underline{CH_2}$), 1.29 (sext, J = 7.3 Hz, 3x$Sn(CH_2)_2\underline{CH_2}$), 1.03-0.93 (m, 6H, $SnCH_2$), 0.88 (t, J = 7.3 Hz, 9H, 3xCH_3).

(*R*)-Tributylstannylmethyl 1-(2-naphthyl)ethyl sulfide [(*R*)-1.69]

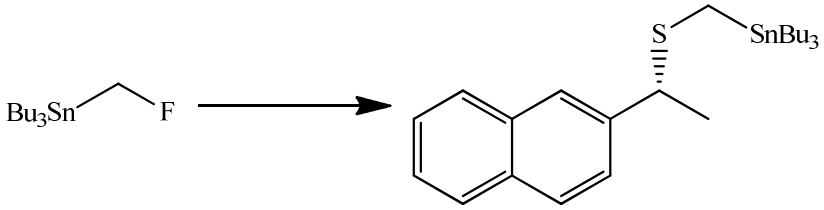

1.62 (*R*)-**1.69**

*n*BuLi (0.2 mmol, 0.125 ml, 1.6M in hexane) was added to a stirred mixture of (*R*)-1-(2-naphthyl)ethylthiol [(*R*)-**1.68**, 0.038 g, 0.2 mmol] in dry THF (3 ml) at 0˚C.[15] After stirring for 15 min, tributyl(fluoromethyl)stannane (**1.62**, 0.043 g, 0.13 mmol) was added and stirring was continued for 18 h at room temperature. The solution was concentrated under reduced pressure and water was added. The mixture was extracted three times with Et_2O and the combined organic layers were washed with water, dried (Na_2SO_4) and concentrated under reduced pressure. The residue was purified by flash chromatography (hexane:dichloromethane = 10:1, R_f = 0.42) to give sulfide (*R*)-**1.69** (0.023 g, 37%) as a colorless oil.

The ^{1}H NMR spectrum was identical to the spectrum reported in the literature.[15]

1-Fluoro-2-phenyl-2-propanol (1.66)

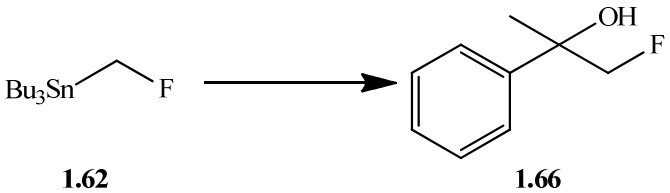

1.62 **1.66**

Methyllithium (0.92 mmol, 0.92 ml, 1M, prepared by mixing a 3M solution in diethoxymethane with dry THF) was added in drops (1 drop every 5 s) to a solution of acetophenone (0.92 mmol, 0.46 ml, 2M in dry THF) and tributyl(fluoromethyl)stannane (**1.62**, 0.149 g, 0.46 mmol) in dry

THF (3 ml) under argon at -95˚C. After stirring for 5 min trifluoroacetic acid (1.012 mmol, 0.506 ml, 2M in CH_2Cl_2) and water were added. The mixture was extracted three times with CH_2Cl_2. The combined organic layers were dried (Na_2SO_4) and concentrated under reduced pressure. The residue (ratio of tributyl(fluoromethyl)stannane (**1.62**):1-fluoro-2-phenyl-2-propanol (**1.66**):2-phenyl-2-propanol (**1.65**):tributylmethylstannane = 1.16:1.03:1.09:1.00, by ^{1}H NMR) was purified by flash chromatography (hexane:ethyl acetate = 10:1, R_f = 0.19 for both alcohols) to give a mixture of the racemic 1-fluoro-2-phenyl-2-propanol and 2-phenyl-2-propanol, (0.059 g, 82%) in a molar ratio of 1.00:0.80 as a colorless oil.

1-Fluoro-2-phenyl-2-propanol (**1.66**)

^{1}H NMR (400.27 MHz, $CDCl_3$): δ = 7.50-7.20 (m, 5H, CH_{ar}), 4.43 (AB-system that couples with F, J_{AB} = 9.2 Hz, J_{AF} = J_{BF} = 48.1 Hz, 2H, FCH_2), 1.59 (d, J_{FH} = 2.1 Hz, 3H, CH_3), 1.90 (br. s, 1H, OH).

2-Phenyl-2-propanol (**1.65**)

^{1}H NMR (400.27 MHz, $CDCl_3$): δ = 7.50-7.20 (m, 5H, CHar), 1.58 (s, 6H, 2xCH_3), 1.90 (br. s, 1H, OH).

The same reaction was performed at -78˚C with tributyl(fluoromethyl)stannane (**1.62**, 0.122 g, 0.38 mmol) with the resulting ratio of tributyl(fluoromethyl)stannane (**1.62**):1-fluoro-2-phenyl-2-propanol (**1.66**):2-phenyl-2-propanol (**1.65**):tributylmethylstannane = 1.00:0.44:1.16:0.39, by ^{1}H NMR). Purification by flash chromatography yielded a mixture (0.049 g, 83%) as a colorless oil: racemic 1-fluoro-2-phenyl-2-propanol (**1.66**) and 2-phenyl-2-propanol (**1.65**) in a molar ratio of 1.00:2.90.

(*R*)-Mosher esters of 1-fluoro-2-phenyl-2-propanol (1.71)

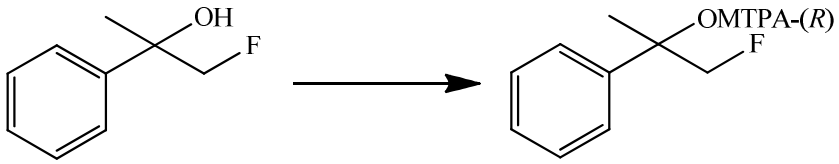

1.66 **1.71**

A solution of (*S*)-MTPACl (0.18 mmol, 0.342 ml, 0.53M in dry dioxane), 1-fluoro-2-phenyl-2-propanol (**1.66**, contained **1.65**, 14 mg, 0.09 mmol), DMAP (0.044 g, 0.36 mmol) and dry dioxane (2 ml) was stirred under argon for 9 h at 50˚C. HCl (2M) was added and it was extracted

three times with CH_2Cl_2. The combined organic layers were washed with a saturated aqueous solution $NaHCO_3$, dried (Na_2SO_4) and concentrated under reduced pressure. The crude product was purified by flash chromatography (hexane:ethyl acetate = 10:1, R_f = 0.35) to give a mixture of diastereomeric Mosher esters **1.71** (14.6 mg, 44%) in a ratio of 3.00:1.88 (^{1}H NMR, signals for OCH_3 at 3.59 and 3.53 ppm) as a colorless oil.

^{1}H NMR (400.27 MHz, $CDCl_3$): δ = 7.70-7.10 (m, CH_{ar}), 4.71 (AB-system, that couples with F, J_{AB} = 9.8 Hz, J_{HF} = 47.7 Hz, 2H, FCH_2, minor diast.), 4.56 (AB-system that couples with F, J_{AB} = 9.9 Hz, J_{HF} = 45.6 Hz, 2H, FCH_2, major diast.), 3.59 (q, J = 1.2 Hz, 3H, OCH_3, major diast.), 3.53 (q, J = 1.0 Hz, 3H, OCH_3, minor diast.), 2.04 (d, J_{HF} = 2.3 Hz, 3H, CH_3, major diast.), 1.94 (d, J_{HF} = 2.3 Hz, 3H, CH_3, minor diast.).

4.3 Chapter 2

Phenyl- and (*R*)-phenyl-[D$_1$]methanol [2.32 and (*R*)-[D$_1$]2.32]

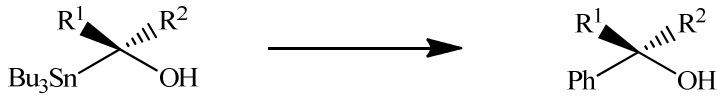

1.67: $R^1 = R^2 = H$
(*S*)-[D$_1$]**1.67**: R^1 = D, $R^2 = H$

2.32: $R^1 = R^2 = H$
(*R*)-[D$_1$]**2.32**: R^1 = D, $R^2 = H$

Dry 1,4-dioxane (4 ml) and bromobenzene (0.141 g, 0.9 mmol, 0.094 ml) were added to tributylstannylmethanol (**1.67**, 0.435 g, 1.35 mmol) and $Pd(PPh_3)_4$ under argon at room temperature.[44] The mixture was stirred for 18 h at 80˚C. After cooling to room temperature it was concentrated under reduced pressure and purified by flash chromatography (hexane:ethyl acetate = 5:1, R_f = 0.32) to yield phenylmethanol (**2.32**, 0.055 g, 57%) as a colorless liquid.

^{1}H NMR (400.13 MHz, $CDCl_3$): δ = 7.36-7.32 (m, 4H, CH_{ar}), 7.30-7.25 (m, 1H, CH_{ar}), 4.67 (s, 2H, CH_2).
^{13}C (100.61 MHz, $CDCl_3$): δ = 140.90 (C_{ar}), 128.56 (2xCH_{ar}), 127.66 (CH_{ar}), 127.01 (2xCH_{ar}), 65.35 (CH_2).

(*R*)-Phenyl-[D$_1$]methanol [(*R*)-[D$_1$]**2.32**]

Similarly, (*S*)-tributylstannyl-[D$_1$]methanol [(*S*)-[D$_1$]**1.67**, 0.312 g, 0.97 mmol] was converted to (*R*)-phenyl-[D$_1$]methanol [(*R*)-[D$_1$]**2.32**, 0.040 g, 38%].

^{1}H NMR (400.27 MHz, $CDCl_3$): δ = 7.38-7.33 (m, 4H, CH_{ar}), 7.32-7.25 (m, 1H, CH_{ar}), 4.66 (t, J = 1.8 Hz, 1H, CHD).

(*R*)-Mosher ester of (*R*)-phenyl-[D_1]methanol [(*R*)-[D_1]2.33]

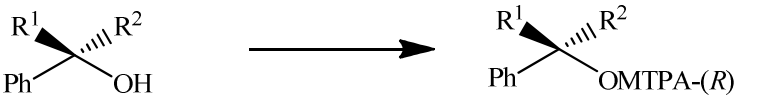

(*R*)-[D_1]**2.32**: R^1 = D, R^2 = H (*R*)-[D_1]**2.33**: R^1 = D, R^2 = H

A mixture of dry pyridine (0.480 g, 6.1 mmol, 0.49 ml), (*S*)-MTPACl (0.295 mmol, 0.60 ml, 0.53M in CH_2Cl_2) and (*R*)-phenyl-[D_1]methanol [(*R*)-[D_1]**2.32**, 0.021 g, 0.19 mmol] in dry CH_2Cl_2 (4 ml) was stirred for 18 h under argon at room temperature. After the addition of water (5 ml) stirring was continued for another 5 min. CH_2Cl_2 and HCl (1M) were added and the phases were separated. The aqueous layer was extracted twice with CH_2Cl_2. The combined organic layers were washed with a saturated aqueous solution of $NaHCO_3$, dried (Na_2SO_4) and concentrated under reduced pressure. The crude product was purified by flash chromatography (hexane:ethyl acetate = 10:1, R_f = 0.38) to yield Mosher ester (*R*)-[D_1]**2.33** (0.033 g, 53%, ee ≥ 99%) as a colorless oil.

^{1}H NMR (400.27 MHz, $CDCl_3$): δ = 7.46-7.41 (m, 2H, CH_{ar}), 7.40-7.30 (m, 8H, CH_{ar}), 5.33 (broadened s, 1H, CHD), 3.50 (q, J = 1.3 Hz, 3H, OCH_3).

1-Tributylstannylmethyl-, (*R*)- and (*S*)-tributylstannyl-[D_1]methyl benzoate [2.35, (*R*)- and (*S*)-[D_1]2.35]

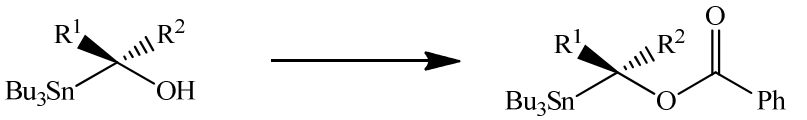

1.67: R^1 = R^2 = H **2.35**: R^1 = R^2 = H
(*R*)-[D_1]**1.67**: R^1 = H, R^2 = D (*R*)-[D_1]**2.35**: R^1 = H, R^2 = D
(*S*)-[D_1]**1.67**: R^1 = D, R^2 = H (*S*)-[D_1]**2.35**: R^1 = D, R^2 = H

A mixture of dry CH_2Cl_2 (4.6 ml), dry pyridine (0.487 g, 6.16 mmol, 0.496 ml), benzoyl chloride (0.433 g, 2.08 mmol, 0.358 ml) and tributylstannylmethanol (**1.67**, 0.496 g, 1.54 mmol) was stirred for 20 h under argon at room temperature. After the addition of water (2 ml) it was stirred for another 10 min. HCl (1M) and CH_2Cl_2 were added and the phases were separated. The

aqueous layer was extracted with CH_2Cl_2 and the combined organic layers were washed with a saturated solution of $NaHCO_3$, dried ($MgSO_4$) and concentrated under reduced pressure. The crude product was purified by flash chromatography (hexane:CH_2Cl_2 = 1:1, R_f = 0.80) to yield benzoate **2.35** (0.551g, 84%) as a colorless oil.

IR (ATR): ν = 2955, 2922, 1708, 1315, 1290, 1105.

^{1}H NMR (400.27 MHz, $CDCl_3$): δ = 8.01-7.95 (m, 2H, CH_{ar}), 7.54-7.49 (m, 1H, CH_{ar}), 7.43-7.37 (m, 2H, CH_{ar}), 4.41 (s, $J(^{117/119}Sn)$ = 11.8 Hz, 2H, CH_2), 1.61-1.41 (m, 6H, 3x $SnCH_2\underline{CH_2}$), 1.27 (sext, J = 7.3 Hz, 6H, 3x$Sn(CH_2)_2\underline{CH_2}$), 1.03-0.86 (m, 6H, 3x$SnCH_2$), 0.85 (t, J = 7.3 Hz, 9H, 3xCH_3).

^{13}C NMR (100.61 MHz, $CDCl_3$): δ = 132.53 (CH_{ar}), 129.36 (2xCH_{ar}), 128.16 (2xCH_{ar}), 56.41 (CH_2), 29.00 ($J(^{117/119}Sn)$ = 21.2 Hz, 3x$SnCH_2\underline{CH_2}$), 27.29 ($J(^{117/119}Sn)$ = 53.4 Hz, 3x$Sn(CH_2)_2\underline{CH_2}$), 13.68 ($CH_3$), 9.69 ($J(^{117/119}Sn)$ = 319.3 Hz, $SnCH_2$), C=O and C_q n.d.

(*R*)-Tributylstannyl-[D_1]methyl benzoate [(*R*)-[D_1]**2.35**]

Similarly, (*R*)-tributylstannyl-[D_1]methanol [(*R*)-[D_1]**1.67**, 0.327 g, 1.01 mmol] was converted to (*R*)-tributylstannyl-[D_1]methyl benzoate [(*R*)-[D_1]**2.35**, 0.369 g, 90%, $[\alpha]_D^{20}$ = -1.24 (c = 18.5), acetone].

(*S*)-Tributylstannyl-[D_1]methyl benzoate [(*S*)-[D_1]**2.35**]

Similarly, (*S*)-tributylstannyl-[D1]methanol [(*S*)-[D_1]**1.67**, 0.334 g, 1.00 mmol] was converted to (*S*)-1-tributylstannyl-[D_1]methyl benzoate [(*S*)-[D_1]**2.35**, 0.351 g, 82%].

^{1}H and ^{13}C NMR spectra for (*R*)- and (*S*)-1-tributylstannyl-[D_1]methanyl benzoate were identical:

^{1}H NMR (400.27 MHz, $CDCl_3$): δ = 8.01-7.95 (m, 2H, CH_{ar}), 7.54-7.48 (m, 1H, CH_{ar}), 7.43-7.38 (m, 2H, CH_{ar}), 4.39 (broadened s, 1H, CHD),1.61-1.41 (m, 6H, 3x $SnCH_2\underline{CH_2}$), 1.27 (sext, J = 7.3 Hz, 6H, 3x$Sn(CH_2)_2\underline{CH_2}$), 1.03-0.86 (m, 6H, 3x$SnCH_2$), 0.85 (t, J = 7.3 Hz, 9H, 3xCH_3).

^{13}C NMR (100.61 MHz, $CDCl_3$): δ = 132.52 (CH_{Ar}), 129.34 (2xCH_{Ar}), 128.27 (2xCH_{Ar}), 56.11 (t, J = 22.3 Hz, CHD), 29.00 ($J(^{117/119}Sn)$ = 21.2 Hz, 3x$SnCH_2\underline{CH_2}$), 27.30 ($J(^{117/119}Sn)$ = 53.4 Hz, 3x$Sn(CH_2)_2\underline{CH_2}$), 13.65 ($CH_3$), 9.66 ($J(^{117/119}Sn)$ = 319.3 Hz, $SnCH_2$), C=O and C_q n.d.

2-Phenyl-2-oxoethyl-, (*R*)- and (*S*)-2-phenyl-2-oxo-[1-D_1]ethyl benzoate [2.36, (*R*)- and (*S*)-[1-D_1]2.36]

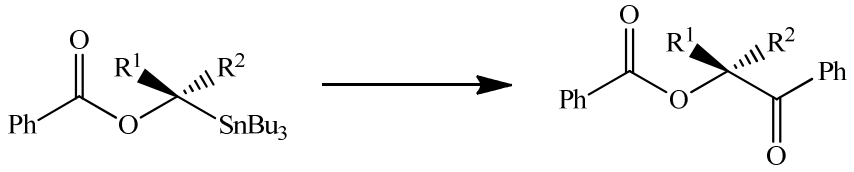

2.35: $R^1 = R^2 = H$
(*R*)-[D_1]**2.35**: $R^1 = D$, $R^2 = H$
(*S*)-[D_1]**2.35**: $R^1 = H$, $R^2 = D$

2.36: $R^1 = R^2 = H$
(*S*)-[1-D_1]**2.36**: $R^1 = D$, $R^2 = H$
(*R*)-[1-D_1]**2.36**: $R^1 = H$, $R^2 = D$

A mixture of benzoyl chloride (0.116 g, 0.82 mmol, 0.095 ml) tributylstannylmethyl benzoate (**2.35**, 0.366 g, 0.86 mmol), $(PPh_3)_2PdCl_2$ (25.3 mg, 0. 039 mmol, 4.5 mol %) and CuCN (8.1 mg, 0.09 mmol, 10.5 mol %) in dry toluene (8 ml) was stirred under argon at 70˚C for 18 h.[41] After cooling to room temperature it was concentrated under reduced pressure and purified by flash chromatography (hexane: ethyl acetate = 5:1, R_f = 0.53) to yield benzoate **2.36** (0.138 g, 67%, contained 28 mol % of an impurity possibly formed from the staring material losing a butyl group) as a crystalline solid.

IR (Si): ν = 2956, 2926, 1720, 1701, 1284.
^{1}H NMR (400.13 MHz, $CDCl_3$): δ = 8.15-8.11 (m, 2H, CH_{ar}), 8.09-8.03 (m, 1 H, CH_{ar}), 7.97-7.93 (m, 1H, CH_{ar}), 7.65-7.55 (m, 2 H, CH_{ar}), 7.52-7.43 (m, 4H, CH_{ar}), 5.56 (s, 2H, CH_2), significant signals of impurity: 4.14 (s, $J(^{117/119}Sn)$ = 27.5 Hz, 2H, OCH_2Sn), and signals for two butyl groups on Sn.

(*R*)-2-Phenyl-2-oxo-[1-D_1]ethyl benzoate [(*R*)-[1-D_1]**2.36**]

Similarly, (*S*)-1-tributylstannyl-[D_1]methyl benzoate [(*S*)-[D_1]**2.35**, 0.188 g, 0.44 mmol] was converted to (*R*)-2-phenyl-2-oxo-[1-D_1]ethyl benzoate [(*R*)-[1-D_1]**2.36**, 0.100 g, 94%, contained 18 mol % of Bu_3SnX and 2 mol % of the unlabeled species].

(*S*)-2-Phenyl-2-oxo-[1-D_1]ethyl benzoate [(*S*)-[1-D_1]**2.36**]

Similarly, (*R*)-1-tributylstannyl-[D_1]methyl benzoate [(*R*)-[D_1]**2.35**, 0.188 g, 0.44 mmol] was converted to (*S*)-2-phenyl-2-oxo-[1-D_1]ethyl benzoate [(*S*)-[1-D_1]**2.36**, 0.100 g, 94%, contained 26 mol % of the same impurity as the unlabeled species and 2 mol % of the unlabeled species].

^{1}H NMR spectra for (*R*)- and (*S*)-2-phenyl-2-oxo-[1-D_1]ethyl benzoate were identical:

^{1}H NMR (400.27 MHz, $CDCl_3$): δ = 8.16-8.10 (m, 2H, CH_{ar}), 7.98-7.93 (m, 2H, CH_{ar}), 7.62-7.55 (m, 2 H, CH_{ar}), 7.52-7.42 (m, 4H, CH_{ar}), 5.56 (s of the unlabeled species), 5.54 (t, J = 2.3 Hz, 1H, CHD).

1-Phenyl-, (*1RS,2R*)- and (*1RS,2S*)-1-phenyl-1,2-[2-D_1]ethanediol [2.37, (*1RS,2R*)- and (*1RS, 2S*)-[2-D_1]2.37]

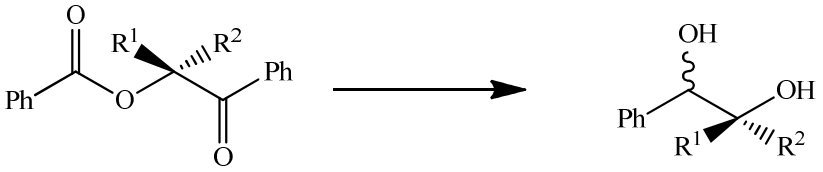

2.36: $R^1 = R^2 = H$
(*R*)-[1-D_1]**2.36**: $R^1 = H$, $R^2 = D$
(*S*)-[1-D_1]**2.36**: $R^1 = D$, $R^2 = H$

2.37: $R^1 = R^2 = H$
(*2R*)-[2-D_1]**2.37**: $R^1 = H$, $R^2 = D$
(*2S*)-[2-D_1]**2.37**: $R^1 = D$, $R^2 = H$

A solution of 2-phenyl-2-oxoethyl benzoate (**2.36**, 0.132 g, 0.50 mmol) in dry THF (2 ml) was added drop wise to $LiAlH_4$ (2 ml, 2M in THF) under argon at 0˚C. It was then stirred at room temperature for 1 h. After cooling to 0˚C, ethyl acetate (2 ml) was carefully added followed by more ethyl acetate and HCl (2M) were added after 15 min at 0˚C and the phases were separated. The aqueous layer was extracted twice with ethyl acetate. The combined organic layers were washed with a saturated aqueous solution of $NaHCO_3$, dried (Na_2SO_4) and concentrated under reduced pressure. The residue was purified by flash chromatography (hexane:ethyl acetate = 1:1, R_f = 0.24) to yield a crystalline diol **2.37** (0.022 g, 32%).

^{1}H NMR (400.13 MHz, $CDCl_3$): δ = 7.37-7.34 (m, 8H, CH_{ar}), 7.31-7.28 (m, 2H, CH_{ar}), 4.82 (d, J = 4.7 Hz, 1H, OCH), 4.82 (d, J = 11.5 Hz, 1H, OCH), 3.76 (dd, J = 11.6, 4.0 Hz, 2H, CH_2), 3.66 (dd, J = 11.2, 8.2 Hz, 2H, CH_2).

(*1RS,2R*)-1-Phenyl-1,2-[2-D_1]ethanediol [(*1RS,2R*)-[2-D_1]**2.37**]

Similarly, (*R*)-2-phenyl-2-oxo-[1-D_1]ethyl benzoate [(*R*)-[1-D_1]**2.36**, 0.095 g, 0.39 mmol] was converted to (*R*)-1-phenyl-1,2-[2-D_1]ethanediol [(*1RS,2R*)-[2-D_1]**2.37**, 0.032 g, 59%].

(*1RS,2S*)-1-Phenyl-1,2-[2-D_1]ethanediol [(*1RS,2S*)-[2-D_1]**2.37**]

Similarly, (*S*)-2-phenyl-2-oxo-[1-D_1]ethyl benzoate [(*S*)-[1-D_1]**2.36**, 0.104 g, 0.43 mmol] was converted to (*S*)-1-phenyl-1,2-[2-D_1]ethanediol [(*1RS,2S*)-[2-D_1]**2.37**, 0.02 g, 37%].

^{1}H and ^{13}C NMR spectra for (*R*)- and (*S*)-1-phenyl-1,2-[2-D_1]ethanediol were identical:

^{1}H NMR (400.27 MHz, $CDCl_3$): δ = 7.37-7.34 (m, 8H, CH_{ar}), 7.31-7.28 (m, 2H, CH_{ar}), 4.80 (d, *J* = 8.0 Hz, 1H, OCH), 4.80 (d, *J* = 3.7 Hz, 1H, OCH), 3.73 (td, *J* = 1.6 Hz, 3.3 Hz, 1H, CHD), 3.63 (td, *J* = 1.5 Hz, 8.2 Hz, 1H, CHD).

^{13}C NMR (100.65 MHz, $CDCl_3$): δ = 140.49 (C_{ar}), 128.55 (2xCH_{ar}), 128.02 (CH_{ar}), 126.04 (2xCH_{ar}), 74.62 and 74.61 (CH of the two diastereomers), 67.75 (t, *J* = 20.8 Hz) and 67.69 (t, *J* = 22.7 Hz) (CHD of the two diastereomers).

(*R*)-Mosher esters of (*1RS,2R*)- and (*1RS,2S*)-1-phenyl-1,2-[2-D_1]ethanediol [(*1RS,2R*)- and (*1RS, 2S*)-[2-D_1]2.38]

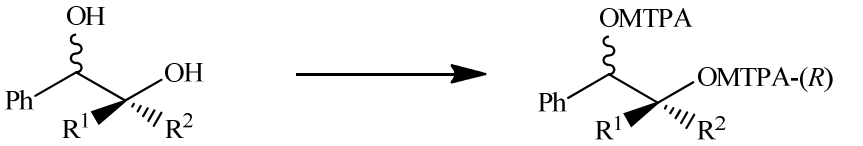

(*2R*)-[2-D_1]**2.37**: R^1 = H, R^2 = D
(*2S*)-[2-D_1]**2.37**: R^1 = D, R^2 = H

(*2R*)-[2-D_1]**2.38**: R^1 = H, R^2 = D
(*2S*)-[2-D_1]**2.38**: R^1 = D, R^2 = H

A mixture of dry pyridine (0.40 ml), (*S*)-MTPACl (1.14 ml of a 0.53M solution in dry CH_2Cl_2) and (*1RS,2R*)-1-phenyl-1,2-[2-D_1]ethanediol [(*1RS,2R*)-[2-D_1]**2.37**, 0.019 g, 0.14 mmol] in dry CH_2Cl_2 (3 ml) was stirred under argon at room temperature for 18 h. After the addition of water (0.40 ml) and stirring for 5 min, CH_2Cl_2 and HCl (2M) were added. The phases were separated and the aqueous layer was extracted twice with CH_2Cl_2. The combined organic layers were washed with a saturated aqueous solution of $NaHCO_3$, dried (Na_2SO_4) and concentrated under reduced pressure. The residue was purified by flash chromatography (hexane:ethyl acetate = 10:1, R_f = 0.38) to yield a 1:1 mixture of diastereomeric (*R*)-Mosher esters (*1RS,2R*)-[2-D_1]**2.38** (0.049 g, 61%, ee > 99%, contained 2% of the unlabeled species) as a colorless oil.

^{1}H NMR (400.27 MHz, $CDCl_3$): δ = 7.45-7.41 (m, 2H, CH_{ar}), 7.39-7.26 (m, 26H, CH_{ar}), 7.20-7.16 (m, 2H, CH_{ar}), 6.26 (d, *J* = 3.9 Hz, 1H, CH), 6.14 (d, *J* = 8.7 Hz, 1H, CH), 4.63 (broadened d, *J* = 3.9 Hz, 1H, CHD), 4.47 (broadened d, *J* = 8.7 Hz, 1H, CHD), 3.45 (q, *J* = 1.0 Hz, 3H, OCH_3), 3.38 (q, *J* = 1.0 Hz, 3H, OCH_3), 3.34 (q, *J* = 1.0 Hz, 3H, OCH_3), 3.32 (q, *J* = 1.3 Hz, 3H, OCH_3).

(*R*)-Mosher esters of (*1RS,2S*)-1-phenyl-1,2-[2-D_1]ethanediol [(*1RS,2S*)-[2-D_1]**2.38**]

Similarly, (*1RS,2S*)-1-phenyl-1,2-[2-D_1]ethanediol [(*1RS,2S*)-[2-D_1]**2.37**, 0.010 g, 0.07 mmol] was converted to a 1:1 mixture of (*R*)-Mosher esters of the (*1RS,2S*)-1-phenyl-1,2-[2-D_1]ethanediol [(*1RS, 2S*)-[2-D_1]**2.38**, 0.028 g, 70%, ee > 99%, contained 2% of the unlabeled species].

^{1}H NMR (400.27 MHz, $CDCl_3$): δ = 7.45-7.41 (m, 2H, CH_{ar}), 7.39-7.26 (m, 26H, CH_{ar}), 7.20-7.16 (m, 2H, CH_{ar}), 6.26 (d, *J* = 7.4 Hz, 1H, CH), 6.15 (d, *J* = 2.8 Hz, 1H, CH), 4.64 (broadened d, *J* = 2.8 Hz, 1H, CHD), 4.46 (broadened d, *J* = 7.4 Hz, 1H, CHD), 3.45 (q, *J* = 1.1 Hz, 3H, OCH_3), 3.39 (q, *J* = 1.1 Hz, 3H, OCH_3), 3.35 (q, *J* = 1.0 Hz, 3H, OCH_3), 3.34 (q, *J* = 1.1 Hz, 3H, OCH_3).

2-Benzylthio-1-phenylethanone (2.42a, reference sample)

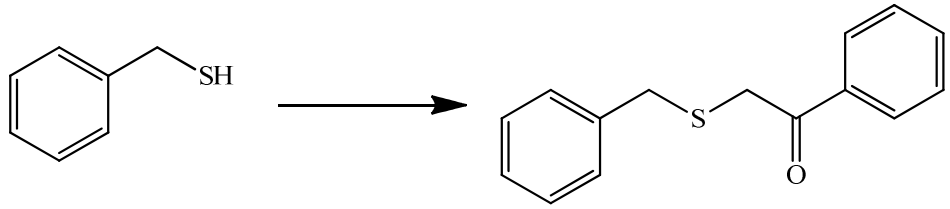

2.49 **2.42a**

A mixture of 2-chloroacetophenone (0.773 g, 5.0 mmol), potassium *t*-butylate (0.617 g, 5.5 mmol) and benzyl mercaptane (**2.49**, 0.621 g, 5.0 mmol) in dry methanol (20 ml) was stirred at room temperature for 18 h.[45] HCl (2M, 2 ml), water and CH_2Cl_2 were added and the phases were separated. The aqueous layer was extracted twice with CH_2Cl_2. All three organic layers were combined and washed with water, dried (Na_2SO_4) and concentrated under reduced pressure. The crude product was purified by flash chromatography (hexane:ethyl acetate = 10:1, R_f = 0.51) and recrystallized from ethanol to give the ketone **2.42a** (0.839 g, 69%) as colorless crystals; mp. 87-88˚C (lit.: [72] 89˚C).

^{1}H NMR (400. 27 MHz, $CDCl_3$): δ = 7.94-7.89 (m, 2H, CH_{ar}), 7.58-7.52 (m, 1H, CH_{ar}), 7.47-7.40 (m, 2H, CH_{ar}), 7.36-7.26 (m, 4H, CH_{ar}), 7.25-7.23 (m, 1H, CH_{ar}), 3.75 (s, 2H, $C(O)CH_2$), 3.66 (s, 2H, SCH_2).

^{13}C NMR (100.65 MHz, $CDCl_3$): δ = 194.43 (C=O), 137.30 (C_{ar}), 135.47 (C_{ar}), 133.31 (CH_{ar}), 129.26 (2xCH_{ar}), 128.69 (2xCH_{ar}), 128.64 (2xCH_{ar}), 128.53 (2xCH_{ar}), 127.23 (CH_{ar}), 36.17 ($C(O)CH_2$), 35.95 (SCH_2).

(±)-2-Benzylthio-1-phenylethanol (2.43, reference sample)

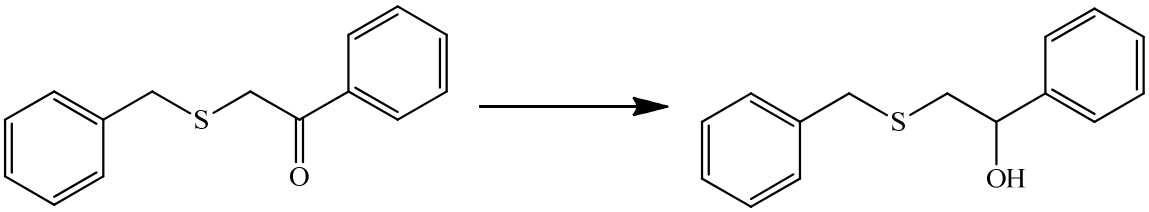

2.42a **2.43**

A mixture of $LiAlH_4$ (0.056 g, 1.5 mmol) and 2-benzylthio-1-phenylethanone (**2.42a**, 0.242 g, 1 mmol) in dry THF (13 ml) was stirred under argon for 2 h at room temperature. After the addition of acetone (0.15 ml) stirring was continued for 10 min. HCl (2M, 2ml) and water (30 ml) were added and the mixture was extracted three times with CH_2Cl_2. The combined organic layers were washed with water, dried (Na_2SO_4) and concentrated under reduced pressure. The residue was purified by flash chromatography (CH_2Cl_2, R_f = 0.53) and recrystallized from diisopropyl ether and hexane to yield the alcohol **2.43** (0.234 g, 96%) as colorless crystals; mp. 49-50˚C (lit.:[73] 47-48˚C)

IR (ATR): 3351, 2919, 1453, 1198, 1053, 987.

^{1}H NMR (400. 27 MHz, $CDCl_3$): δ = 7.35-7.21 (m, 10H, CH_{ar}), 4.66 (dd, J = 9.2, 3.7 Hz, 1H, CHOH), 3.71 (AB system, J_{AB} = 14.2 Hz, 2H, $PhCH_2S$), 2.71 (AB part of ABX-system, J_{AB} = 14. 0 Hz, J_{AX} = 3.7 Hz, J_{BX} = 9.2 Hz, 2H, SCH_2), 2.45 (br.s, 1H, OH).

^{13}C NMR (100.65 MHz, $CDCl_3$): δ = 142.50 (C_{ar}), 137.89 (C_{ar}), 128.94 (2xCH_{ar}), 128.64 (2xCH_{ar}), 128.49 (2xCH_{ar}), 127.85 (CH_{ar}), 127.26 (CH_{ar}), 125.74 (2xCH_{ar}), 71.76 (CH), 40.97 (CH$\underline{CH_2}$), 36.20 (SCH_2).

Dibenzylsulfide (2.47a, reference sample)

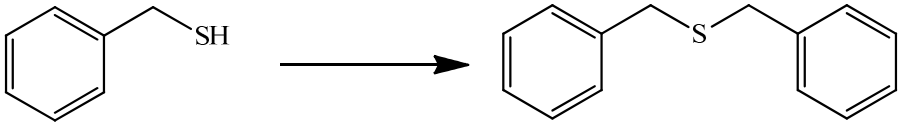

2.49 **2.47a**

A solution of benzyl chloride (0.253 g, 2.0 mmol), KOH (0.133 g, 2.37 mmol) and benzyl mercaptane (**2.49**, 0.248 g, 2.0 mmol) in ethanol (16 ml) was refluxed for 2 h, cooled and diluted with water.[47] The mixture was extracted twice with CH_2Cl_2. The combined organic layers were washed with a warm aqueous solution of KOH (25%), water and a saturated aqueous solution of

NaCl, dried (Na_2SO_4) and concentrated under reduced pressure. The crude product was purified by flash chromatography (hexane:ethyl acetate = 10:1, R_f = 0.68) to give the sulfide **2.47a** (0.410 g, 96%) as a colorless oil.

^{1}H NMR (400. 27 MHz, $CDCl_3$): δ = 7.29-7.16 (m, 10H, CH_{ar}), 3.56 (s, 4H, 2xSCH_2).

_S_-Tributylstannylmethyl thioacetate (2.45b)

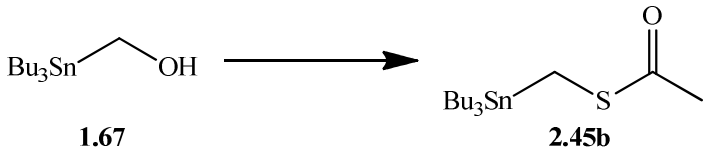

1.67 **2.45b**

A mixture of triphenylphosphane (0.882 g, 3.36 mmol) and DIAD (0.680 g, 3.36 mmol, 0.662 ml) in dry THF (8 ml) was stirred for 30 min under argon before a solution of tributylstannylmethanol (**1.67**, 0.864 g, 2.69 mmol) and thioacetic acid (0.409 g, 5.28 mmol, 0.385 ml) in dry THF (3 ml) was added.[49] The solution color changed from yellow to green and then turned back to yellowish brown after a few minutes. Stirring was continued for 16 h and then the reaction mixture was concentrated under reduced pressure. The residue was purified by flash chromatography (hexane:dichloromethane = 10:1, R_f = 0.11) to give the thioacetate **2.45b** (0.852 g, 84%) as a colorless oil.

IR (ATR): 2956, 2921, 1738, 1692, 1675, 1457, 1376, 1217, 1131.

^{1}H NMR (400. 27 MHz, $CDCl_3$): δ = 2.29 (s, 3H, CH_3), 2.04 (s, J($^{117/119}$Sn) = 34.4 Hz, 2H, SCH_2), 1.59-1.38 (m, 6H, 3xSnCH$_2$$\underline{CH_2}$), 1.29 (sext, J = 7.3 Hz, 6H, 3x$\underline{CH_2}CH_3$), 1.00-0.82 (m, 6H, 3x$SnCH_2$), 0.88 (t, J = 7.3 Hz, 9H, 3xCH_3).

^{13}C NMR (100.65 MHz, $CDCl_3$): δ = 198.96 (C=O), 29.83 (C(O)CH_3), 28.92 (J($^{117/119}$Sn) = 28.0 Hz, 3xSnCH$_2$$\underline{CH_2}$), 27.28 ($J$($^{117/119}$Sn) = 56.1 Hz, 3x$\underline{CH_2}CH_3$), 13.68 (3x$CH_3$), 10.01 ($J$($^{117/119}$Sn) = 341.6, 321.2 Hz, 3x$SnCH_2$), 4.99 (J($^{117/119}$Sn) = 216.7 Hz, SCH_2).

Anal. calcd. for $C_{15}H_{32}OSSn$: C 47.51%, H 8.51%, S 8.46%; found: C 47.48%, H 8.44%, S 8.57%.

Preparation of *N*-Tributylstannylmethyl- and (*R*)-*N*-tributylstannyl-[D_1]methylphthalimide [2.54 and (*R*)-[D_1]2.54]

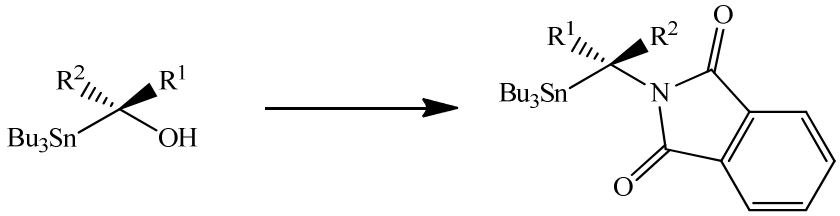

1.67: $R^1 = R^2 = H$
(*S*)-[D_1]**1.67**: $R^1 = D$, $R^2 = H$

2.54: $R^1 = R^2 = H$
(*R*)-[D_1]**2.54**: $R^1 = D$, $R^2 = H$

DEAD (0.982 g, 5.64 mmol, 0.888 ml) was added to a stirred mixture of tributylstannylmethanol (**1.67**, 1.497 g, 4.7 mmol), triphenylphosphane (1.48 g, 5.64 mmol), phthalimide (0.830 g, 5.64 mmol) in dry THF (23.5 ml) under argon at 0˚C and stirring was continued at room temperature for 16 h.[15] After the addition of water (few drops), it was concentrated under reduced pressure and purified by flash chromatography (hexane:ethyl acetate = 15:1, R_f = 0.57) to give phthalimide **2.54** (1.955 g, 92%) as a yellow oil.

^{1}H NMR (400.27 MHz, $CDCl_3$): δ = 7.80-7.75 (m, 2H, CH_{ar}), 7.67-7.62 (m, 2H, CH_{ar}), 3.22 (s, $J(^{117/119}Sn)$ = 13.3 Hz, 2H, NCH_2), 1.50-1.45 (m, 6H, 3x$SnCH_2\underline{CH_2}$), 1.25 (sext, J = 7.3 Hz, 6H, 3x$Sn(CH_2)_2\underline{CH_2}$), 0.95-0.90 (m, 6H, 3x$SnCH_2$), 0.83 (t, J = 7.3 Hz, 9H, 3xCH_3).
^{13}C NMR (100.65 MHz, $CDCl_3$): δ = 168.80 (2xC=O), 133.57 (2xCH_{ar}), 132.40 (2xC_{ar}), 122.77 (2xCH_{ar}), 28.90 ($J(^{117/119}Sn)$ = 20.9 Hz, 3x$SnCH_2\underline{CH_2}$), 27.26 ($J(^{117/119}Sn)$ = 54.4 Hz, 3x$Sn(CH_2)_2\underline{CH_2}$), 21.21 ($NCH_2$), 13.62 (3x$CH_3$), 10.46 ($J(^{117/119}Sn)$ = 318.1 Hz, 3x$SnCH_2$).

(*R*)-*N*-Tributylstannyl-[D_1]methylphthalimide [(*R*)-[D_1]**2.54**]

Similarly, (*S*)-tributylstannyl-[D_1]methanol [(*S*)-[D_1]**1.67**, 0.385 g, 1.2 mmol] was converted to (*R*)-*N*-tributylstannyl-[D_1]methylphthalimide [(*R*)-[D_1]**2.54**, 0.496 g, 91%, contained 2% of the unlabeled species].

^{1}H NMR (400.27 MHz, $CDCl_3$): δ = 7.80-7.75 (m, 2H, CH_{ar}), 7.67-7.62 (m, 2H, CH_{ar}), 3.22 (s, unlabeled species), 3.20 (broadened s, $J(^{117/119}Sn)$ = 26.1 Hz, 1H, NCHD), 1.50-1.45 (m, 6H, 3x$SnCH_2\underline{CH_2}$), 1.25 (sext, J = 7.3 Hz, 6H, 3x$Sn(CH_2)_2\underline{CH_2}$), 0.95-0.90 (m, 6H, 3x$SnCH_2$), 0.83 (t, J = 7.3 Hz, 9H, 3xCH_3).
^{13}C NMR (100.65 MHz, $CDCl_3$): δ = 168.83 (2xC=O), 133.56 (2xCH_{ar}), 132.37 (2xC_{ar}), 122.76 (2xCH_{ar}), 28.90 ($J(^{117/119}Sn)$ = 20.9 Hz, 3x$SnCH_2\underline{CH_2}$), 27.28 ($J(^{117/119}Sn)$ = 54.4 Hz,

3xSn(CH_2)$_2$<u>CH_2</u>), 20.98 (t, *J* = 21.6 Hz, NCH_2), 13.62 (3xCH_3), 10.44 (*J*($^{117/119}$Sn) = 318.1 Hz, 3xSnCH_2).

1-Phenyl-2-phthalimidoethan-1-one (2.55, reference sample)

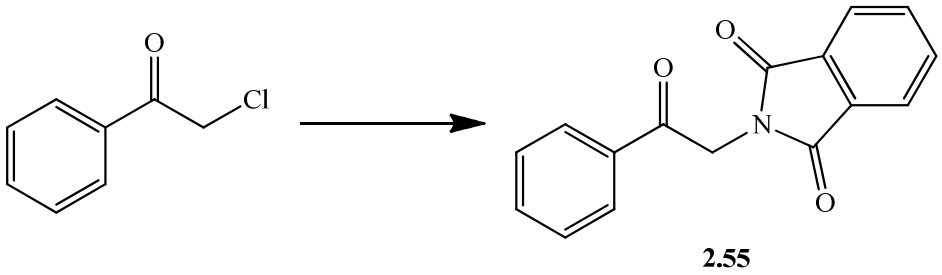

2.55

A mixture of α-chloroacetophenone (0.773 g, 5 mmol) and potassium phthalimide (0.926 g, 5 mmol) in dry acetonitrile (10 ml) was refluxed for 5 h.[50] After the addition of water it was extracted three times with CH_2Cl_2. The combined organic layers were washed with water, dried (Na_2SO_4) and concentrated under reduced pressure. The residue was recrystallized from ethanol to yield the ketone **2.55** (1.235 g, 93%) as colorless crystals; mp. 163-164˚C (lit.: [74] 165-166˚C).

^{1}H NMR (400.27 MHz, $CDCl_3$): δ = 8.04-7.97 (m, 2H, CH_{ar}), 7.91-7.86 (m, 2H, CH_{ar}), 7.77-7.71 (m, 2H, CH_{ar}), 7.64-7.60 (m, 1H, CH_{Ar}), 7.53-7.48 (m, 2H, CH_{ar}), 5.11 (s, 2H, CH_2).
^{13}C NMR (100.65 MHz, $CDCl_3$): δ = 190.97 (C=O), 167.88 (2xC=O), 134.48 (C_{ar}), 134.12 (2xCH_{ar}), 134.03 (CH_{ar}), 132.30 (2xC_{ar}), 128.91 (2xCH_{ar}), 128.15 (2xCH_{ar}), 123.57 (2xCH_{ar}), 44.20 (NCH_2).

1-Phenyl-2-phthalimido- and (*S*)-1-phenyl-2-phthalimido-[2-D$_1$]ethan-1-one [2.55 and (*S*)-[2-D$_1$]2.55]

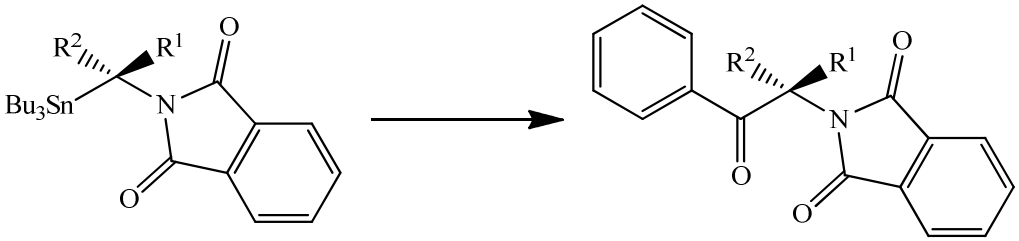

2.54: $R^1 = R^2 = H$
(*R*)-[D$_1$]**2.54**: $R^1 = H$, $R^2 = D$

2.55: $R^1 = R^2 = H$
(*S*)-[D$_1$]**2.55**: $R^1 = H$, $R^2 = D$

A mixture of benzoyl chloride (0.067 g, 0.475 mmol, 0.054 ml), *N*-tributylstannylmethyl phthalimide (**2.54**, 0.336 g, 0.5 mmol), $(PPh_3)_4Pd$ (23.1 mg, 0.02 mmol, 4 mol%) and CuCN (4.7

mg, 0.04 mmol, 8 mol%) in dry toluene (6 ml) was stirred under argon at 75˚C for 20 h.[41] After cooling it was concentrated under reduced pressure and the residue was purified by flash chromatography (CH_2Cl_2, R_f = 0.31) to yield the substituted phthalimide **2.55** (0.104 g, 78%) as colorless crystalline solid.

The ^1H and ^{13}C NMR spectra were identical to the ones of the above reference example.

(*S*)-1-Phenyl-2-phthalimido-[2-D_1]ethan-1-one [(*S*)-[2-D_1]**2.55**]

Similarly, (*R*)-*N*-tributylstannyl-[D_1]methylphthalimide [(*R*)-[D_1]**2.54**, 0.242 g, 0.53 mmol] was converted to (*S*)-1-phenyl-2-phthalimido-[2-D_1]ethan-1-one [(*S*)-[2-D_1]**2.55**, 0.109 g,77%].

^1H NMR (400.27 MHz, $CDCl_3$): δ = 8.02-7.97 (m, 2H, CH_{Ar}), 7.90-7.86 (m, 2H, CH_{ar}), 7.79-7.71 (m, 2H, CH_{ar}), 7.64-7.59 (m, 1H, CH_{ar}), 7.55-7.48 (m, 2H, CH_{ar}), 5.10 (t, *J* = 2.1 Hz, 1H, CHD).
^{13}C NMR (100.65 MHz, $CDCl_3$): δ = 190.96 (C=O), 167.89 (2xC=O), 134.48 (C_{ar}), 134.11 (2xCH_{ar}), 134.03 (CH_{ar}), 132.29 (2xC_{ar}), 128.90 (2xCH_{ar}), 128.15 (2xCH_{ar}), 123.55 (2xCH_{ar}), 49.97 (t, *J* = 21.4 Hz, NCHD).

2-Phthalimido-1-phenyl- and (*1RS,2S*)-2-phthalimido-1-phenyl-[2-D_1]ethanol [2.56 and (*1RS,2S*)-[2-D_1]2.56]

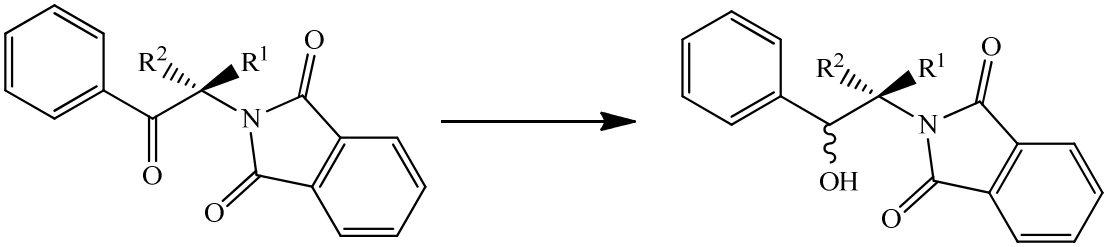

2.55: $R^1 = R^2 = H$
(*S*)-[2-D_1]**2.55**: R^1 = H, R^2 = D

2.56: $R^1 = R^2 = H$
(*2S*)-[2-D_1]**2.56**: R^1 = H, R^2 = D

A mixture of 1-phenyl-2-phthalimidoethan-1-one (**2.55**, 0.133 g, 0.5 mmol) and 10% Pd/C (66.3 mg, 50 weight %) in dry ethyl acetate (p. A., 15 ml) was hydrogenated in a Parr apparatus (4 h, 60 psi, room temperature).[51] The mixture was filtered and concentrated under reduced pressure. The residue was recrystallized from dichlorethane/diisopropyl ether to give the alcohol **2.56** (0.103 g, 0.39 mmol, 77%) as colorless crystals; mp. 166-167˚C (lit.: [75] 164-165˚C).

^{1}H NMR (400.27 MHz, $CDCl_3$): δ = 7.87-7.81 (m, 2H, CH_{ar}), 7.73-7.68 (m, 2H, CH_{ar}), 7.47-7.40 (m, 2H, CH_{ar}), 7.37-7.32 (m, 2H, CH_{ar}), 7.30-7.25 (m, 1H, CH_{ar}), 5.06 (dd, J = 8.4, 3.7 Hz, 1H, OCH), 3.97 (AB part of the ABX-system, J_{AB} = 14.2 Hz, J_{AX} = 8.4 Hz, J_{BX} = 3.7 Hz, 2H, NCH_2), 2.80 (br. s, 1H, OH).

^{13}C NMR (100.65 MHz, $CDCl_3$): δ = 168.75 (2xC=O), 141.06 (C_{ar}), 134.14 (2xCH_{ar}), 131.91 (2xC_{ar}), 128.62 (2xCH_{ar}), 128.13 (CH_{ar}), 125.87 (2xCH_{ar}), 123.48 (2xCH_{ar}), 72.71 (CH), 45.79 (NCH_2).

(*1RS,2S*)-2-Phthalimido-1-phenyl-[2-D_1]ethanol [(*1RS,2S*)-[2-D_1]**2.56**]

Similarly, (*S*)-1-phenyl-2-phthalimido-[2-D_1]ethan-1-one [(*S*)-[2-D_1]**2.55**, 0.052 g, 0.20 mmol] was converted to (*1RS,2S*)-2-phthalimido-1-phenyl-[2-D_1]ethanol [(*1RS,2S*)-[2-D_1]**2.56**, 0.021 g, 41%).

^{1}H NMR (400.27 MHz, $CDCl_3$): δ = 7.87-7.81 (m, 4H, CH_{Ar}), 7.73-7.68 (m, 4H, CH_{ar}), 7.47-7.40 (m, 4H, CH_{ar}), 7.37-7.32 (m, 4H, CH_{ar}), 7.30-7.25 (m, 2H, CH_{ar}), 5.05 (d, J = 3.7 Hz, 1H, CHOH), 5.05 (d, J = 8.3 Hz, 1H, CHOH), 3.99 (d, J = 8.8 Hz, 1H, CHD), 3.92 (bs, 1H, CHD).

^{13}C NMR (100.65 MHz, $CDCl_3$): δ = 168.74 (2xC=O), 141.05 (C_{ar}), 134.13 (2xCH_{ar}), 131.91 (2xC_{ar}), 128.61 (2xCH_{ar}), 128.11 (CH_{ar}), 125.86 (2xCH_{ar}), 123.46 (2xCH_{ar}), 72.65 (CH), 45.49 (t, J = 21.6 Hz, NCHD).

(*R*)-Mosher esters of 2-phthalimido-1-phenyl- and (*1RS,2S*)-2-phthalimido-1-phenyl-[2-D_1]ethanol [2.57 and (*1RS,2S*)-[2-D_1]2.57]

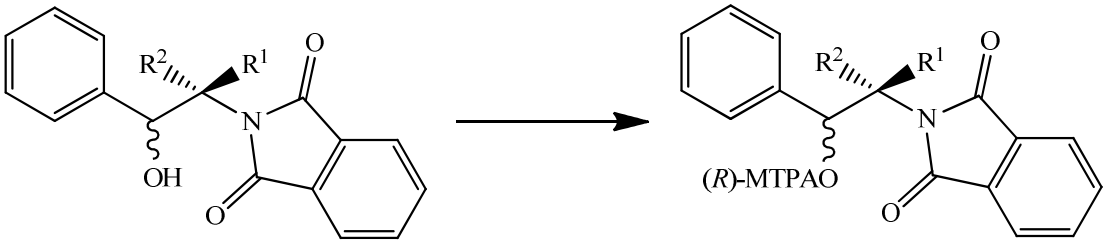

2.56: $R^1 = R^2 = H$
(*2S*)-[2-D_1]**2.56**: $R^1 = H$, $R^2 = D$

2.57: $R^1 = R^2 = H$
(*2S*)-[2-D_1]**2.57**: $R^1 = H$, $R^2 = D$

A solution of (*S*)-MTPACl (0.09 mmol, 0.171 ml of a solution 0.53M in dry CH_2Cl_2), 2-phthalimido-1-phenylethanol (**2.56**, 11.9 mg, 0.045 mmol), dry CH_2Cl_2 (0.5 ml) and pyridine (3 drops) was stirred under argon at room temperature for 18 h. It was concentrated under reduced pressure and water was added. The mixture was extracted three times with CH_2Cl_2 and the

combined organic layers were washed with HCl (2M), a saturated aqueous solution of $NaHCO_3$, dried (Na_2SO_4) and concentrated under reduced pressure. The crude product was purified by flash chromatography (hexane:ethyl acetate = 5:1, R_f = 0.32) to give a 1:1 diastereomeric mixture of (*R*)-Mosher esters **2.57** (19.8 mg, 91%) as colorless oil.

^{1}H NMR (200.27 MHz, $CDCl_3$): δ = 7.85-7.80 (m, 2H, CH_{ar}), 7.77-7.68 (m, 5H, CH_{ar}), 7.51-7.46 (m, 2H, CH_{ar}), 7.42-7.30 (m, 8H, CH_{ar}), 7.28-7.20 (m, 6H, CH_{ar}), 7.15-7.08 (m, 3H, CH_{ar}), 7.07-7.00 (m, 2H, CH_{ar}), 6.34 (dd, *J* = 10.2, 4.1 Hz, 1H, OCH), 6.28 (dd, *J* = 9.8, 4.3 Hz, 1H, OCH), 4.27 (dd, *J* = 14.4, 9.8 Hz, 1H, NCH), 4.26 (dd, *J* = 14.4, 10.2 Hz, 1H, NCH), 3.86 (dd, *J* = 14.4, 4.2 Hz, 1H, NCH), 3.79 (dd, *J* = 14.4, 4.2 Hz, 1H, NCH), 3.39 (q, *J* = 1.1 Hz, 3H, OCH_3), 3.36 (q, *J* = 1.1 Hz, 3H, OCH_3).

(*R*)-Mosher esters of (*1RS,2S*)-2-phthalimido-1-phenyl-[2-D_1]ethanol [(*1RS,2S*)-[2-D_1]**2.57**]
Similarly, (*1RS,2S*)-2-phthalimido-1-phenyl-[2-D_1]ethanol [(*1RS,2S*)-[2-D_1]**2.56**, 0.010 g, 0.038 mmol] was converted to the (*R*)-Mosher esters (*1RS,2S*)-[2-D_1]**2.57** (0.013 g, 71%, de > 98%).

^{1}H NMR (600.13 MHz, $CDCl_3$): δ = 7.85-7.80 (m, 2H, CH_{ar}), 7.77-7.68 (m, 5H, CH_{ar}), 7.51-7.46 (m, 2H, CH_{ar}), 7.42-7.30 (m, 8H, CH_{ar}), 7.28-7.20 (m, 6H, CH_{ar}), 7.15-7.08 (m, 3H, CH_{ar}), 7.07-7.00 (m, 2H, CH_{ar}), 6.33 (d, *J* = 10.2 Hz, 1H, OCH), 6.28 (d, *J* = 4.2 Hz, 1H, OCH), 4.24 (d, *J* = 10.2 Hz, 1H, NCH), 3.79 (d, *J* = 4.2 Hz, 1H, NCH), 3.39 (q, *J* ~ 1 Hz, 3H, OCH_3), 3.36 (q, *J* ~ 1 Hz, 3H, OCH_3).

***N*-Phenylmethylphthalimide (2.59, reference sample)**

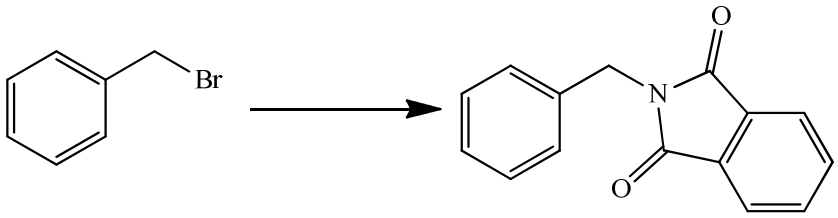

2.59

A mixture of benzyl bromide (0.513 g, 3 mmol) and potassium phthalimide (0.741 g, 4 mmol) in dry acetonitrile (10 ml) was refluxed for 3 h. After cooling, water was added and the mixture was extracted twice with CH_2Cl_2. The combined organic layers were washed with NaOH (2M) and water, dried (Na_2SO_4) and concentrated under reduced pressure. The crude product was

recrystallized from ethanol to give the substituted phthalimide **2.59** (0.6742 g, 2.8 mmol, 95%) as colorless crystals; mp. 116-117˚C (lit.: [76] 115-116˚C).

^{1}H NMR (400.27 MHz, $CDCl_3$): δ = 7.86-7.80 (m, 2H, CH_{ar}), 7.70-7.65 (m, 2H, CH_{ar}), 7.42-7.38 (m, 2H, CH_{ar}), 7.32-7.20 (m, 3H, CH_{ar}), 4.83 (s, 2H, CH_2)
^{13}C NMR (100.65 MHz, $CDCl_3$): δ = 168.01 (2xC=O), 136.36 (C_{ar}), 133.94 (2xCH_{ar}), 132.15 (2xC_{ar}), 128.65 (2xCH_{ar}), 128.59 (2xCH_{ar}), 127.80 (CH_{ar}), 123.32 (2xCH_{ar}), 41.60 (NCH_2).

***N*-Phenyl-, (*R*)- and (*S*)-*N*-phenyl-[D$_1$]methylphthalimide [2.59, (*R*)- and (*S*)-[D$_1$]2.59]**

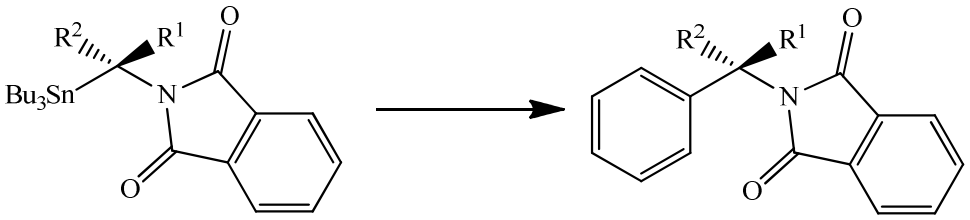

2.54: $R^1 = R^2 = H$
(*R*)-[D$_1$]**2.54**: $R^1 = H$, $R^2 = D$
(*S*)-[D$_1$]**2.54**: $R^1 = D$, $R^2 = H$

2.59: $R^1 = R^2 = H$
(*S*)-[D$_1$]**2.59**: $R^1 = H$, $R^2 = D$
(*R*)-[D$_1$]**2.59**: $R^1 = D$, $R^2 = H$

A mixture of bromobenzene (0.117 g, 0.75 mmol, 0.079 ml), *N*-tributylstannylmethyl phthalimide (**2.54**, 0.225 g, 0.5 mmol), $Pd(PPh_3)_2Cl_2$ (28 mg, 0.04 mmol, 8 mol %) and CuCN (7.1 mg, 0.08 mmol, 16 mol %) in dry dioxane (6 ml) was stirred under argon at 100˚C for 6 h.[41] After cooling it was concentrated under reduced pressure and a 5% aqueous solution of KF was added. The mixture was extracted twice with CH_2Cl_2. The combined organic layers were dried (Na_2SO_4) and concentrated under reduced pressure. The crude product was purified by flash chromatography (CH_2Cl_2, R_f = 0.44) to yield the *N*-phenylmethylphthalimide [**2.59**, 0.043 g, 37%] as colorless crystals.

The ^{1}H and ^{13}C NMR spectra were identical to the ones of the above reference compound.

(*R*)-*N*-Phenyl-[D$_1$]methylphthalimide [(*R*)-[D$_1$]**2.59**]

Similarly, (*S*)-*N*-tributylstannyl-[D$_1$]methylphthalimide [(*S*)-[D$_1$]**2.54**, 0.301 g, 0.67 mmol] was converted in dry toluene to (*R*)-*N*-phenyl-[D$_1$]methylphthalimide [(*R*)-[D$_1$]**2.59**, 0.084 g, 53%].

(*S*)-*N*-Phenyl-[D_1]methylphthalimide [(*S*)-[D_1]**2.59**]

Similarly, (*R*)-*N*-tributylstannyl-[D_1]methylphthalimide [(*R*)-[D_1]**2.54**, 0.206 g, 0.46 mmol] was converted in dry dioxane to (*S*)-*N*-phenyl-[D_1]methylphthalimide [(*S*)-[D_1]**2.59**, 0.031 g, 29%].

The ^{1}H NMR spectra of (*R*)- and (*S*)-*N*-phenyl-[D_1]methylphthalimide were identical:
^{1}H NMR (400.27 MHz, $CDCl_3$): δ = 7.86-7.80 (m, 2H, CH_{ar}), 7.71-7.66 (m, 2H, CH_{ar}), 7.44-7.39 (m, 2H, CH_{ar}), 7.32-7.22 (m, 3H, CH_{ar}), 4.83-4.80 (broadened s, 1H, CHD).

(*S*)-*N*-Phenyl-[D_1]methylphthalimide (2.59, reference sample)

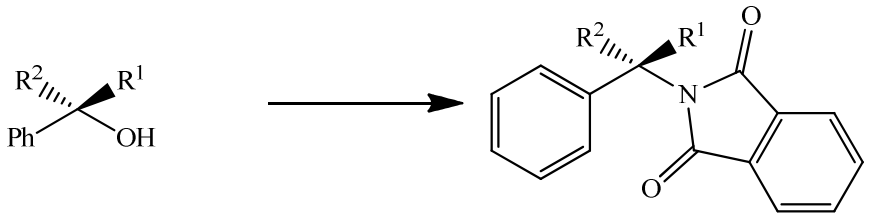

(*R*)-[D_1]**2.60**: R^1 = D, R^2 = H

(*S*)-[D_1]**2.59**: R^1 = H, R^2 = D

DIAD (1.03 mmol, 0.203 ml) was added to a stirred mixture of (*R*)-phenyl-[D_1]methanol [(*R*)-[D_1]**2.60**, 0.094 g, 0.86 mmol], triphenylphosphane (0.270 g, 10.03 mmol) and phthalimide (0.150 g, 1.03 mmol) in dry THF (8 ml) under argon at 0˚C and stirring was continued for 2 days at room temperature.[49] After water (0.5 ml) was added it was concentrated under reduced pressure. The crude product was purified by flash chromatography (hexane:ethyl acetate = 2:1, R_f = 0.73) to give the phthalimide [(*S*)-[D_1]**2.59**, 0.148 g, 72%] as colorless crystals.

The ^{1}H NMR spectra were identical to the compound prepared by the Stille coupling.

Phenyl-, (*R*)- and (*S*)-phenyl-[D_1]methylamine [2.61, (*R*)- and (*S*)-[D_1]2.61]

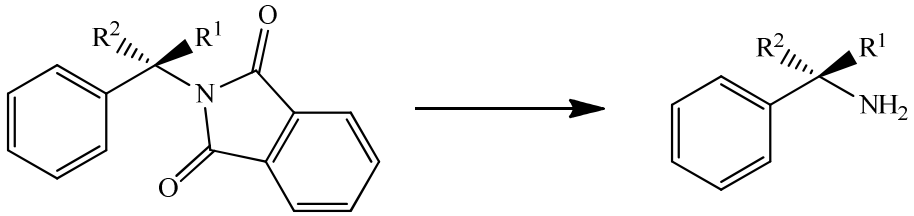

2.59: R^1 = R^2 = H
(*R*)-[D_1]**2.59**: R^1 = D, R^2 = H
(*S*)-[D_1]**2.59**: R^1 = H, R^2 = D

2.61: R^1 = R^2 = H
(*R*)-[D_1]**2.61**: R^1 = D, R^2 = H
(*S*)-[D_1]**2.61**: R^1 = H, R^2 = D

A mixture of hydrazine hydrate (0.327 g, 5.03 mmol, 0.306 ml) and *N*-phenylmethylphthalimide (**2.59**, 0.194 g, 0.8 mmol) in dry ethanol (7 ml) was refluxed for 2 h. After cooling it was centrifuged to remove the crystalline byproduct. The pellet was washed with Et_2O and the combined organic layers were concentrated under reduced pressure. Et_2O (10 ml) and NH_3 (25%, 3 drops) were added and the mixture was first washed with a half saturated aqueous solution of NaCl (2 ml) and then with a saturated aqueous solution of NaCl (2 ml).[52] After the addition of dry ethanol (5 ml) to the organic layer it was concentrated under reduced pressure. Then dry dichloroethane (5 ml) was added, the mixture was filtered and the filtrate was concentrated under reduced pressure and dried in vacuo (0.5 mbar, 3 min) to give the amine **2.61** (18 mg, 21%) as a colorless liquid which was immediately derivatised with (*S*)-MTPACl in case of labeled species.

(*R*)-Phenyl-[D_1]methylamine [(*R*)-[D_1]**2.61**]

Similarly, (*R*)-*N*-phenyl-[D_1]methylphthalimide [(*R*)-[D_1]**2.59**, 0.148 g, 0.62 mmol] was converted to (*R*)-phenyl-[D_1]methylamine [(*R*)-[D_1]**2.61**, 0.037 g, 55%].

(*S*)-Phenyl-[D_1]methylamine [(*S*)-[D_1]**2.61**]

Similarly, (*S*)-*N*-phenyl-[D_1]methylphthalimide [(*S*)-[D_1]**2.59**, 0.030 g, 0.12 mmol] was converted to (*S*)-phenyl-[D_1]methylamine [(*S*)-[D_1]**2.61**, 0.014 g, 99%].

(*R*)-Mosher amides of phenyl-, (*R*)- and (*S*)-phenyl-[D_1]methylamine [2.62, (*R*)- and (*S*)-[D_1]2.62]

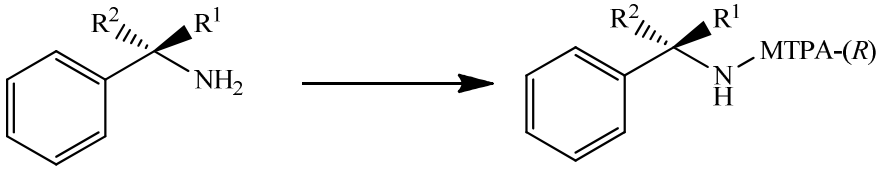

2.61: $R^1 = R^2 = H$
(*R*)-[D_1]**2.61**: $R^1 = D$, $R^2 = H$
(*S*)-[D_1]**2.61**: $R^1 = H$, $R^2 = D$

2.62: $R^1 = R^2 = H$
(*R*)-[D_1]**2.62**: $R^1 = D$, $R^2 = H$
(*S*)-[D_1]**2.62**: $R^1 = H$, $R^2 = D$

A mixture of phenylmethylamine (**2.61**, 12.8 mg, 0.12 mmol), dry pyridine (6 drops) and (*S*)-MTPACl (0.24 mmol, 0.45 ml of a 0.53M solution in dry CH_2Cl_2) in dry CH_2Cl_2 (2 ml) was stirred under argon at room temperature for 18 h. Water was added after it was concentrated under reduced pressure. The mixture was extracted three times with CH_2Cl_2 and the combined organic layers were washed with HCl (2M) and a saturated solution of $NaHCO_3$, dried ($MgSO_4$) and concentrated under reduced pressure. The residue was purified by flash chromatography

(hexane:ethyl acetate = 5:1, R_f = 0.44) to yield the (*R*)-Mosher amide **2.62** (23.5 mg, 61%) as a colorless solid.

^{1}H NMR (400.27 MHz, $CDCl_3$): δ = 7.55-7.49 (m, 2H, CH_{ar}), 7.41-7.36 (m, 3H, CH_{ar}), 7.35-7.23 (m, 5H, CH_{ar}), 7.08 (br. s, 1H, NH), 4.51 (AB part of ABX-system, J_{AB} = 14.8 Hz, J_{AX} = 6.0 Hz, J_{BX} = 8.8 Hz, 2H, NCH_2), 3.37 (q, J = 1.5 Hz, 3H, OCH_3).

(*R*)-Mosher amide of (*R*)-phenyl-[D_1]methylamine [(*R*)-[D_1]**2.62**]

Similarly, (*R*)-phenyl-[D_1]methylamine [(*R*)-[D_1]**2.61**, 0.012 g, 0.11 mmol] was converted to the (*R*)-Mosher amide (*R*)-[D_1]**2.62** (0.023 g, 65%, de > 69%).

^{1}H NMR (400.27 MHz, $CDCl_3$): δ = 7.55-7.49 (m, 2H, CH_{ar}), 7.41-7.36 (m, 3H, CH_{ar}), 7.35-7.23 (m, 5H, CH_{ar}), 7.08 (br. s, 1H, NH), 4.52 (td, J = 5.8, 2.0 Hz, 0.83H, NCHD) 4.46 (td, J = ~5.8, ~2 Hz, 0.15H, NCHD), 3.37 (q, J = 1.4 Hz, 3H, OCH_3).

(*R*)-Mosher amide of (*S*)-phenyl-[D_1]methylamine [(*S*)-[D_1]**2.62**]

Similarly, (*S*)-phenyl-[D_1]methylamine [(*S*)-[D_1]**2.61**, 0.013 g, 0.12 mmol] was converted to the (*R*)-Mosher amide (*S*)-[D_1]**2.62** (0.005 g, 13%, de > 52%).

^{1}H NMR (400.27 MHz, $CDCl_3$): δ = 7.55-7.49 (m, 2H, CH_{ar}), 7.41-7.36 (m, 3H, CH_{ar}), 7.35-7.23 (m, 5H, CH_{ar}), 7.08 (br. s, 1H, NH), 4.52 (td, J = 5.8, 2.0 Hz, 0.24H, NCHD), 4.46 (td, J = ~5.8, ~2 Hz, 0.76H, NCHD), 3.37 (q, J = 1.4 Hz, 3H, OCH_3).

(*R*)-Mosher amide of (*S*)-phenyl-[D_1]methylamine [(*S*)-[D_1]**2.62**] (reference sample)

Similarly, (*S*)-phenyl-[D_1]methylamine [(*S*)-[D_1]**2.61**, 0.011 g, 0.10 mmol] was converted to the (*R*)-Mosher amide (*S*)-[D_1]**2.62** (0.005 g, 15%, de > 99%).

^{1}H NMR (400.27 MHz, $CDCl_3$): δ = 7.55-7.49 (m, 2H, CH_{ar}), 7.41-7.36 (m, 3H, CH_{ar}), 7.35-7.23 (m, 5H, CH_{ar}), 7.08 (br. s, 1H, NH), 4.46 (td, J = 5.6, ~2 Hz, 1H, NCHD), 3.37 (q, J = 1.4 Hz, 3H, OCH_3).

4.4 Chapter 3

Diisopropyl tributylstannylmethyl-, (*R*)- and (*S*)-diisopropyl tributylstannyl-[D_1]methyl phosphate [3.30, (*R*)- and (*S*)-[D_1]3.30]

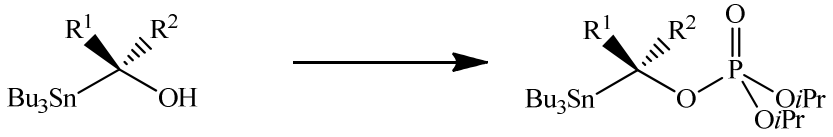

1.67: $R^1 = R^2 = H$
(*R*)-[D_1]**1.67**: $R^1 = H$, $R^2 = D$
(*S*)-[D_1]**1.67**: $R^1 = D$, $R^2 = H$

3.30: $R^1 = R^2 = H$
(*R*)-[D_1]**3.30**: $R^1 = H$, $R^2 = D$
(*S*)-[D_1]**3.30**: $R^1 = D$, $R^2 = H$

Bromine (3.15 mmol, 3.18 ml of a 1.01M solution in dry CH_2Cl_2) was added to a stirred solution of triisopropyl phosphite (0.703 g, 3.38 mmol, 0.83 ml) in dry CH_2Cl_2 (9 ml) under argon at -50˚C.[67] After stirring for 30 min at 0˚C it was cooled to -50˚C and a mixture of tributylstannylmethanol (**1.67**, 0.723 g, 2.25 mmol) and dry pyridine (0.72 ml) in dry CH_2Cl_2 (4.5 ml) was added. After stirring for 1 h at room temperature water (10 ml) and CH_2Cl_2 (10 ml) were added and stirring was continued for another 15 min. The phases were separated and the aqueous layer was extracted twice with ethyl acetate. The combined organic layers were washed with HCl (2M) and a saturated aqueous solution of $NaHCO_3$, dried (Na_2SO_4) and concentrated under reduced pressure. The residue was purified by flash chromatography (hexane:ethyl acetate = 5:1, R_f = 0.32) to give the phosphate **3.30** (0.412 g, 38%) as a colorless oil.

^{1}H NMR (400.27 MHz, $CDCl_3$): δ = 4.57 (oct, J = 6.3 Hz, 2H, 2xCH), 4.17 (d, J = 6.2 Hz, $J(^{117/119}Sn)$ = 12.8 Hz, 2H, PCH_2), 1.60-1.38 (m, 6H, 3x$SnCH_2\underline{CH_2}$), 1.29 (d, J = 6.3 Hz, 12H, 4xCH_3), 1.27 (sext, J = 7.2 Hz, 6H, 3x$\underline{CH_2}CH_3$), 1.02-0.82 (m, 6H, 3x$SnCH_2$), 0.86 (t, J = 7.3 Hz, 9H, 3x$CH_2\underline{CH_3}$).

<u>(*R*)-Diisopropyl tributylstannyl-[D_1]methyl phosphate [(*R*)-[D_1]**3.30**]</u>
Similarly, (*R*)-tributylstannyl-[D_1]methanol [(*R*)-[D_1]**1.67**, 0.389 g, 1.21 mmol] was converted to (*R*)-diisopropyl tributylstannyl-[D_1]methylphosphate [(*R*)-[D_1]**3.30**, 0.359 g, 61%].

<u>(*S*)-Diisopropyl tributylstannyl-[D_1]methyl phosphate [(*S*)-[D_1]**3.30**]</u>
Similarly, (*S*)-tributylstannyl-[D_1]methanol [(*S*)-[D_1]**1.67**, 0.421 g, 1.31 mmol] was converted to (*S*)-diisopropyl tributylstannyl-[D_1]methylphosphate [(*S*)-[D_1]**3.30**, 0.469 g, 74%].

^{1}H NMR spectra for (*R*)- and (*S*)-diisopropyl tributylstannyl-[D_1]methyl phosphate were identical:

^{1}H NMR (400.27 MHz, $CDCl_3$): δ = 4.57 (oct, *J* = 6.3 Hz, 2H, 2xCH), 4.15 (broadened d, *J* = 6.2 Hz, *J*($^{117/119}$Sn) = 12.8 Hz, 2H, PCHD), 1.60-1.38 (m, 6H, 3x$SnCH_2\underline{CH_2}$), 1.29 (d, *J* = 6.3 Hz, 12H, 4xCH_3), 1.27 (sext, *J* = 7.2 Hz, 6H, 3x$\underline{CH_2}CH_3$), 1.02-0.82 (m, 6H, 3x$SnCH_2$), 0.86 (t, *J* = 7.3 Hz, 9H, 3x$CH_2\underline{CH_3}$).

Diisopropyl hydroxymethyl-, (*R*)- and (*S*)-diisopropyl hydroxy-[D_1]methylphosphonate [3.31, (*R*)- and (*S*)-[D_1]3.31]

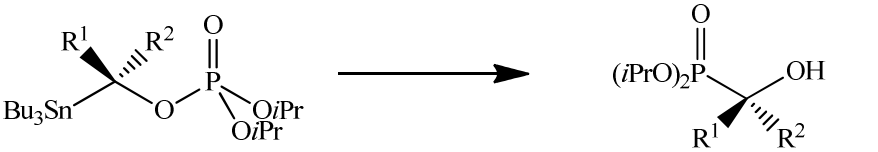

3.30: $R^1 = R^2 = H$
(*R*)-[D_1]**3.30**: $R^1 = H$, $R^2 = D$
(*S*)-[D_1]**3.30**: $R^1 = D$, $R^2 = H$

3.31: $R^1 = R^2 = H$
(*R*)-[D_1]**3.31**: $R^1 = D$, $R^2 = H$
(*S*)-[D_1]**3.31**: $R^1 = H$, $R^2 = D$

*n*BuLi (0.68 mmol, 0.42 ml of a 1.6M solution in hexane) was added in drops to a stirred solution of diisopropyl tributylstannylmethyl phosphate (**3.30**, 0.366 g, 0.75 mmol) and TMEDA (0.68 mmol, 0.102 ml) in dry Et_2O (5 ml) under argon at -78˚C and stirring was continued for 30 min.[24] After the addition of acetic acid (1.5 ml of a 2M solution in Et_2O) and water (4 ml) stirring was continued for 5 min. The phases were separated and the organic phase was extracted four times with Et_2O. The combined organic layers were dried (Na_2SO_4) and concentrated under reduced pressure. The residue was purified by flash chromatography (ethyl acetate, R_f = 0.22) to yield the phosphonate **3.31** (0.103 g, 77%) as a an oil.

^{1}H NMR (400.27 MHz, $CDCl_3$): δ = 4.72 (oct, *J* = 6.2, 1.2 Hz, 2H, 2xCH), 3.81 (d, *J* = 6.1 Hz, 2H, CH_2), 1.31 (dd, *J* = 6.2, 1.2 Hz, 12H, 4xCH_3).

<u>(*R*)-Diisopropyl hydroxy-[D_1]methylphosphonate [(*R*)-[D_1]**3.31**]</u>

Similarly, (*R*)-diisopropyl tributylstannyl-[D_1]methyl phosphate [(*R*)-[D_1]**3.30**, 0.359 g, 0.74 mmol] was converted to (*R*)-diisopropyl hydroxy-[D_1]methylphosphonate [(*R*)-[D_1]**3.31**, 0.093 g, 64%].

(*S*)-Diisopropyl hydroxy-[D_1]methylphosphonate [(*S*)-[D_1]**3.31**]

Similarly, (*S*)-diisopropyl tributylstannyl-[D_1]methyl phosphate [(*S*)-[D_1]**3.30**, 0.241 g, 0.50 mmol] was converted to (*S*)-diisopropyl hydroxy-[D_1]methylphosphonate [(*S*)-[D_1]**3.31**, 0.048 g, 54%].

The ^{1}H NMR spectra for (*R*)- and (*S*)-diisopropyl tributylstannyl-[D_1]methylphosphonate were identical:

^{1}H NMR (400.27 MHz, $CDCl_3$): δ = 4.72 (oct, *J* = 6.2 Hz, 2H, 2xCH), 3.81 (broadened d, *J* = 4.2 Hz, 1H, CHD), 3.23 (br.s, 1H, OH), 1.31 (dd, *J* = 6.2, 0.7 Hz, 12H, 4xCH_3).

1-Hydroxymethyl-, (*R*)- and (*S*)-1-hydroxy-[D_1]methylphosphonic acid [3.14, (*R*)- and (*S*)-[D_1]3.14]

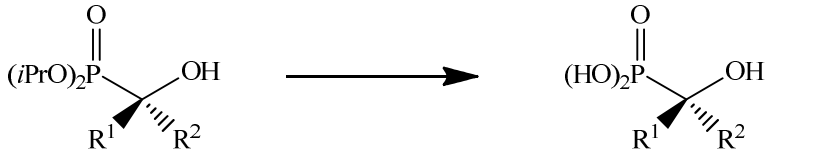

3.31: $R^1 = R^2 = H$
(*R*)-[D_1]**3.31**: R^1 = D, R^2 = H
(*S*)-[D_1]**3.31**: R^1 = H, R^2 = D

3.14: $R^1 = R^2 = H$
(*R*)-[D_1]**3.14**: R^1 = D, R^2 = H
(*S*)-[D_1]**3.14**: R^1 = H, R^2 = D

Allyltrimethylsilane (0.71 g, 6.25 mmol, 0.99 ml) and bromotrimethylsilane (3.83 g, 25 mmol, 3.25 ml) were added drop wise to a solution of diisopropyl hydroxymethylphosphonate (**3.31**, 0.98 g, 5 mmol) in dry 1,2-dichloroethane (18.75 ml) under argon at 0 °C.[68] After heating for 18 h at 50 °C and then cooling to room temperature, volatile components were removed in vacuo (0.5 mbar) at room temperature. The residue was twice dissolved in dry CH_2Cl_2 (5 ml each time) and concentrated again in vacuo as before (0.5 mbar, at first at room temperature, then 40 °C). Water (10 ml) was added and the mixture was stirred for 5 min and then concentrated under reduced pressure. Water (20 ml) was added again and removed by lyophilisation. The phosphonic acid **3.14** (0.668 g, contained water; yield was assumed to be 95%) was a colorless oil.

^{1}H NMR (400.27 MHz, D_2O): δ = 3.76 (d, *J* = 7.2 Hz, 2H, PCH_2).

^{13}C NMR (100.65 MHz, D_2O): δ = 56.78 (d, *J* = 159.9 Hz, PCH_2).

^{31}P NMR (162.03 MHz, D_2O): δ = 22.01.

(*R*)-1-Hydroxy-[D_1]methylphosphonic acid [(*R*)-[D_1]**3.14**]

Similarly, (*R*)-diisopropyl hydroxy-[D_1]methylphosphonate [(*R*)-[D_1]**3.31**, 0.083 g, 1.42 mmol] was converted to (*R*)-1-hydroxy-[D_1]methylphosphonic acid [(*R*)-[D_1]**3.14**, 0.069 g, contained water]. It was converted to the ammonium salf for storage: The acid was dissolved in water and a few drops of concentrated ammonia were added. The solution was concentrated by lyophilization.

(*S*)-1-Hydroxy-[D_1]methylphosphonic acid [(*S*)-[D_1]**3.14**]

Similarly, (*S*)-diisopropyl hydroxy-[D_1]methylphosphonate [(*S*)-[D_1]**3.31**, 0.037 g, 0.19 mmol] was converted to (*S*)-1-hydroxy-[D_1]methylphosphonic acid [(*S*)-[D_1]**3.14**, 0.027 g, contained water]. It was converted to the ammonium salf for storage: The acid was dissolved in water and a few drops of concentrated ammonia were added. The solution was concentrated by lyophilization.

The NMR spectra for (*R*)- and (*S*)-1-hydroxy-[D_1]methylphosphonic acid were identical:

^{1}H NMR (400.27 MHz, D_2O): δ = 3.83 (broadened d, J = 7.1 Hz, 1H, PCHD), (R)-enantiomer contained 2% of unlabeled species.

^{13}C (100.65 MHz, D_2O): δ = 56.31 (td, J = 157.1, 22.9 Hz, PCHD).

^{31}P NMR (162.03 MHz, D_2O): δ = 21.97.

Dimethyl hydroxymethylphosphonate (3.34, reference sample)

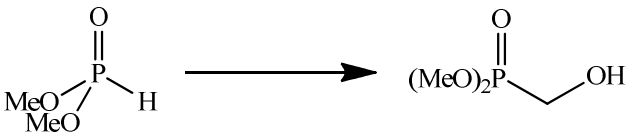

3.34

DBU (5 drops) was added to a mixture of dimethyl phosphite (2.20 g, 20 mmol, 1.83 ml) and paraformaldehyde (0.66 g, 22 mmol) at room temperature.[77] It was stirred for 20 min in a cold water bath. The crude product was purified by flash chromatography (ethyl acetate: hexane: methanol = 40:20:1, R_f = 0.25) to yield the phosphonate **3.34** (1.77 g, 63%) as a colorless oil.

IR (ATR): ν = 3303, 2959, 2854, 1450, 1227, 1184, 1018.

^{1}H NMR (400.13 MHz, $CDCl_3$): δ = 4.23 (brq, J = 6.0 Hz, 1H, OH), 3.91 (t, J = 6.0 Hz, 2H, PCH_2), 3.78 (d, J = 10.5 Hz, 6H, 2xOCH_3).

^{13}C (100.61 MHz, $CDCl_3$): δ = 56.38 (d, J = 161.9 Hz, PCH_2), 53.12 (d, J = 7.0 Hz, OCH_3).

^{31}P NMR (161.97 MHz, $CDCl_3$): δ = 27.81.

Dimethyl hydroxymethyl-, (*R*)- and (*S*)-dimethyl hydroxy-[D_1]methylphosphonate [3.34, (*R*)- and (*S*)-[D_1]3.34]

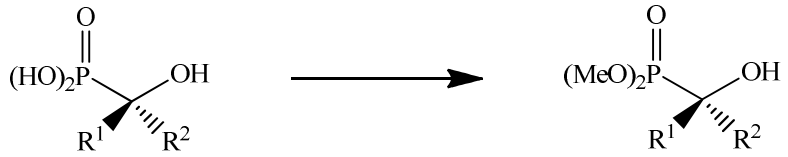

3.14: $R^1 = R^2 = H$
(*R*)-[D_1]**3.14**: $R^1 = D$, $R^2 = H$
(*S*)-[D_1]**3.15**: $R^1 = H$, $R^2 = D$

3.34: $R^1 = R^2 = H$
(*R*)-[D_1]**3.34**: $R^1 = D$, $R^2 = H$
(*S*)-[D_1]**3.34**: $R^1 = H$, $R^2 = D$

A distilled ethereal solution of diazomethane was added to a solution of hydroxymethylphosphonic acid (**3.14**, 0.053 g, 0.47 mmol) in dry methanol (5 ml) until yellow color persisted for a few seconds.[69] The solvent was then evaporated under reduced pressure to give **3.34** (contained 6% of dimethyl methoxymethylphosphonate) as a colorless oil.

The ^1H, ^{13}C and ^{31}P NMR spectra were identical to the spectra of the above reference sample except for the following peaks corresponding to dimethyl methoxymethylphosphonate:
^1H NMR (400.13 MHz, $CDCl_3$): δ = 3.75 (d, J = 8.5 Hz, 2H, PCH_2), 3.45 (d, J = 1.0 Hz, 3H, OCH_3).
^{31}P NMR (161.97 MHz, $CDCl_3$): δ = 23.67.

(*R*)-Dimethyl hydroxy-[D_1]methylphosphonate [(*R*)-[D_1]**3.34**]
Similarly, (*R*)-1-hydroxy-[D_1]methylphosphonic acid [(*R*)-[D_1]**3.14**, 0.023 g, 0.20 mmol] was converted to (*R*)-dimethyl hydroxy-[D_1]methylphosphonate [(*R*)-[D_1]**3.34**, 0.021 g, contained 12% of the dimethyl methoxy-[D_1]methylphosphonate].

(*S*)-Dimethyl hydroxy-[D_1]methylphosphonate [(*S*)-[D_1]**3.34**]
Similarly, (*S*)-1-hydroxy-[D_1]methylphosphonic acid [(*S*)-[D_1]**3.14**, 0.027 g, 0.20 mmol] was converted to (*S*)-dimethyl hydroxy-[D_1]methylphosphonate [(*S*)-[D_1]**3.34**, 0.023 g].

^1H and ^{31}P NMR spectra for (*R*)- and (*S*)-dimethyl hydroxy-[D_1]methylphosphonate were identical:
^1H NMR (400.27 MHz, $CDCl_3$): δ = 4.50 (br. s, 1H, OH), 3.90 (td, J = 5.5, 2.0 Hz 1H, CHD), 3.79 (d, J = 10.6 Hz, 6H, 2xOCH_3), significant signals for dimethyl methoxy-[D_1]methylphosphonate: 3.71 (td, J = 8.5, 2.0 Hz, 1H, CHD), 3.43 (d, J = 1.3 Hz, 3H, OCH_3).

^{31}P NMR (162.03 MHz, $CDCl_3$): δ = 26.59.

(*R*)-Mosher esters of dimethyl hydroxymethyl-, (*R*)- and (*S*)-dimethyl hydroxy-[1-D_1]methylphosphonates [3.35, (*R*)- and (*S*)-[D_1]3.35]

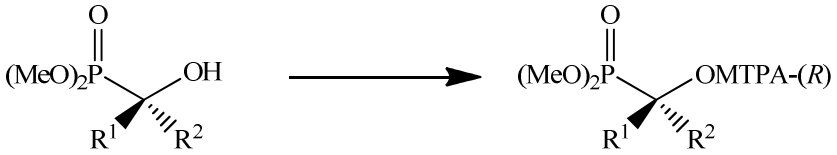

3.34: $R^1 = R^2 = H$
(*R*)-[D_1]**3.34**: $R^1 = D$, $R^2 = H$
(*S*)-[D_1]**3.34**: $R^1 = H$, $R^2 = D$

3.35: $R^1 = R^2 = H$
(*R*)-[D_1]**3.35**: $R^1 = D$, $R^2 = H$
(*S*)-[D_1]**3.35**: $R^1 = H$, $R^2 = D$

(*S*)-MTPACl (0.25 mmol, 0.47 ml of a 0.53 M solution in dry CH_2Cl_2) and dry pyridine (5 drops) were added to a solution of dimethyl hydroxylmethylphosphonate (**3.34**, 0.017 g, 0.12 mmol) in dry dichloromethane (1 ml) under argon at room temperature.[15] After 20 h at 4˚C it was concentrated under reduced pressure. Water and CH_2Cl_2 were added and the phases were separated. The organic layer was first washed with HCl (2M), then with a saturated solution of $NaHCO_3$, dried ($MgSO_4$) and concentrated under reduced pressure. The residue was purified by flash chromatography (ethyl acetate, R_f = 0.62) to yield Mosher ester **3.35** (0.037 g, 86%) as colorless oil.

^{1}H NMR (400.13 MHz, $CDCl_3$): δ = 7.55 – 7.49 (m, 2H, CH_{ar}), 7.42 – 7.36 (m, 3H, CH_{ar}), 4.60 (AB part of ABX-system, δ_A = 4.55, δ_B = 4.64, J_{AB} = 14.3 Hz, J_{AP} = J_{BP} = 8.6 Hz, 2H, PCH_2), 3.75 (d, J = 10.8 Hz, 3H, $POCH_3$), 3. 72 (d, J = 10.9 Hz, 3H, $POCH_3$), 3.55 (q, J = 1.2 Hz, 3H, $COCH_3$).
^{31}P NMR (161.97 MHz, $CDCl_3$): δ = 20.74.

(*R*)-Mosher ester of (*R*)-dimethyl hydroxy-[1-D_1]methylphosphonate [(*R*)-[D_1]**3.35**]
Similarly, crude (*R*)-dimethyl hydroxy-[D_1]methylphosphonate [(*R*)-[D_1]**3.34**, 0.021 g, 0.15 mmol] was converted to (*R*)-Mosher ester of (*R*)-dimethyl hydroxy-[D_1]methylphosphonate [(*R*)-[D_1]**3.35**, 0.044 g, 82%, ee > 99%, contained 2% of the unlabeled species].

^{1}H NMR (400.13 MHz, $CDCl_3$): δ = 7.55 – 7.49 (m, 2H, CH_{ar}), 7.42 – 7.36 (m, 3H, CH_{ar}), 4.54 (td, J = 8.6 Hz, ~ 1.5 Hz, 1H, CHD), 3.75 (d, J = 10.9 Hz, 3H, $POCH_3$), 3.72 (d, J = 10.9 Hz, 3H, $POCH_3$), 3.55 (q, J = 1.2 Hz, 3H, $COCH_3$).

^{31}P NMR (161.97 MHz, $CDCl_3$): δ = 20.74.

(*R*)-Mosher ester of (*S*)-dimethyl hydroxy-[D_1]methylphosphonate [(*S*)-[D_1]**3.35**]

Similarly, crude (*S*)-dimethyl hydroxy-[D_1]methylphosphonate [(*S*)-[D_1]**3.34**, 0.023 g, 0.17 mmol] was converted to (*R*)-Mosher ester of (*S*)-dimethyl hydroxy-[D_1]methylphosphonate [(*S*)-[D_1]**3.35**, 0.024 g, 40%, ee > 99%, contained 2% of the unlabeled species].

^{1}H NMR (400.13 MHz, $CDCl_3$): δ = 7.55 – 7.49 (m, 2H, CH_{ar}), 7.42 – 7.36 (m, 3H, CH_{ar}), 4.63 (td, *J* = 8.5 Hz, ~ 1.5 Hz, 1H, CHD), 3.75 (d, *J* = 10.9 Hz, 3H, $POCH_3$), 3.72 (d, *J* = 10.9 Hz, 3H, $POCH_3$), 3.55 (q, *J* = 1.2 Hz, 3H, $COCH_3$).
^{31}P NMR (161.97 MHz, $CDCl_3$): δ = 20.75.

Diethyl *N*-tributylstannylmethyl-, (*R*)- and (*S*)-diethyl *N*-tributylstannyl-[D_1]methyl- *N*-(*t*-butoxycarbonyl)phosphoramidate [3.36, (*R*)- and (*S*)-[D_1]3.36]

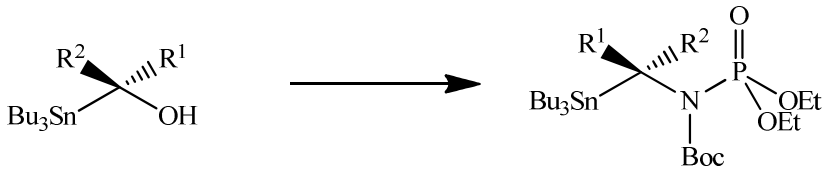

1.67: $R^1 = R^2 = H$
(*S*)-[D_1]**1.67**: $R^1 = H$, $R^2 = D$
(*R*)-[D_1]**1.67**: $R^1 = D$, $R^2 = H$

3.36: $R^1 = R^2 = H$
(*R*)-[D_1]**3.36**: $R^1 = H$, $R^2 = D$
(*S*)-[D_1]**3.36**: $R^1 = D$, $R^2 = H$

DEAD (0.435 g, 2.5 mmol, 0.393 ml) was added to a stirred mixture of tributylstannylmethanol (**1.67**, 0.678 g, 2.1 mmol), diethyl *N*-(*t*-butoxycarbonyl)phosphoramidate (0.647 g, 2.5 mmol) and triphenylphosphane (0.655 g, 2.5 mmol) in dry THF (10 ml) under argon at 0˚C.[15] Stirring was continued for 30 min at 0˚C and then at room temperature for 24 h. After the addition of water (7 drops), it was concentrated under reduced pressure. The residue was purified by flash chromatography (hexane:ethyl acetate = 5:1, R_f = 0.37) to give the phosphoramidate **3.36** (0.953 g, 82%) as a colorless oil.

^{1}H NMR (400.27 MHz, $CDCl_3$): δ = 4.18-4.00 (m, 4H, 2x$POCH_2$), 3.18 (d, *J* = 8.2 Hz, $J(^{117/119}Sn)$ = 23.8 Hz, 2H, NCH_2Sn), 1.55-1.40 (m, 6H, 3x$SnCH_2\underline{CH_2}$), 1.45 (s, 9H, 3xCH_3), 1.31 (td, *J* = 7.1, 0.9 Hz, 6H, 2x$POCH_2\underline{CH_3}$), 1.27 (sext, *J* = 7.3 Hz, 6H, 3x$Sn(CH_2)_2\underline{CH_2}$), 0.95-0.75 (m, 6H, 3x$SnCH_2$), 0.86 (t, *J* = 7.3 Hz, 9H, 3xCH_3).

(*R*)-Diethyl *N*-tributylstannyl-[D_1]methyl- *N*-(*t*-butoxycarbonyl)phosphoramidate [(*R*)-[D_1]**3.36**]
Similarly, (*S*)-tributylstannyl-[D_1]methanol [(*S*)-[D_1]**1.67**, 0.366 g, 1.14 mmol] was converted to (*R*)-diethyl *N*-tributylstannyl-[D_1]methyl-*N*-(*t*-butoxycarbonyl)phosphoramidate [(R)-[D_1]**3.36**, 0.493 g, 78%].

(*S*)-Diethyl *N*-tributylstannyl-[D_1]methyl- *N*-(*t*-butoxycarbonyl)phosphoramidate [(*S*)-[D_1]**3.36**]
Similarly, (*R*)-tributylstannyl-[D1]methanol [(*R*)-[D_1]**1.67**, 0.412 g, 1.28 mmol] was converted to (*S*)-diethyl *N*-tributylstannyl-[D_1]methyl-*N*-(*t*-butoxycarbonyl)phosphoramidate [(*S*)-[D_1]**3.36**, 0.599 g, 84%].

The ^{1}H NMR spectra for (*R*)- and (*S*)-diethyl *N*-tributylstannyl-[D_1]methyl-*N*-(*t*-butoxycarbonyl)phosphoramidate were identical:
^{1}H NMR (400.27 MHz, $CDCl_3$): δ = 4.20-4.00 (m, 4H, 2x$POCH_2$), 3.16 (d, J = 8.1 Hz, $J(^{117/119}Sn)$ = 19.7 Hz, 1H, CHD), 1.50-1.40 (m, 6H, 3x$SnCH_2CH_2$), 1.46 (s, 9H, 3xCH_3), 1.31 (td, J = 0.9 Hz, J = 7.1 Hz, 6H, 2x$POCH_2CH_3$), 1.27 (sext, J = 7.3 Hz, 6H, 3x$Sn(CH_2)_2CH_2$), 0.95-0.75 (m, 6H, 3x$SnCH_2$), 0.86 (t, J = 7.3 Hz, 9H, 3xCH_3).

Diethyl *N*-(*t*-butoxycarbonyl)aminomethyl- , (*R*)- and (*S*)-diethyl *N*-(*t*-butoxycarbonyl)amino-[D_1]methylphosphonate [3.37, (*R*)- and (*S*)-[D_1]3.37]

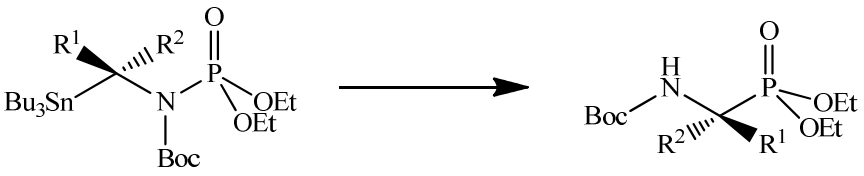

3.36: $R^1 = R^2 = H$
(*R*)-[D_1]**3.36**: R^1 = H, R^2 = D
(*S*)-[D_1]**3.36**: R^1 = D, R^2 = H

3.37: $R^1 = R^2 = H$
(*R*)-[D_1]**3.37**: R^1 = H, R^2 = D
(*S*)-[D_1]**3.37**: R^1 = D, R^2 = H

Methyllithium (0.81 mmol, 0.27 ml, 3M in diethoxymethane) was added drop wise to a stirred solution of diethyl *N*-tributylstannylmethyl-*N*-(*t*-butoxycarbonyl)phosphoramidate (**3.36**, 0.450 g, 0.81 mmol) and TMEDA (0.89 mmol, 0.133 ml) in dry Et_2O (5 ml) under argon at -78˚C.[15] After stirring for 5 min, acetic acid (2 mmol, 2 ml, 1M in H_2O) was added. The layers were separated and the aqueous layer was extracted twice with Et_2O. The combined organic layers were dried ($MgSO_4$) and concentrated under reduced pressure. The residue was purified by flash

chromatography (ethyl acetate, R_f = 0.35) to give the aminophosphonate **3.37** (0.143 g, 66%) as colorless oil.

^{1}H NMR (400.27 MHz, $CDCl_3$): δ = 4.76 (brs, 1H, NH), 4.20-4.00 (m, 4H, 2xOCH_2), 3.53 (dd, J = 11.1, 6.0 Hz, 2H, NCH_2P), 1.42 (s, 9H, 3xCH_3), 1.31 (t, J = 7.1 Hz, 6H, 2x$POCH_2\underline{CH_3}$).

(*R*)-Diethyl *N*-(*t*-butoxycarbonyl)amino-[D_1]methylphosphonate [(*R*)-[D_1]**3.37**]

Similarly, (*R*)-diethyl *N*-tributylstannyl-[D_1]methyl *N*-(*t*-butoxycarbonyl)phosphoramidate [(*R*)-[D_1]**3.36**, 0.419 g, 0.75 mmol] was converted to (*R*)-diethyl *N*-(*t*-butoxycarbonyl)amino-[D_1]methylphosphonate [(*R*)-[D_1]**3.37**, 0.134 g, 73%].

(*S*)-Diethyl *N*-(*t*-butoxycarbonyl)amino-[D_1]methylphosphonate [(*S*)-[D_1]**3.37**]

Similarly, (*S*)-diethyl *N*-tributylstannyl-[D_1]methyl *N*-(*t*-butoxycarbonyl)phosphoramidate [(*S*)-[D_1]**3.36**, 0.573 g, 1.03 mmol] was converted to (*S*)-diethyl *N*-(*t*-butoxycarbonyl)amino-[D_1]methylphosphonate [(*S*)-[D_1]**3.37**, 0.252 g, 91%].

The ^{1}H NMR spectra for (*R*)- and (*S*)-diethyl *N*-(*t*-butoxycarbonyl)aminomethylphosphonate were identical:

^{1}H NMR (400.27 MHz, $CDCl_3$): δ = 4.75 (brs, 1H, NH), 4.20-4.00 (m, 4H, 2xOCH_2), 3.51 (broadened dd, J = 10.6, 6.0 Hz, 1H, NCHD), 1.42 (s, 9H, 3xCH_3), 1.31 (t, J = 7.0 Hz, 6H, 2xCH_2CH_3).

Diethyl *N*-(triphenylmethylamino)methylphosphonate (3.42)

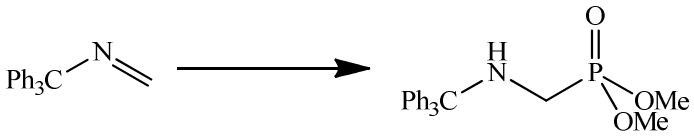

3.42

Dry toluene (10 ml) was added to a mixture of *N*-(triphenylmethyl)methylimine (2.165 g, 8.0 mmol) and dimethyl phosphite (4.40 g, 4.0 mmol, 3.66 ml) at 100˚C.[71] The mixture was refluxed for 5 min and concentrated under reduced pressure. Excess dimethyl phosphite was removed in vacuo (20 mm Hg, 100˚C). The crude phosphonate **3.42** (3.49 g) still contained some dimethyl phosphite and was immediately deprotected without any further purification.

Aminomethylphosphonic acid (3.26)

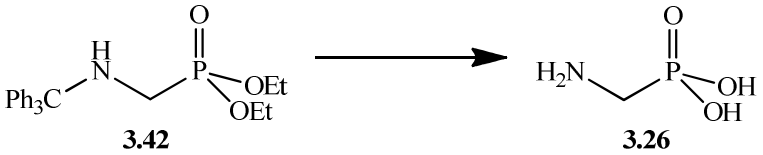

3.42 **3.26**

A mixture of diethyl *N*-(triphenylmethylamino)methylphosphonate (**3.42**, 3.49 g, 9.1 mmol) and HCl (6M, 22 ml) was refluxed for 2 h. After cooling to room temperature the reaction mixture was extracted three times with CH_2Cl_2. The organic layer was discarded and the aqueous layer was concentrated under reduced pressure. The residue was dried in a vacuum dessicator (KOH) for 18 h and purified by ion-exchange chromatography (Dowex 50x8, H^+,water as eluent). Fractions containing product (detected by using a solution of 0.2% ninhydrin in 96% EtOH and heating) were pooled and concentrated under reduced pressure to give crystalline product that was recrystallized from water and ethanol to yield colorless crystals of aminophosphonic acid **3.26** (0.608 g, 60%, contained 8 mol % of EtOH); mp. 336-338˚C (decomp) (lit.:[71] 342-345˚C).

^{1}H NMR (400.27 MHz, D_2O): δ = 3.15 (d, J = 12.7 Hz, 2H, NCH_2).
^{13}C NMR (100.65 MHz, D_2O): δ = 36.16 (d, J = 141.4 Hz).
^{31}P (162.03 MHz, D_2O): δ = 10.82.

(*R*)- and (*S*)-Amino-[D_1]methylphosphonic acid [(*R*)- and (*S*)-[D_1]3.26]

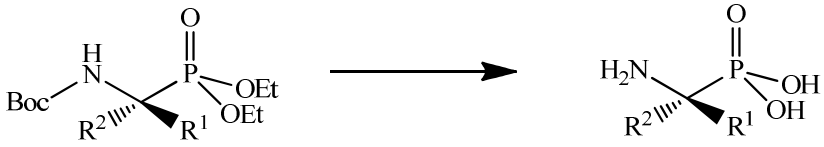

(*R*)-[D_1]**3.37**: R^1 = H, R^2 = D
(*S*)-[D_1]**3.37**: R^1 = D, R^2 = H

(*R*)-[D_1]**3.26**: R^1 = H, R^2 = D
(*S*)-[D_1]**3.26**: R^1 = D, R^2 = H

A mixture of (*R*)-diethyl *N*-(*t*-butoxycarbonyl)amino-[D_1]methylphosphonate [(*R*)-[D_1]**3.37**, 0.106 g, 0.37 mmol] and HCl (6M, 3 ml) was refluxed for 6 h. The mixture was concentrated under reduced pressure and dried over KOH in vacuum dessicator for 18 h. The residue was purified by ion-exchange chromatography (Dowex 50x8, H^+, water as eluent) to give the phosphonic acid (*R*)-[D_1]**3.26** (0.017 g, 41%) as colorless crystals that were used for Mosher amide.

(*S*)-Amino-[D_1]methylphosphonic acid [(*S*)-[D_1]**3.26**]

Similarly, (*S*)-diethyl *N*-(*t*-butoxycarbonyl)amino-[D_1]methylphosphonate [(*S*)-[D_1]**3.37**, 0.218 g, 0.81 mmol] was converted to (*S*)-amino-[D_1]methylphosphonic acid [(*S*)-[D_1]**3.26**, 0.018 g, 20%].

Analytical samples of both (*R*)- and (*S*)-amino-[D_1]methylphosphonic acid were recrystallized (water: ethanol = 1:1) and their NMR spectra were identical:

^{1}H NMR (400.27 MHz, D_2O, 4.8): δ = 3.13 (d, J = 12.4 Hz, 1H CHD).

^{13}C NMR (100.61 MHz, D_2O): δ = 36.26 (td, J = 142.1, 21.6 Hz, CHD).

^{31}P (162.03 MHz, D_2O): δ = 10.78.

(*R*)-Mosher amides of dimethyl aminomethyl- and (*R*)-dimethyl amino[D_1]methylphosphonate and (*S*)-Mosher amide of (*S*)-dimethyl amino-[D_1]methylphosphonate [3.44, (*R*)- and (*S*)-[D_1]3.44]

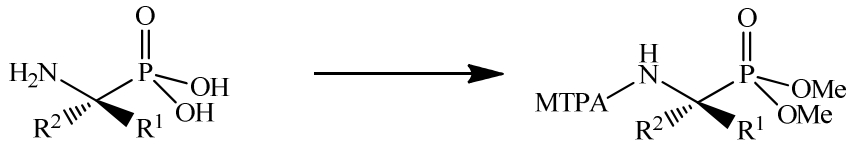

3.26: $R^1 = R^2 = H$
(*R*)-[D_1]**3.26**: $R^1 = H$, $R^2 = D$
(*S*)-[D_1]**3.26**: $R^1 = D$, $R^2 = H$

3.44: $R^1 = R^2 = H$
(*R*)-[D_1]**3.44**: $R^1 = H$, $R^2 = D$
(*S*)-[D_1]**3.44**: $R^1 = D$, $R^2 = H$

Trimethylchlorosilane (0.105 g, 0.97 mmol, 0.123 ml) was added to a mixture of aminomethylphosphonic acid (**3.26**, 13.5 mg, 0.12 mmol) and dry pyridine (2 ml) under argon. It was heated to 100˚C for 3 min to dissolve the phosphonic acid and then cooled to ambient temperature. After the addition of (*S*)-MTPACl (0.24 mmol, 0.453 ml, 0.53 M in dry CH_2Cl_2) stirring was continued for 18 h. Water (5 drops) was added and the mixture was stirred for 5 min and then concentrated under reduced pressure. HCl (2M, 5 ml) and water (5 ml) were added and the mixture was extracted with Et_2O. The organic layer was discarded and the aqueous layer was concentrated under reduced pressure. The residue was dissolved in water and passed through Dowex 50x8, H^+ (water as eluent). The eluate was concentrated under reduced pressure and dried in vacuo. Dry methanol (5ml) was added and a distilled ethereal solution of diazomethane was added until the solution remained yellow. It was concentrated under reduced pressure and purified by flash chromatography (ethyl acetate, R_f = 0.23) to yield (*R*)-Mosher amide **3.44** (16.5 mg, 39%) as a colorless oil.

^{1}H NMR (600.13 MHz, toluene-d_8): δ = 7.64 (d, J = 7.7 Hz, 2H, CH_{ar}), 7.09-7.01 (m, 3H, CH_{ar}), 6.91 (br. s, 1H, NH), 3.50 (ddd, J = 15.7, 11.9, 6.7 Hz, 1H, NCH), 3.33 (d, J = 10.8 Hz, 3H, $POCH_3$), 3.28 (d, J = 10.8 Hz, 3H, $POCH_3$), 3.28 (ddd, overlaps with signals from $POCH_3$, J = 6.0 Hz, 1H, NCH), 3.22 (q, J = 1.5 Hz, 3H, OCH_3).
^{1}H NMR (400.27 MHz, Tol): δ = 7.64 (d, J = 7.6 Hz, 2H, CH_{ar}), 7.09-7.01 (m, 3H, CH_{ar}), 6.87 (br. s, 1H, NH), 3.49 (ddd, J = 15.8, 11.8, 6.5 Hz, 1H, NCH), 3.33 (d, J = 10.8 Hz, 3H, $POCH_3$), 3.29 (d, J = 10.8 Hz, 3H, $POCH_3$), 3.29 (ddd, overlaps with signals from $POCH_3$, J = 6.0 Hz – only this one could be determined, 1H, NCH), 3.21 (q, J = 1.5 Hz, 3H, OCH_3).
^{31}P NMR (161.98 MHz, $CDCl_3$): δ = 25.40.

(*R*)-Mosher amide of (*R*)-dimethyl amino-[D_1]methylphosphonate [(*R*)-[D_1]**3.44**]

Similarly, (*R*)-amino-[D_1]methylphosphonic acid [(*R*)-[D_1]**3.26**, 0.012 g, 0.11 mmol] was converted to the (*R*)-Mosher amide (*R*)-[D_1]**3.44** (0.024 g, 62%, de > 94%).

(*S*)-Mosher amide of (*S*)-dimethyl amino-[D_1]methylphosphonate [(*S*)-[D_1]**3.44**]

Similarly, (*S*)-amino-[D_1]methylphosphonic acid [(*S*)-[D_1]**3.26**, 0.011 g, 0.10 mmol] and (*R*)-MTPACl (0.050 g, 0.2 mmol) were converted to the (*S*)-Mosher amide (*S*)-[D_1]**3.44** (0.023 g, 66%, de > 94%).

The ^{1}H and ^{31}P NMR spectra for (*R*)- and (*S*)-Mosher amides were identical:
^{1}H NMR (400.13 MHz, toluene-d_8): δ = 7.64 (d, J = 7.6 Hz, 2H, CH_{ar}), 7.09-7.01 (m, 3H, CH_{ar}), 6.87 (br. s, 1H, NH), 3.34 (d, J = 10.8 Hz, 3H, $POCH_3$), 3.29 (d, J = 10.8 Hz, 3H, $POCH_3$), 3.29 (dd, overlaps with signals from $POCH_3$, 1H, NCH), 3.23 (q, J = 1.5 Hz, 3H, OCH_3).
^{31}P (161.98 MHz, $CDCl_3$): δ = 25.35.

5 References

1. Wallis, E. S.; Adams, F. H. *J. Am. Chem. Soc.* **1933**, *55*, 3838-3851.
2. Carey, F. A.; Sunberg, R. J. *Advanced Organic Chemistry, Part A: Structure and Mechanisms*, 5th ed.; Springer, **2007**
3. Still, W. C.; Sreekumar, C. *J. Am. Chem. Soc.* **1980**, *102*, 1201-1202.
4. Fraenkel, G.; Henrichs, M.; Hewitt, J. M.; Su, B. M.; Geckle, M. J. *J. Am. Chem. Soc.* **1980**, *102*, 3345-3350.
5. Fraenkel, G.; Henrichs, M.; Hewitt, J. M.; Su, B. M. *J. Am. Chem. Soc.* **1984**, *106*, 255-256.
6. Kapeller, D. C. *Diplomarbeit*, Universität Wien, **2005**.
7. Carey, F. A.; Sunberg, R. J. *Advanced Organic Chemistry, Part B:Reactions and Synthesis*, 5th ed.; Springer, **2007**
8. Clayden, J. *Tetrahedron Organic Chemistry Series, Volume 23, Organolithiums: Selectivity for Synthesis*, 1st ed.; Pergamon, **2002**.
9. Still, W. C. *J. Am. Chem. Soc.* **1978**, *100*, 1481-1487.
10. Meyer, N.; Seebach, D. *Chem. Ber.* **1980**, *113*, 1290-1303.
11. Reich, H. J.; Phillips, N. H. *J. Am. Chem. Soc.* **1986**, *108*, 2102-2103.
12. Letsinger, R. L. *J. Am. Chem. Soc.* **1950**, *72*, 4842.
13. Beak, P.; Reitz, D. B. *Chem. Rev.* **1978**, *78*, 275-316.
14. Cram, D. J. *Fundamentals of Carbanion Chemistry*, Academic Press, **1965**.
15. Kapeller, D. C. *Dissertation*, Universität Wien, **2008**.
16. Basu, A.; Thayumanavan, S. *Angew. Chem. Int. Ed.* **2002**, *41*, 716-738.
17. Hoffmann, R. W.; Lanz, J.; Metternich, R.; Tarara, G.; Hoppe, D. *Angew. Chem. Int. Ed. Engl.* **1987**, *26*, 1145-1146.
18. Linderman, R. J.; Ghannam, A. *J. Am. Chem. Soc.* **1990**, *112*, 2392-2398.
19. Hoppe, D.; Hense, T. *Angew. Chem.* **1997**, *109*, 2376-2410.
20. Elworthy, T. R.; Meyers, A. I. *Tetrahedron* **1994**, *60*, 6089-6096.
21. Kerrick, S. T.; Beak, P. *J. Am. Chem. Soc.* **1991**, *113*, 9708-9710.
22. Beak, P.; Zajdel, W. J.; Reitz, D. B. *Chem. Rev.* **1984**, *84*, 471-523.
23. Kapeller, D. C.; Hammerschmidt, F. *J. Am. Chem. Soc.* **2008**, *130*, 2329-2335.
24. Kapeller, D. C.; Barth, R.; Mereiter, K., Hammerschmidt, F. *J. Am. Chem. Soc.* **2007**, *129*, 914-923.

25. Boche, G.; Lohrenz, J. C. W. *Chem. Rev.* **2001**, *101*, 697-756.
26. Espinet, P.; Echavarren, A. M. *Angew. Chem. Int. Ed.* **2005**, *43*, 4704-4734.
27. Azarian, D.; Dua, S. S.; Eaborn, C.; Walton, D. R. M. *J. Organomet. Chem.* **1976**, *117*, C55-C57.
28. Kosugi, M.; Fugami, K. *J. Organomet. Chem.* **2002**, *653*, 50-53.
29. Milstein, D.; Stille, J. K. *J. Am. Chem. Soc.* **1978**, *100*, 3636-3638.
30. Mateo, C.; Cárdenas, D. J.; Fernández-Rivas, C.; Echavarren, A. M. *Chem. Eur. J.* **1996**, *2*, 1596-1606.
31. Stille, J. K. *Angew. Chem.* **1986**, *98*, 504-519.
32. Vicente, J.; Arcas, A.; Bautista, D. *Organometallics* **1997**, 2127-2138.
33. Amatore, C.; Jutand, A. *Acc. Chem. Res.* **2000**, *33*, 314-321.
34. Amatore. C.; Jutand, A.; Suarez, A. *J. Am. Chem. Soc.* **1993**, *115*, 9531-9541.
35. Casares, J. A.; Espinet, P.; Salas, G. *Chem. Eur. J.* **2002**, *8*, 4843-4853.
36. Cross, R. J. *Adv. Inorg. Chem.* **1989**, *34*, 219-292.
37. Romeo, R. *Comments Inorg. Chem.* **1990**, *11*, 21-57.
38. Casado, A. L.; Espinet, P.; Gallego, A. M. *J. Am. Chem. Soc.* **2000**, *122*, 11771-11782.
39. Casado, A. L.; Espinet, P. *J. Am. Chem. Soc.* **1998**, *120*, 8978-8985.
40. Brown, J. M.; Cooley, N. A. *Chem. Rev.* **1988**, *88*, 1031-1046.
41. Ye, J.; Bhatt, R. K.; Falck, J. R. *J. Am. Chem. Soc.* **1994**, *116*, 1-5.
42. Farina, V.; Kapadia, S.; Krishnan, B.; Wang, C.; Liebeskind, L. S. *J. Org. Chem.* **1994**, *59*, 5905-5911.
43. Fouquet, E.; Rodriguez, A. L. *Synlett* **1998**, 1323-1324.
44. Kosugi, M.; Sumiya, T.; Ohhashi, K.; Sano, H.; Migita, T. *Chem. Lett.* **1985**, 997-998.
45. Loghmani-Khouzani, H.; Poorheravi, M. R.; Sadeghi, M. M. M.; Caggiano, L.; Jackson, R. F. W. *Tetrahedron* **2004**, *64*, 7419-7425.
46. Littke, A. F.; Schwarz, L.; Fu, G. C. *J. Am. Chem. Soc.* **2002**, *124*, 6343-6348.
47. Kosugi, M.; Sumiya, T.; Ogata, T.; Sano, H.; Migita, T. *Chem. Lett.* **1984**, 1225-1226.
48. Givens, R. S.; Hrinczenko, B.; Liu, J. H. S.; Matuszewski, B.; Tholen-Collison, J. *J. Am. Chem. Soc.* **1984**, *106*, 1779-1789.
49. But, T. Y. S.; Toy, P. H. *Chem. Asian J.* **2007**, *2*, 1340-1355.
50. Al-Mousawi, S. M.; El-Apasery, M. A.; Al-Kanderi, N. H. *ARKIVOC* **2008**, *XVI*, 268-278.
51. Gupta, P.; Shah, B. A.; Parshad, R.; Quazi, G. N.; Taneja, S. T. *Green Chem.* **2007**, *9*, 1120-1125.

52. Pearson, W. H.; Postich, M. J. *J. Org. Chem.* **1992**, *57*, 6354-6357.
53. Metcalf, W. W.; van der Donk, W. A. *Annu. Rev. Biochem.* **2009**, *78*, 65-94.
54. Clark, L. L.; Ingall E. D.; Benner R. *Am. J. Sci.* **1999**, *2999*, 724-737.
55. Wanke, C.; Amrhein, N. *Eur. J. Biochem.* **1993**, *218*, 861-870.
56. Loeff, I.; Stein, G. *Nature* **1959**, *184*, 901-902.
57. Kukhar, V. P.; Hudson, H. R. *Aminophosphonic and Aminophosphinic Acids*; John Wiley & Sons, **2000**.
58. Cooper, G. W.; Onwo, W. M.; Cronin, J. R. *Geochem. Cosmochem. Acta* **1992**, *56*, 4109-4115.
59. Whitteck, J. T.; Cicchillo, R. M.; van der Donk, W. A. *J. Am. Chem. Soc.* **2009**, *131*, 16225-16232.
60. Blodgett, J. A. V.; Thomas, P. M.; Li, G.; Velasquez, J. E.; van der Donk, W. A.; Kelleher, N. L.; Metcalf, W. W. *Nature Chem. Biol.* **2007**, *3*, 480-485.
61. Abell, L. M.; Villafranca, J. J. *Biochemistry* **1991**, *30*, 6135-6141.
62. Faber, K. *Biotransformations in Organic Chemistry*, 5th ed, Springer, **2004**.
63. Cicchillo, R. M.; Zhang, H.; Blodgett, J. A. V.; Whitteck, J. T.; Li, G.; Nair, S. K.; van der Donk, W. A.; Metcalf, W. W. *Nature* **2009**, *459*, 871-875.
64. Higgins, L. J.; Yan, F.; Liu, P.; Drennan, C. L. *Nature* **2005**, *437*, 838-844.
65. Liu, P.; Murakami, K.; Seki, T.; He, X.; Yeung, S.-M.; Kuzuyama, T.; Seto, H.; Liu, H.-W. *J. Am. Chem. Soc.* **2001**, *123*, 4619-4620.
66. Ryzhkov, V. L.; Kabachnik, M. I.; Tarasevich, L. M.; Medved, T. Y.; Zeitlenok, N. A.; Marchenko, N. K.; Vagzhanova, V. A. *Chem Abstr.* **1955**, *49*, 3404b.
67. Hammerschmidt, F.; Schmidt, S. *Monatsh. Chem.* **1997**, *128*, 1173-1180.
68. Hammerschmidt, F. *Liebigs Ann. Chem.* **1991**, 469-475.
69. McGrath, J. W.; Hammerschmidt, F.; Preusser, W.; Quinn, J. P., Schweifer, A. *Org. Biomol. Chem.* **2009**, *7*, 1944-1953.
70. Zwierzak, A.; Pilichowska, S. *Synthesis* **1982**, 922-924.
71. Soroka, M.; Zygmunt, J. *Synthesis* **1988**, *5*, 370-372.
72. Wahl, C. *Chem. Ber.* **1922**, *55*, 1449-1457.
73. Rondestvedt, C. S. Jr. *J. Org. Chem.* **1956**, *21*, 911-912.
74. John H. M. Hill, J. H. M. *J. Org. Chem.* **1965**, *30*, 620-622.
75. Terada, A. *Nippon Kagaku Zasshi* **1956**, *77*, 1265-1267, *Chem. Abstr.* **1959**, *53*, 5185.
76. Gabriel, S. *Chem. Ber.* **1887**, *20*, 2224-2236.
77. Guanti, G.; Zannetti, M. T.; Banfi, L.; Riva, R. *Adv. Synth. Catal.* **2001**, *343*, 682-691.

6 Summary

(*R*)- and (*S*)-tributylstannyl-[D_1]methanol were transformed into a variety of chiral methylmetals to determine their reactivity and configurational stability. The transformations were optimized in the unlabelled series. Tributyl(fluoromethyl)stannane was transmetalated with methyllithium. The fluoromethyllithium formed in the presence of acetophenone reacted with it at -78°C and -95°C to give a tertiary alcohol. Surprisingly, fluoromethyllithium is chemically stable for its short lifetime. This information justifies later experiments in the labelled series.

The Stille coupling was performed with enantiomers of tributylstannyl-[D_1]methanol, tributylstannyl-[D_1]methyl benzoate and *N*-protected amino-[D_1]methylstannanes and benzoyl chloride or bromobenzene in toluene and 1,4-dioxane at temperatures ranging from room temperature to 100 °C. Palladium(0) in combination with triphenylphosphane or tris(*t*-butyl)phosphane was used as catalyst, sometimes with copper(I) cyanide as additive. According to the generally accepted mechanism for the Stille reaction, Pd(II) complexes containing a benzoyl or a phenyl group and phosphane ligands reacted with the various stannanes to give chiral methylpalladium complexes, which undergo reductive elimination to form coupling products. These were converted to compounds, whose configuration at the deuterium bearing carbon atom could be determined by ^{1}H NMR spectroscopy. It was found that the oxygen-substituted chiral [D_1]methylpalladium complexes are configurationally stable relative to the reductive elimination. Furthermore, the C-C bonds are formed with retention of configuration at the stereogenic centre. *N*-Protected chiral aminomethylstannes can be Stille coupled with benzoyl chloride giving products with the enantiomeric excesses of 99%, but with bromobenzene with partial razemisation. Sulfur-substituted methylpalladium complexes could not be formed.

Phosphinothricin, a glutamine synthetase inhibitor produced by various strains of *Streptomyces*, is a commercially important herbicide, used especially with certain transgenic plants. Its biosynthesis is very challenging. To unravel the stereochemistry of the 2-hydroxyethylphosphonate dioxygenase (HEPD), that converts 2-hydroxyethylphosphonate to hydroxymethylphosphonate and formic acid, the enantiomers of (*R*)- and (*S*)-hydroxy-[D_1]methylphosphonate were prepared using microscopically configurationally stable chiral phosphinyloxy-[D_1]methyllithiums as intermediates. The cooperation partner converted the enantiomers of 2-hydroxy-[1-D_1]ethylphosphonate using HEPD to labelled hydroxy-[D_1]methylphopshonates. The samples were derivatized and found by ^{1}H NMR spectroscopy to be racemic.

Finally, the enantiomers of amino-[D_1]methylphosphonic acid with the enantiomeric excesses of at least 94% were synthesized via phosphoramidate-aminophosphonate rearrangement of chiral *N*-phosphorylated amino-[D_1]methyllithiums.

7 Zusammenfassung

(*R*)- und (*S*)-Tributylstannyl-[D_1]methanol wurden in verschiedene chirale Methylmetall-Verbindungen überführt, um ihre Reaktivität und konfigurative Stabilität zu untersuchen. Die Umwandlungen wurden in der nicht markierten Serie optimiert. Tributyl(fluormethyl)stannan wurde mit Methyllithium transmetalliert. Das Fluormethyllithium wurde in Gegenwart von Acetophenon gebildet und reagierte damit bei -78°C und -95°C zu einem tertiären Alkohol. Überraschenderweise ist Fluormethyllithium während seiner Lebensdauer chemisch stabil. Diese Information rechtfertigt spätere Experimente in der markierten Serie.

Die Stille-Kupplung wurde mit Enantiomeren von Tributylstannyl-[D_1]methanol, Tributylstannyl-[D_1]methylbenzoat und *N*-geschützten Amino-[D_1]methylstannanen und Benzoylchlorid oder Brombenzol in Toluol oder 1,4-Dioxan bei Temperaturen von Raumtemperatur bis 100°C durchgeführt. Palladium(0) in Kombination mit Triphenylphosphin oder Tris(*t*-butyl)phosphin wurde als Katalysator verwendet, manchmal auch mit Kupfer(I)cyanid als Additiv. Gemäß des allgemein akzeptierten Mechanismus der Stille-Reaktion reagierten Pd(II)-Komplexe mit einer Benzoyl- oder Phenyl-Gruppe und Phosphinliganden mit den verschiedenen Stannanen zu chiralen Methylpalladium-Komplexen, die eine reduktive Eliminierung zu Kopplungsprodukten eingingen. Diese wurden in Verbindungen überführt, deren Konfiguration am Deuterium-tragenden Kohlenstoffatom mittels ^{1}H-NMR-Spektroskopie bestimmt wurde. Es wurde festgestellt, dass die Sauerstoff-substituierten chiralen [D_1]Methylpalladium-Komplexe relativ zur reduktiven Eliminierung konfigurativ stabil sind. Außerdem wurden die C-C-Bindungen mit Retention der Konfiguration am stereogenen Zentrum gebildet. *N*-Geschützte chirale Aminomethylstannane konnten mit Benzoylchlorid zu Produkten mit einem Enantiomerenüberschuß von 99% Stille-gekuppelt werden, aber mit Brombenzen zu partiell racemischen Produkten. Schwefel-substituierte Methylpalladium-Komplexe konnten nicht gebildet werden.

Phosphinothricin, ein Inhibitor der Glutaminsynthetase, das von verschiedenen *Streptomyceten*-Stämmen produziert wird, ist ein kommerziell wichtiges Herbizid, insbesondere bei bestimmten transgenen Pflanzen. Seine Biosynthese ist sehr anspruchsvoll. Um die Stereochemie der 2-Hydroxyethylphosphonat-Dioxygenase (HEPD), die das 2-Hydroxyethylphosphonat in Hydroxymethylphosphonat und Ameisensäure umwandelt, zu untersuchen, wurden die Enantiomere von (*R*)- und (*S*)-Hydroxy-[D_1]methylphosphonat mit der Hilfe von mikroskopisch konfigurativ stabilen chiralen Phosphinyloxy-[D_1]methyllithium-Verbindungen als

Zwischenprodukte synthetisiert. Der Kooperationspartner wandelte die Enantiomere von 2-Hydroxy-[1-D_1]ethylphosphonat mit der Hilfe der HEPD in die markierten Hydroxy-[D_1]methylphopshonate um. Die Proben wurden derivatisiert und mittels ^{1}H-NMR-Spektroskopie untersucht. Beide Proben waren racemisch.

Zuletzt wurden die Enantiomere der Amino-[D_1]methylphosphonsäure mit einem Enantiomerenüberschuß von mindestens 94% mit Hilfe der Phosphoramidat-Aminophosphonat-Umlagerung von chiralen *N*-phosphorylierten Amino-[D_1]methyllithium-Verbindungen sythetisiert.

8 Lebenslauf

Petra Malová

Geburtsdatum: 19.06.1986
Geburtsort: Bratislava, Slowakei

Ausbildung	
universität wien 	*Oktober 2008 – Sommer 2010* Universität Wien, Wien, Österrreich ▪ Masterstudium, geplanter Titel: Master of Science ▪ Fächer: Organische Chemie, Analytische Chemie, Biologische Chemie ▪ Masterarbeit: Betreuer - Ao. Univ.-Prof. Dr. Friedrich Hammerschmidt – Chiral Methylmetals – Configurational Stability and Applications *August 2005 – Mai 2008* Valparaiso University, Valparaiso, Indiana, USA ▪ Titel: Bachelor of Science, Programm: Chemie ▪ Notendurchschnitt: 3.93 (Skala: 4.00 am besten, 1.00 am schlechtesten) *September 2004 – Mai 2005* Faculty of Natural Sciences, Comenius University, Bratislava, Slowakei ▪ Programm: Biologie *1996 – 2004* Gymnázium sv. Uršule, Bratislava, Slowakei *2002 – 2003* Bear Creek High School, Stockton, California, USA
Erfahrungen	
universität wien 	*Juli 2009* Universität Wien, Wien, Österrreich ▪ Forschungsassistentin bei Ao. Univ.-Prof. Dr. Friedrich Hammerschmidt ▪ Synthese von potentiellen Tumormarker *2006 - 2008* Valparaiso University, Valparaiso, Indiana, USA ▪ Laborassistentin für Biochemie und Analytische und Organische Chemie ▪ Lehrassistentin für organische Chemie, Physik und Mathematik

Auszeichnungen	
	2006 Undergraduate Award for Achievement in Organic Chemistry (Valparaiso University) *2007* Undergraduate Award in Analytical Chemistry (Valparaiso University) *2008* Valparaiso University Outstanding Senior Chemistry Award (Valparaiso University) Mitglied von Phi Lambda Upsilon (The National Honorary Chemical Society, USA) Mitglied von The Phi Beta Kappa Society (Academic Honor Society, USA) Hochschulabschluss mit Summa cum Laude